Topics in Spatial Statistics*

Nils Lid Hjort[a,b] **and Henning Omre**[a]

Norwegian Computing Centre[a] *and University of Oslo*[b]

-- March 1992 --

ABSTRACT. An overview is given over a fair range of topics within spatial and spatial-temporal statistics. The theory presented is motivated by and illustrated with actual applications to real world problems. We describe and discuss models for three basic types of spatial processes: continuous random surfaces, mosaic phenomena, and events-against-background processes. Various combinations of these sometimes occur naturally in applications, like Gaußian noise on top of a Markov random field in image restoration problems. Some of these combinations are also discussed. The applications we discuss are drawn from the areas of medical image analysis, pollution monitoring, characterisation of oil reservoirs, estimation of fish and whale stock, forestry surveillance via satellite, statistical meteorology, and symbol recognition.

KEY WORDS: *Bayesian methods; covariance function; event processes; hidden Markov fields; image restoration; Kriging; marked point processes; Markov random fields; parameter estimation; pseudo-likelihood; quasi-likelihood; semi-Markov random fields; spatial classification; spatial sampling strategy; stochastic simulation*

1. Introduction

1.1. What's special about spatial? Spatial statistical problems call for evaluation by exploratory data analysis, prediction and classification, simulation, and confirmatory statistics, and are accordingly in that respect well within traditional statistics. To pinpoint differences, consider a spatial process $\{Y(x): x \in D\}$ with some m-dimensional $Y(x)$ defined over some s-dimensional spatial or spatial-temporal reference region D. We have encountered $s = 2, 3, 4$ in our applications. Traditional statistical dependence between variables may occur in the Y-space, while the spatial reference x allows for dependencies in the reference dimensions. This is challenging from a stochastic modelling point of view and usually adds complexity to the sampling and estimation stages. The presence of a reference variable points to the importance of scale and changes from one scale to the other. The choice of scale is always crucial in spatial statistics.

Spatial phenomena are complicated to understand and model. The objective of a study is often to evaluate characteristics of a single realisation $\{y(x): x \in D\}$, for example, the hydrocarbon present in one particular petroleum reservoir. In this setting the data points $y(x_1), \ldots, y(x_n)$ are 'non-repeatable' and the observations may be dependent through their spatial locations. In traditional statistics the underlying assumptions usually include 'repeatability' in the form of (nearly) independent and (nearly) identically distributed observations. In spatial statistics some sort of 'pseudo-repeatability' is often obtained by postulating various forms of spatial stationarity. Typical model assumptions could be a constant mean $EY(x) = m$ and/or a stationary covariance function

* *Invited forum lectures at the Nordic Conference on Mathematical Statistics, Odense, June 1990*

$\mathrm{cov}\{Y(x_1), Y(x_2)\} = C(x_1 - x_2)$. There are parallels to modelling of time series, but spatial problems are often a full degree more complicated, due to lack of ordering in the reference space, the fact that border areas of the reference domain often constitute a large proportion of D, and the large variety of sampling options which appear when the dimensionality of D increases. The ergodicity assumption needed in both time series and spatial statistics is much harder to justify in the latter, since the dependence structure often is strong and D seldomly, with reasonable imagination, can be extended to infinity. Spatial correlation also tends to die out much more slowly than for a dependent one-dimensional process like time series.

In easier i.i.d.-type problems there is always a Glivenko–Cantelli type theorem which says that one can be ambitious and fit even sophisticated realistic models; the problems are 'one-dimensionally' tied to a couple of underlying distributions and nothing else, and the information content of a data set is sufficient to assess intricate features of these. In complex spatial problems, on the other hand, the information content is more thinly spread out in a much larger quilt of interwoven problems. Just think of inferring the underlying probabilistic structure of a two-dimensional continuous random function from just observing its values in a finite number of locations for a single realisation!

We have mentioned that sampling of spatial phenomena has several special features. The sampling support B is defined as the domain of the volume over which the sampling is averaged, i.e. $y_B(x_i) = |B|^{-1} \int_B y(x_i - u)\,du$, writing $|B|$ for the volume (or area) of B. A sampling support of zero is in many cases impossible. In petroleum applications, observations in wells are made on about $.03 \times .03 \times .05\,\mathrm{meter}^3$, which is of approximate zero support relative to the extent of the reservoir which is typically of size $2500 \times 5000 \times 100\,\mathrm{meter}^3$. Seismically collected data have a considerable support, however, approximately $100 \times 100 \times 10\,\mathrm{meter}^3$, and this must be accounted for when the two types of data are combined.

Data representativity in the form of a random sampling hypothesis is usually a basic assumption in traditional statistics. Sampling in non-regular regimes is frequent in applications of spatial statistics, however. 'Preferential sampling' of some sort is often performed in practice, planned or no-planned. One is of course tempted to use available data and knowledge about spatial continuity in order to confirm 'favourable areas' with extreme values of the process. This makes sense from most points of view except from the traditional statistical one. In the petroleum industry one is using seismic data in order to locate the first well in a prospect such that the chances for hitting oil is maximised. The fact that each exploratory well costs about US$ 30 million makes this even more sensible and almost mandatory. Consequently one particular challenge of spatial statistics is to correct for preferential sampling when for example predicting the total hydrocarbone volume.

The spatial dependence entails that the information content in each sample may vary. In image analysis and remote sensing where regular sampling occurs the redundancy in the sometimes enormous data set is usually substantial. The amount of information in the set of observations is often much smaller than what traditionally would have been anticipated.

Measurements of the variable of interest are often expensive or complicated to obtain. Spatial problems frequently involve indirect measurements, like seismic data, in order to improve the spatial coverage of the data. This calls for multivariate spatial models, and often for multivariate calibration methods.

The spatial reference in $\{Y(x): x \in D\}$ provides good opportunities for stochastic modelling. The fact that sampling is scarce and that the spatial dependence complicates the exploratory data analysis renders model verification a very difficult task. When preparing a development plan for a North Sea oil reservoir only about $10^{-8}\%$ of the reservoir volume is directly observable from well data. Geological experience and indirect seismic data are other sources of knowledge, and make the evaluation possible. The verification of the model must often be based on experience.

In typical spatial models with extensive dependence between observations one can only seldomly find explicit closed-form estimators with good efficiency properties. Usually one has to rely on model fitting to the observations through iterative procedures and cross validation. Note that jackknife and bootstrap procedures are difficult to apply in spatial problems because of the complex dependence structure.

We have so far primarily discussed spatial problems. Problems containing both spatial and temporal elements are considered with increasing interest, however. In this type of problems the samples are often abundant, particularly in the time dimension. This is caused by the increasing use of automatic sensors, and again there are often difficulties stemming from a high degree of data redundancy. The interdependence structure is even more complicated than for spatial problems, and even simple exploratory data analysis may turn out to be very complicated.

1.2. Three ways of applying statistics. Let us return to 'general statistics' and its philosophy and use in spatial statistics problems. It seems appropriate and convenient to distinguish between three ways of applying statistical methodology:

(i) Exploratory statistics is primarily concerned with the observations $y(x_1), \ldots, y(x_n)$ and their characteristics. When exploring them a minimum of model assumptions is enforced. Usually only some statements about representativity are made, hence data displays and plots associated with summary statistics can be provided. Exploratory statistics is an important but still underused part of applied statistics. Its uses include generating hypotheses justifying model choices.

(ii) Predictive statistics is primarily concerned with prediction and classification of realisations, either because the actual realisation is not observed or because it is observed with noise. An example of the former is interpolation from $y(x_1), \ldots, y(x_n)$ to estimation of $y(x)$ in other positions, perhaps with an uncertainty measure included, and an example of the latter is image restoration. Model assumptions are made only to meet the objective of prediction. In other words, the stochastic model is often constructed more for reasons of pragmatism and convenience than for ambitiously and realistically describing the phenomenon under study. Thus a model could have only vague, intuitive connections to the physical phenomenon. Some clear relations from phenomenon to model are of course preferable, since this eases the justification of the model towards the users, but in the end the quality of the model is judged solely by its predictive success. This viewpoint, whereby statisticians finetune parameters of algorithms rather than estimate parameters of models, can of course be adopted also in more traditional frameworks of perhaps one-dimensional

independent or nearly independent realisations of some phenomenon, but is, we feel, particularly relevant for complex spatial problems. Model fitting is frequently made by cross validation based on the available observations. Prediction and classification methods find numerous uses in all sectors of applied statistics.

(iii) Confirmatory statistics is mostly occupied with properties of the underlying phenomenon $\{Y(x): x \in D\}$. It requires a stochastic model which in a stronger sense than with predictive statistics truly reflects the key features of the phenomenon, and model parameters must be interpreted in terms of it. The observations $y(x_i)$ are used to express the significance of these parameters. An example is the test for significant correlation between permeability and porosity in sandstone petroleum reservoirs. The quality of this statement is crucially dependent on the validity of the model. Confirmatory statistics are used primarily in such scientific contexts.

The problems addressed in this article will utilise spatial statistics in a predictive setting. Stochastic modelling constitutes a considerable part of the studies presented. This is necessary in order to integrate the different types of available information for the purpose of prediction or classification. Expert experience often constitutes an important source of information, which sometimes invites Bayesian and empirical Bayesian approaches. The Bayesian formalism has proved useful in pragmatic modelling, and since formal testing is seldom performed the disadvantages of the formalism are seldom exposed. Large data volumes with complicated intercorrelation structures and computer intensive solution algorithms are other characteristics.

1.3. Stochastic modelling. Phenomena that vary in space and/or time are frequently observed in nature. The use of stochastic models and statistics in surveying such phenomena has proven useful. Stochastic modelling constitutes the artistic part of the analysis, and some rules of thumb should be kept in mind. The model formulation must be tailored to the question to be answered. Classification of discrete objects, predictions of a continuous surface, and identification of discontinuities require different model formulations. If extensive knowledge about the phenomenon to be evaluated is available it should be used in the modelling. The scale at which the model is valid has to be specified. Consider a porous medium like sandstone; at micro scale a discrete spatial model based on pores and sand grains would be suitable, while on macro scale porosity could be represented by a continuous spatial model. The amount of available data will also influence the modelling. The problem of overfitting is well recognised in statistics, and in spatial-temporal settings the number of parameters is often large and one encounters redundancies in the data. This makes the problem even more crucial. Bayesian approaches with prior qualified guesses on parameter valuies based on phenomenological information will reduce the problems of overfitting. As previously mentioned data analysis is often complex and efficient model estimators of known form are rarely available in spatial-temporal settings. Hence the possibilities for model verification, and for interpretation of and estimation of parameters, should be taken into consideration when choosing the statistical model.

Spatial problems appear with complex interdependence structures, and a large variety of spatial models can be imagined. In this presentation a division into three natural main model classes has been made, and this corresponds roughly to the three types of models most frequently encountered in spatial statistics literature. The division is into classes of well-defined mathematical objects, but is mainly motivated by the form of real spatial problems and by the form of the available data sources.

(i) Models for continuous random surfaces, say $\{Z(x): x \in D\}$ with $Z(x)$ in some m-dimensional Euclidian space. The model most frequently used is the Gaußian random function model, perhaps after an initial scale-transformation like taking logarithms. It maintains most of the favourable properties from non-spatial models when introducing higher dimensional spatial references. Typical tasks to be carried out include interpolation by estimated conditional expected value $E\{Z(x)|z(x_1),\ldots,z(x_n)\}$ and data-conditional simulation of $\{Z_{\text{sim}}(x): x \in D|z(x_1),\ldots,z(x_n)\}$.

(ii) Models for mosaic phenomena, say $\{L(x): x \in D\}$ with $L(x) \in \{1,\ldots,K\}$. The Markov random fields constitute the most popular class of models, but tesselation techniques are also used. These form an extremely large class of models and only small parts of their potential have been explored. Unfortunately, the nice mathematical properties found in the one-dimensional case are not maintained when higher-dimensional spatial references are introduced. The lack of ordering causes this. Most applications include stochastic simulations, as a means in itself or as some intermediate block, with the Metropolis algorithm or Gibbs sampler providing ways of generating realisations.

(iii) *Models for events-against-background processes*, say $\{(x_1,S_1),\ldots,(x_n,S_n)\}$, in which S_i is a set of attributes assigned to reference location x_i. The models most frequently used are related to the theory of marked point processes. An example could be a simultaneous model for locations and heights of trees in a forest. This model can also be defined in a general manner, but usually only pairwise dependencies of marked points are modelled. Few exact analytical results are available for processes outside the simpler Poisson type ones. Statistical analysis of this type of models is typically carried out through simulation using variations of Ripley–Kelly's spatial birth-and-death algorithm.

1.4. The present article. The material is organised as follows. Section 2 presents a generous list of application examples, sorted into problem areas. The emphasis is on describing problems and modelling ideas, and is not on 'solutions'. The applications have been chosen from a much longer list of projects we have worked on, with fellow statisticians at the Norwegian Computing Centre and surroundings and with clients. We have strived to represent the most important dimensions in this high-dimensional space of all spatial statistics applications. We have partly been guided by the degree of problem-solving success as criterion but also by the methodologically inclined statistician's view of what constitute interesting models and interesting problems. One of our aims is to show to the statistical community the kind of statistical problems that are currently deemed important to user groups. The application examples presented come from projects that are actually paid for by clients. Judging the usefulness of applied statistical models, methods and expertise by the willingness of users to spend money on them is not uninteresting.

Section 3 presents basic methodology, introduces the most useful stochastic models, and discusses ways of analysing them. In particular models for the three main types of phenomena noted above are discussed, as well as a couple of 'combinations' where two different models work together. Four of Section 2's list of applications are returned to in

Section 4 for a more complete and more careful treatment, and suggested solutions to the actual real problems are described. Finally Section 5 gives some concluding remarks and points to some topics for future work.

This is partly a review of several topics in spatial statistics with a broad range of examples. Some basic references about models in and uses of spatial statistics include Matern (1960), Yaglom (1962), Matheron (1973), Journel and Huijbregts (1978), Diggle (1983), Ripley (1981, 1988), Stoyan, Kendall, and Mecke (1987), and Cressie (1991). For the convenience of some readers we point out here what is supposed to be 'new contributions', or perhaps only modest new insights into the use of old methods, in our article: The extended 'conjugate family' analysis for Bayesian Kriging in 3.1.C; some new reliable simulation methods for Gaußian surfaces in 3.1.D; the quasi likelihood method in Section 3.1.E for estimating covariance function parameters; comparison of maximum likelihood and maximum pseudo-likelihood for Markov chains in 3.2.B; the semi-Markov type random field models of 3.2.E; the ways of imposing global constraints on realisations from Markov random fields and marked point processes in Sections 3.2 and 3.4 respectively; and generalisations of Geman and Geman and of Besag methods in image restoration problems with correlated noise, in 3.4. In addition we hope that the ways by which we approach and solve some of the real world problems in Sections 2 and 4 contain some novel ideas in the respective problem areas.

2. Range of applications

In the following a collection of application examples are briefly described. Four of these are returned to in Section 4 for a more complete treatment, leading to suggested solutions to the actual real problems.

2.1. Medical Image Analysis.

2.1.A. Tumor identification [Lundervold, Moen, and Taxt (1988)]. Identification and classification of tumors in the human brain is obviously a problem of great importance. Magnetic resonance equipment provides the possibility for indirect measurement of various characteristics of the brain with three-dimensional spatial references. The data can be collected without surgery, hence minimising the chance of complications. The observations are indirect and the signal to noise ratio is low. A model based on hidden Markov random field theory with Gaußian noise is often used for segmenting the three-dimensional brain into various pathological units. The pathological units are modelled by requiring $p(X_{ij} = k|\text{rest of image})$ to depend upon units in the 5×5 neighbourhood of pixel (i,j) only. Here X_{ij} denotes pathological unit type at pixel (i,j). The noise component is usually of the white noise type, or it may be spatially auto-correlated within some neighbourhood. See Sections 3.2 and 3.4. Usually no direct observations will be available, which means that unsupervised classification of the units must be made. Spatial models are required because of the areal extent of the pathological units and the spatially correlated noise.

Experiences with medical image analysis have so far been encouraging, and the methods will hopefully be in commercial use in the near future. From a statistical point of view the traditional Markov random field theory has several shortcomings as a model for the pathological units. The problem surfaces in parameter estimation, where good estimators for model parameters are hard to construct. Further studies of other models that are more directably suitable for segmentation are needed.

2.1.B. Identification of heart dysfunction [Taxt, Lundervold, and Angelsen (1990), Storvik and Switzer (1992)]. Heart defects may appear as reduction in pumping capacity, reduced volume pumped, and as decline in elasticity of the heart walls. The dynamic behaviour of the heart can be observed by repeated three-dimensional grey-tone ultrasound images at 25–35 Hz. The signal-to-noise ratio in each image is normally very poor, hence the time repetitions must be utilised. See Section 4.2 for further discussion.

2.1.C. Noise reduction in Nuclear Magnetic Resonance imaging [Godtliebsen (1989)]. The common technique for reducing noise in NMR images is to take several measurements on the same slice and then average. This is time-consuming, expensive, and the patients sometimes move during acquisition time, thereby introducing additional noise. Hence a natural challenge is to devise statistical noise reduction algorithms that work on a single slice. One approach is to model the observed image as $y_i = x_i + \varepsilon_i$ in pixel i, where the collection of x_i's come from some Markov random field and the ε_i's are independent Gaußian zero mean noise. Studies indicate that the latter assumption is quite acceptable. The Markov random field assumption is less realistic, but can be used to derive image enhancement and image noise reduction techniques. Examples of such methods are in Section 3.4. Another method which can be motivated by the model assumptions is to replace observed grey level in a pixel with some weighted average of grey levels over the pixel and neigbouring pixels, with weights determined by the spread of the local data. This can be done in a suitable empirical Bayesian fashion. The study found that sound statistical techniques were able to reduce noise in a single picture with a factor of about three. This particular study was unusual in that a good approximation to the 'true scene' was available, taken to be the average of eight consecutive images of the same slice. Accordingly measures of restoration performance could be proposed and compared for different image analysis methods.

2.2. Pollution Monitoring.

2.2.A. Status of forest [Strand (1989)]. The decline in the quality of forest may be linked to increased pollution, and the Norwegian authorities have initiated an extensive sampling program. Sampling takes place in more than 2000 sites in a regular $9 \times 9\,\mathrm{km}^2$ grid over Norway every second year. Each site is $100\,\mathrm{m}^2$ and each tree is located and characteristics like age, size, top density are sampled. The general environment at each site is also carefully sampled. A spatial regression model is used to analyse the data, see Section 3.1. The model is $S(x) = \sum_{i=1}^{p} \beta_i f_i(x) + \varepsilon(x)$, where $S(x)$ is some variable representing status of forest and the $f_i(x)$'s are known explanatory regressor functions like elevation, soil quality etc. The residuals $\varepsilon(x)$ are treated as a random function and its regional properties are evaluated in order to find differences due to unexplained factors, which could include air pollution. The data analysis exposes reasonably large regional differences, which at this stage is believed to be linked to pollution level. An extended analysis is planned.

2.2.B. Air quality [Halvorsen and Strand (1987), Høst, Omre, and Switzer (1991)]. The decline in air quality over Europe is a problem of concern. There are several sources for the pollution, which is transported over long distances. Its solution calls for international cooperation. The European Meteorological Environment Program has established more than one hundred monitoring stations all over Europe. The air quality is characterised by the volume content of several chemical components, particle density, etc. Sampling is made on a daily basis. Consequently the pollution monitoring can be considered as a time- and space problem, and one approach for evaluation of the problem is further discussed in Section 4.4.

2.2.C. Combining satellite data with field data in pollution monitoring [Høst, Omre, and Sæbø (1991)]. Some water quality variables from the Hvaler area in Norway have been analysed on the basis of both hard-to-get direct measurements and easy-to-get satellite data. The satellite data are abundant but of course very 'indirect', having a small positive correlation with the water quality variables. The challenge is to build a model that makes it possible to integrate these very different data types. On the basis of a validated model a map of the estimated water quality was produced, along with a map of the estimated uncertainty of the estimate.

2.3. Reservoir Characterisation.

2.3.A. Seismic Depth conversion [Omre, Halvorsen, and Berteig (1989), Abrahamsen, Omre, and Lia (1991), Abrahamsen (1992)]. The petroleum is usually trapped under a geologic horizon having non-permeable characteristics, for example shale. Fortunately, these types of horizons can also be identified from seismic data. The sesmic data have good spatial coverage and consist of two-way reflection times down to the horizon. Note that the unit here is time, while the geologists are interested in depth to the horizon. By using depth observations in a small number of wells, seismic reflection time data and basic laws of physics, a model for depth conversion can be constructed. This is further discussed in Section 4.1.

2.3.B. Simulation of facies architecture [Clemetsen, Hurst, Knarud, and Omre (1989), Hjort, Holden, and Omre (1989), Høiberg, Omre, and Tjelmeland (1989, 1990), Omre (1992), Georgsen and Omre (1992), Tjelmeland and Holden (1992)]. The petroleum reservoirs in the North Sea appear as heterogeneous in the sense that several units of good and poor quality are packed. The units usually correspond to different rock types or facies. Their packing is according to certain geologic processes. The heterogeneity in the reservoirs has proven to have large impact on the production potential.

The facies architecture is a consequence of the geologic processes, the dynamics of which are partly understood by the geologists. This constitutes the primary base for the modelling. The facies distribution can be observed in the wells, and this provides constraints on the model. Both Markov random fields and marked point processes have been used in modelling the facies architecture, see Sections 3.2 and 3.3. The former model postulates that $p(X_{ij} = k|\text{all other facies})$ is only dependent upon the neighbourhood facies, with X_{ij} facies type in pixel location (i, j) and $k \in \{1, \ldots, K\}$ facies type. Sometimes there are as many as $K = 12$ facies types on the scene. Simulations of pseudo-reality constrained by some known values of x_{kl} are required. Simulation procedures from recent literature seem to converge very slowly, and exploring their properties is a difficult and time-consuming task. The marked point process traditionally applied has density of the form $f_n(m_1, \dots, m_n) = \text{const.} \exp\{-\sum_{i=1}^{n} b(m_i) - \sum_{i<j} c(m_i, m_j)\}$, with m_i's being the marked points with information on location, size, shape, and facies characteristics. Often global constraints are necessary, and simulated realisations are pushed in the wished for direction by certain tricks. New model formulations of the 'semi-Markov' process type have also been studied and seem promising. In order to evaluate the impact of the heterogeneity on the production of petroleum, simulations of fluid flow are performed on realisations of the facies architecture.

2.3.C. Simulation of fractures and faults [Omre and Sølna (1990), Omre, Sølna, Dahl, and Tørudbakken (1992)]. The petroleum reservoirs in the North Sea are of sedimentary origin, and they have been changed by considerable tectonic activity. This has forced a complicated fracture and fault pattern on to the reservoirs. The location of large fault zones, i.e. those with offset above 10 m, can be observed on the seismic data. The actual break pattern in the zone has been studied by geologists and is found to consist of swarms of smaller faults. This hetereogeneity is important for fluid flow. A more thorough presentation of the problem and model appear in Section 4.3.

2.3.D. Interpretation of well log data [Bølviken and Helgeland (1989), Bølviken, Helgeland, and Storvik (1991)]. The petroleum reservoirs in the North Sea are located at a depth of approximately 3000 m. Wells are drilled to penetrate the reservoir in order to collect information about its characteristics. Few direct observations are available even in the wells. Logging tools are lowered down the well, however, and indirect measurements of radioactivity, acoustic reflection, conductivity etc., are collected every .25 m in the reservoir zone. From these data the geologists would like to infer the geologic environment from which the reservoir originates. This entails determining the geologic sequences or sequence of rock types down the wells. The problem can be considered as a spatial segmentation problem based on multivariate data from the log tools.

The model is based on hidden and in fact even on hidden hidden Markov random processes with Gaußian noise, see Sections 3.1 and 3.4. There are three ordered stages in the evaluation, say $S \to L \to X$, with sedimentary processes S creating a sequence of lithofacies L which again influence the responses of the logs X. The corner stone in the model used is that the unobservable part (S, L) has been generated by a Markov process while L can be observed with white Gaußian noise through X. The geological processes makes some sequences more probable a priori than others, hence a Bayesian dimension is added to the model. A general model has been constructed and is expected to be widely applicable, but the set of parameters must be reservoir specific, and has to be estimated for each reservoir.

2.4. Sea Resources.

2.4.A. Stock of capelin [Hjort and Murray (1912), Omre and Sølna (1990)]. The fisheries in Norway are important for employment in the western and northern parts of the country and for the national export volume. The fish resources are renewable, but the reproduction cycle varies among the species. For capelin it is approximately four years in the Barent Sea. While capelin is a consumer of low level organisms like plancton it is being predated by cod in the winter season. The migration of capelin south to the Norwegian coast for spawning in winter causes the contact with cod. Both capelin and cod are of commercial value, hence a multi-species catching strategy is required.

There are surprising amounts of data available. Acoustic data, indirectly observing the echo-sounding reflected by fish with a three-dimensional reference, is abundant. There are thrawl samples as well. For several thousand capelin multi-dimensional observations of age, length, weight, stadium, etc. with space-time references are available each year. For large amounts of cod stomach content has been analysed with respect to fraction and volume of capelin. Presently only single-species models are operable, and time is the only reference variable. Multi-species models between capelin/cod are being developed, and both time and space references are discussed. It is at present problematic to verify a significant interaction between the two species based on available observations. A reliable space-time model for the species would compensate for some of the time and space variability, and may contribute to a more reliable analysis. Work is in progress on such matters.

2.4.B. Stock of Minke whale [Schweder, Øien, and Høst (1990), Schweder and Høst (1991)]. Minke whales have been considered an endangered species and have been protected by the International Whaling Commission since 1986. The Norwegian authorities have during the last few years performed surveys in order to estimate the size of the stock. 'Official estimates' have been suprisingly low compared to historical catch successes. A serious downward bias is expected in the predictions since these have been based on the assumption of complete sampling in the surveyed areas. Due to the fact that each whale surfaces only about 30 times per hour and that they can be difficult to detect in rough sea the actual detection success rate for whales passing close to the survey vessel, $g(0)$, is probably significantly smaller than 1.

There are two stochastic elements in the final estimator of the population size. One is the hazard probability $Q(x, r)$, the probability of sighting a whale surfacing at polar coordinates (x, r) relative to the vessel, given that the whale has not been observed before. The parametric form of $Q(x, r)$ is a subject of continued discussion. Its parameters can be estimated from data provided by test surveys where two vessels were run in parallell and covered the same area. The second random element is the surfacing frequency for whales. This has been reproduced by simulation from a spatial Poisson. From this model the sampling success rate $g(0)$ was found to be approximately 0.5, which means that about one out of two whales were observed. Thus the predicted number of whales is about twice as large as first anticipated.

Methods developed here are partly of a general nature, and aim at being able to integrate very different types of data (viz. 'micro' and 'macro' data) in a consistent and meaningful framework. They should find applications in other areas as well.

2.5. Other areas of application.

2.5.A. Mapping of seabed: Spatial sampling strategy to find all shallow areas [Helgeland, Hjort, and Sæbø (1984)]. Let $Z(x)$ be depth to the seabed in geographical location x. Mapping of $Z(x)$ based on point sampling is another problem of spatial interpolation, see Section 3.1. Suppose however that it is considered important to find all shallow banks, say where $Z(x)$ is smaller than some level u. Term sets of the type $\{x: Z(x) < u\}$ by Z_u-areas. A question of spatial sampling strategy is therefore: what is a good regime for detecting all Z_u-areas, and what is the probability of not detecting such an area? A solution based on approximate shapes of excursion sets for Gaußian random fields is given in the above reference.

2.5.B. Automatic recognition of handwritten symbols [Hjort (1986), Hjort and Taxt (1988), Pripp (1991)]. Automatic recognition of printed or handwritten symbols is an established field with several well-explored approaches. Among these are several which are statistical in nature. The usual method comprises two main steps. The first is to extract a feature vector for the symbols, typically of dimension 10 or less. The second is to model the behaviour of feature vectors for each symbol type, and then estimate parameters, perhaps in cheap semi-automatic ways. Finally statistical discriminant analysis is used on future symbols.

A more direct approach would be to model the statistical behaviour of the symbols themselves. We have some experience with modelling the boundaries of symbols as random closed curves in the plane, giving rather successful rates of correct classification. This is perhaps not a genuine spatial example since we merely model one-dimensional objects. But the following approach is spatial. Suppose the candidate symbol is digitised to form 0's and 1's on a rectangular grid. Thus a hand-drawn '8' could be digitised on a 20×20 grid and be represented by the resulting collection of 400 0's and 1's. Then a possibility is to model the mosaic process of 1's on this lattice as a Markov random field, see Section 3.2. Each symbol class (say a hand-written '8') has its own mrf specification of the conditional probability of having a '1' in pixel location (i, j), given the rest of the image. It is of a certain form involving various 'award functions' designated by the modeller to encourage or discencourage certain types of local behaviour, and various parameters, some of which may be class-dependent and may vary over the scene. It is sometimes fruitful to impose global constraints too. The mrf parameters can be estimated from data by maximising the product of individual pseudo-likelihoods, see Section 3.2. Finally the estimated models are used to construct a classifier.

2.5.C. Meteorology: Combining new satellite data with other information sources to improve prognoses [Homleid (1992)]. The Norwegian Institute of Meteorology uses two numerical weather prognosis models for the atmosphere. Input data for such models are observations from ships, radio buoys and sondes, and land based stations. One is also interested in exploiting satellite data, for example temperature and humidity profiles processed from the TOVS satellite, to build better models for prognosis. Several methods have been tried out but so far the results are not convincingly better. One is currently exploring better ways of combining these very different data sources. The task seems to require (i) simply assessing the current data quality from the satellite, (ii) constructing a successful spatial-temporal statistical model, drawing on both meteorology physics and empirical statistics, (iii) estimating necessary parameters and implementing prognosis formulas, and (iv) evaluating the performance compared to existing methods. Although satellite data obviously add important information to the problem, the improvements in prognosis quality by their inclusion seems to be rather small with the existing prognosis techniques. Research that aims at refining the statistical model formulations, and at a better statistical understanding of why the current improvements are so small, are under way.

3. Theoretical tools

This section presents basic statistical theory that has been developed to solve problems like those listed in Section 2. As mentioned above a fruitful division of the various stochastic processes encountered is into continuous random surfaces, finitely-valued or mosaic phenomena, and events-against-background processes. Subsections 1, 2, 3 study these three basic types. In many problems different data sources may have to be combined, and some combination or other of the three basic model types is called for. Some situations of this sort are discussed in 3.4.

3.1. Continuous random surfaces. The simplest spatial statistical model capable of describing interesting continuous or near continuous random surfaces is one with some smooth trend surface plus a spatially correlated Gaußian residual process. This model is introduced in the course of 3.1.A below. Various aspects of such models are discussed, including theory for spatial interpolation, Bayesian Kriging, simulation, and for estimating parameters in spatial covariance functions.

3.1.A. The basic model. Let $z = z(x)$ be a continuous or nearly continuous surface defined over some domain D of x-values, for example a rectangle in the plane. Suppose $z(x_i)$-data on $z(.)$ are collected in n distinct locations $x_1, \dots, x_n$, and that some problem of interest can be phrased in terms of $z(.)$, like that of spatial interpolation. The spatial statistical way of approaching such problems is to view $z(.)$ as a realisation of a stochastic process $Z(.)$. The idea is to translate prior knowledge to a suitable class of models for $Z(.)$, typically viewed as a smooth trend surface plus spatially correlated residual, use data to estimate parameters, and answer the original $z(.)$-question under the model assumption and given all available information. To be specific, suppose that $Z(.)$ is Gaußian with regression type trend surface plus zero mean Gaußian residual, say

$$Z(x) = m(x, \beta) + \varepsilon(x) = \sum_{j=1}^{p} \beta_j f_j(x) + \varepsilon(x), \tag{3.1}$$

where the $f_j(x)$'s are known regressor functions ($f_1(x)$ would typically be the constant 1), the β_j's are coefficient parameters, and where the covariance function

$$\mathrm{cov}\{Z(x), Z(y)\} = \mathrm{cov}\{\varepsilon(x), \varepsilon(y)\} = \sigma^2 K(x, y) \tag{3.2}$$

describes the variability and the degree of spatial continuity of the residual process. One often postulates shift invariance, so that $K(x, y)$ is of the form $K_0(x - y)$ for appropriate $K_0(.)$ function, and in such cases it is convenient to choose $K(x, x) = K_0(0) = 1$ so that $\mathrm{Var}\, Z(x) = \sigma^2$. The random function is isotropic if in addition $K(x, y)$ only depends on the distance $\|x - y\|$, as in the popular case $K(x, y) = \exp\{-c\|x - y\|\}$.

At this point it is worth noting that the covariance function is only defined when $Z(x)$ has finite variance. A richer class of measures for second order spatial characteristics is the so-called semi-variogram

$$\gamma(x, y) = \tfrac{1}{2}\mathrm{Var}\{Z(x) - Z(y)\}, \tag{3.3}$$

which requires only the variances of differences to be finite. When K is shift invariant and $\operatorname{Var} Z(x) = \sigma^2 < \infty$ one has $\gamma(x,y) = \sigma^2\{1 - K(x,y)\}$. The idea of and value of requiring finite variances of only certain linear combinations of $Z(.)$ is developed in the theory of intrinsic random functions, see remarks at the end of this section. The possible choices for semi-variogram functions are linked to the choice of p and $f_j(x)$'s together with the requirement of producing nonnegative prediction variances; see also remarks below. We have chosen to present most of the general Gaußian random function theory in terms of spatial covariance functions.

3.1.B. Spatial interpolation by universal Kriging, and its precision. Suppose interpolation is called for. Let x be a new location point, and let us follow the program above. Under the Gaußian assumption

$$\begin{pmatrix} Z(x) \\ Z_{\text{dat}} \end{pmatrix} \sim N_{n+1}\Big\{\begin{pmatrix} f(x)'\beta \\ F\beta \end{pmatrix}, \sigma^2 \begin{pmatrix} K(x,x) & k' \\ k & K \end{pmatrix}\Big\},$$

in which K is the $n \times n$ matrix of $K(x_i, x_j)$, k and Z_{dat} are the vectors with components respectively $K(x, x_i)$ and $Z(x_i)$, and finally F is the $n \times p$ matrix whose i'th row is $f(x_i)' = (f_1(x_i), \ldots, f_p(x_i))$. Hence

$$Z(x)|\text{data} \sim N\{m(x,\beta) + k'K^{-1}(Z_{\text{dat}} - m(\beta)), \sigma^2(K(x,x) - k'K^{-1}k)\},$$

writing $m(\beta)$ for the vector of $m(x_i, \beta)$. Of course $m(\beta) = F\beta$ in the present case, but the notation is meant to suggest its natural generalisation to other regression functions.

Specification and estimation of $K(.,.)$ is discussed in 3.1.E below. Suppose for now that a covariance function has been decided on. The natural estimator of β then emerges by minimising $(Z_{\text{dat}} - F\beta)'K^{-1}(Z_{\text{dat}} - F\beta)$. This is the weighted least squares as well as the maximum likehood principle, when the covariance function is assumed known. The result is

$$\widehat{\beta} = HF'K^{-1}Z_{\text{dat}} \quad \text{where } H = (F'K^{-1}F)^{-1},$$

constituting an unbiased estimator with covariance matrix $\sigma^2 H$. The spatial interpolator used in the end is the estimated mean value of $Z(x)$ given the data, that is

$$\widehat{Z}(x) = m(x, \widehat{\beta}) + k'K^{-1}(Z_{\text{dat}} - m(\widehat{\beta})) = f(x)'\widehat{\beta} + k'K^{-1}(Z_{\text{dat}} - F\widehat{\beta}). \tag{3.4}$$

Note that it is unbiased predictor in the sense of having $E\{\widehat{Z}(x) - Z(x)\} = 0$. The interpolation variance, or prediction error, can be shown to be

$$\begin{aligned} \sigma_{\text{pe}}(x)^2 &= E\{\widehat{Z}(x) - Z(x)\}^2 \\ &= \sigma^2\big[K(x,x) - k'K^{-1}k + (f(x) - F'K^{-1}k)'H(f(x) - F'K^{-1}k)\big]. \end{aligned} \tag{3.5}$$

Note that the mean squared error is computed w.r.t. (the random) $Z(x)$ and not its mean value $f(x)'\beta$, since the intention is to guess $Z(x)$ for the surface under study and not its trend surface. In particular $\sigma_{\text{pe}}(x)^2$ is not the same as $\operatorname{Var} \widehat{Z}(x)$.

The interpolator (3.4) is itself independent of the scale factor σ^2, which however is needed to assess the uncertainty as in (3.5). To estimate σ^2, when some covariance structure $K(.)$ has been decided on, note that $Z_{\rm dat} - F\widehat{\beta}$ has variance matrix $\sigma^2(K - FHF')$, from which it follows that $Q(\widehat{\beta}) = (Z_{\rm dat} - F\widehat{\beta})'K^{-1}(Z_{\rm dat} - F\widehat{\beta})$ has mean value equal to σ^2 times the trace of $K^{-1}(K - FHF')$, which is $\mathrm{Tr}(I_n - HF'K^{-1}F) = \mathrm{Tr}(I_n - I_p) = n - p$ by usual tricks. Thus $Q(\widehat{\beta})/(n-p)$ is unbiased, even in the present setting with correlated data. The maximum likelihood solution, trusting normality, is $\widehat{\sigma}^2 = Q(\widehat{\beta})/n$. We should stress that σ^2 and $K(.)$ are defined 'together' and should be estimated together. Modelling and estimating $K(.)$ is the harder task, see 3.1.E below; σ can be estimated as just described for given $K(.)$. It is also usual in geostatistics to estimate σ^2 by cross validation techniques, see Davis (1973) and Solow (1990).

Spatial interpolation of a random function with drift can be considered from a somewhat different perspective as well, that of choosing an optimal linear combination, under different assumptions about spatial smoothness. Consider the interpolator $Z^*(x_0) = \sum_{i=1}^n c_i Z(x_i)$ at point $x = x_0$, where the weights c_i are to be determined. Unbiasedness, in the sense of $E\{Z^*(x_0) - Z(x_0)\} = 0$, is ensured by the constraints $\sum_{i=1}^n c_i f_j(x_i) = f_j(x_0)$ for $j = 1, \ldots, p$. A natural avenue is to minimise the interpolation variance $\mathrm{Var}\{Z^*(x_0) - Z(x_0)\}$ under these constraints. This may be formulated as minimising $\mathrm{Var}\sum_{i=0}^n c_i Z(x_i)$ under $\sum_{i=0}^n c_i f_j(x_i) = 0$, $j = 1, \ldots, p$, where $c_0 = -1$, and the task is solved by the Lagrange technique. The result is in fact $\widehat{Z}(x)$ of (3.4), and this Lagrangian way of deriving it is the usual one in the geostatistics tradition. It is the called the universal Kriging interpolator, see for example Journel and Huijbregts (1978). Note that the Gaußian assumption, which was used to reach (3.4), is unnecessary in this construction.

One sometimes uses (3.4), in that form or computed by constrained minimisation, with $K(x, y)$ functions that are not genuine nonnegative definite covariance functions. The minimum requirements on the K function for guaranteeing nonnegative interpolation variances are that

$$\mathrm{Var}\sum_{i=0}^n c_i Z(x_i) = \sum_{i=0}^n \sum_{l=0}^n c_i c_j K(x_i - x_j) = \begin{pmatrix} -1 \\ c \end{pmatrix}' \begin{pmatrix} 1 & k' \\ k & K \end{pmatrix} \begin{pmatrix} -1 \\ c \end{pmatrix} \geq 0$$

for all $x_0, x_1, \ldots, x_n$ and all $c_1, \ldots, c_n$ satisfying the $\sum_{i=0}^n c_i f_j(x_i) = 0$ constraints above. It is assumed here that $K(x, y) = K(x - y)$.

Consider cases for which $f_1(x)$ is the constant 1, i.e. the trend surface contains a constant β_1, and $\sum_{i=1}^n c_i = 1$ among other constraints. Nonnegative interpolation variances are ensured by $c'Kc \geq 0$ for all c vectors obeying certain constraints, where K is the matrix of $K(x_i - x_j)$. In terms of the semi-variogram function (3.3) the criterion becomes $c'\Gamma c \leq 0$ with constraints on c, where Γ is the matrix of $\gamma(x_i - x_j)$.

Assume in particular that the regressor functions $f_j(x)$ are polynomials in the coordinates of x, of order k or less. The random functions having this property are called 'generalised intrinsic functions of order k', and the associated function $K(.)$ is termed 'generalised covariance function of order k'. It is clear that this class of generalised covariance functions is larger than the class of simply nonnegative definite functions.

By enforcing stronger assumptions on the form of the expected value one can choose among a larger class of generalised covariance functons. This approach to spatial interpolation is widely used in the geostatistics school, see Matheron (1973). It resembles the 'integration approach' used in time series analysis, see Box and Jenkins (1976). It can be shown, however, that interpolations based on assumptions of intrinsic random function hypotheses, of any given order k, are equivalent to those obtained from an appropriate universal Kriging with a Gaußian random function model, see Christensen (1990).

REMARKS. (i) A sound implementation is vital here, since inverting large matrices can be slow and unstable if done directly. Rather than using the mathematically and statistically informative (3.4) and (3.5) a good interpolation package would typically use derived formulae from Choleski triangularisation; see for example Ripley (1981, Section 4.4). (ii) One valid variogram function, among others, is

$$\gamma(h) = \sigma^2 h^{2H}, \quad \sigma > 0, \quad 0 \leq H < 1.$$

This family of variogram functions is said to have affine similarity properties and are used to model fractal phenomena, see for example Feder (1988). The H constant is called the Hurst exponent. The Brownian motion process in one dimension is of this type, with $H = \frac{1}{2}$. (iii) Note that $\widehat{Z}(x_i) = z(x_i)$ and $\sigma^2_{\mathrm{pe}}(x_i) = 0$, that is, the interpolator respects the data points. This is as it should be, since the real interest is interpolation of the actual $z(.)$, rather than its underlying trend surface. In applications of classical nonparametric regression the problem is typically the opposite one of estimating the smooth trend, based on unrelated realisations at different locations. (iv) In locations x far from all sampled x_i's the interpolator is close to the trend estimate $m(x, \widehat{\beta})$. (v) More robust estimates than the least squares $\widehat{\beta}$ could be used as well, without seriously affecting the reasoning or the results. The same remark applies also to more general forms for $m(x, \beta)$ than the linear one; $\exp(\beta' x)$ is a case in point. (vi) The geostatistical Kriging techniques have been extended to cover multivariate cases, see for example the so-called co-Kriging method of Journel and Huijbregts (1978). Another extension is called factorial Kriging, see Sandjivy (1984), consisting in separating a random function into smoothly varying trend and a correlated residual term. (vii) The term Kriging was originally used for linear predictors, i.e. linear in the data points $Z(x_i)$. A couple of nonlinear predictors have also adopted the Kriging term, however. Disjunctive Kriging is based on a Hermitean expansion of the bivariate characteristics of the random function, thereby extending the familiar correlation framework, see Matheron (1976). Indicator Kriging is based on a discretisation of the univariate variable into a set of linear combinations of indicator variables, hence providing estimates of the fractiles of the conditional distribution, see Journel (1983). (viii) Markovian properties of Gaußian random functions in the onedimensional case are easily defined and well understood. There are unexpected difficulties with the different possible definitions of Markovness in higher dimensions, however, and some of these lead to too restricted classes. See Adler (1981, Appendix) for a review.

3.1.C. Bayesian Kriging. In some situations there is rather too little data to do interpolation like above with the wished for precision, but there is some prior knowledge about the trend surface. This invites Bayesian and empirical Bayesian considerations. The following treatment partly extends that of Omre (1987) and Omre and Halvorsen (1989). Other relevant references are Pilz (1990) and Le and Zidek (1991).

Let the model be as in (3.1) and (3.2) conditionally on β, and suppose β is given some Gaußian prior distribution, which we parameterise as $N_p\{\beta_0, \sigma^2 T\}$. For the moment we take σ^2 to be known. The joint distribution of β and data Z_{dat} is easily found to be

$$\begin{pmatrix} \beta \\ Z_{\text{dat}} \end{pmatrix} \sim N_{p+n}\Big\{\begin{pmatrix} \beta_0 \\ F\beta_0 \end{pmatrix}, \sigma^2 \begin{pmatrix} T & TF' \\ FT & K + FTF' \end{pmatrix}\Big\}.$$

In particular the posterior distribution of β is still normal. After using the convenient matrix identity $(K + FTF')^{-1} = K^{-1} - K^{-1}FG_T F'K^{-1}$, where $G_T = (H^{-1} + T^{-1})^{-1}$, one finds

$$\begin{aligned} \widetilde{\beta} = E\{\beta|\text{data}\} &= \beta_0 + TF'(K + FTF')^{-1}(Z_{\text{dat}} - F\beta_0) \\ &= G_T H^{-1}\widehat{\beta} + (I - G_T H^{-1})\beta_0, \\ \text{VAR}\{\beta|\text{data}\} &= \sigma^2\{T - TF'(K + FTF')^{-1}FT\} \\ &= \sigma^2(I - G_T H^{-1})T. \end{aligned} \tag{3.6}$$

Note that the Bayes estimator $\widetilde{\beta}$ is a combination of the prior guess β_0 and the usual estimate $\widehat{\beta}$. Note also that in the case of a flat prior, which corresponds to moving the elements of T so that its eigenvalues tend to infinity, then $G_T H^{-1} \doteq I - HT^{-1}$, in particular G_T tends to H, $\widetilde{\beta}$ tends to $\widehat{\beta}$, and VAR$\{\beta|\text{data}\}$ becomes $\sigma^2 H$.

This is information of value, but the imminent interest is interpolation and its uncertainty. We find

$$\begin{pmatrix} Z(x) \\ Z_{\text{dat}} \end{pmatrix} \sim N_{n+1}\Big\{\begin{pmatrix} f(x)'\beta_0 \\ F\beta_0 \end{pmatrix}, \sigma^2 \begin{pmatrix} K(x,x) + f(x)'Tf(x), & (k + FTf(x))' \\ k + FTf(x), & K + FTF' \end{pmatrix}\Big\}.$$

Our Bayesian Kriger becomes

$$\begin{aligned} \widehat{Z}_B(x) = E\{Z(x)|\text{data}\} &= f(x)'\beta_0 + (k + FTf(x))'(K + FTF')^{-1}(Z_{\text{dat}} - F\beta_0) \\ &= f(x)'\widetilde{\beta} + k'K^{-1}(Z_{\text{dat}} - F\widetilde{\beta}), \end{aligned} \tag{3.7}$$

with associated Bayesian prediction error

$$\begin{aligned} \sigma_{\text{be}}(x)^2 &= E\{(\widehat{Z}_B(x) - Z(x))^2|\text{data}\} \\ &= \text{Var}\{Z(x)|\text{data}\} \\ &= \sigma^2\big[K(x,x) + f(x)'Tf(x) - (k + FTf(x))'(K + FTF')^{-1}(k + FTf(x))\big]. \end{aligned} \tag{3.8}$$

Again there is a natural correspondence for a flat prior, in that the Bayesian interpolator converges to $\widehat{Z}(x)$ when the covariance matrix T for the β prior tends to infinity, and $\sigma_{\text{be}}(x)$ tends to $\sigma_{\text{pe}}(x)$. More informatively, calculations show that

$$\widehat{Z}_B(x) = \widehat{Z}(x) - (f(x) - F'K^{-1}k)'(I - G_T H^{-1})(\widehat{\beta} - \beta_0),$$

and $G_T H^{-1}$ is close to $I - HT^{-1}$ when T is large compared to H. This means that in situations where T is large (vague prior information) and/or $\widehat{\beta}$ is close to β_0 (good prior guess) the Bayesian and the traditional viewpoints lead to the same quantitative results, regarding interpolator and prediction variance, but with two quite different perspectives. Many statisticians have learned from experience that users very often prefer and relate better to the Bayesian interpretation.

The case of $T = 0$ corresponds to certainty about trend surface $f(x)'\beta = f(x)'\beta_0$, and $\widehat{Z}_B(x) = f(x)'\beta_0 + k'K^{-1}(Z_{\text{dat}} - F\beta_0)$ is as in so-called simple Kriging with known trend. The other extreme is when T is very large, corresponding to prior ignorance about β, where $\widehat{Z}_B(x)$ becomes as in universal Kriging. There is accordingly a 'Bayesian bridge' from simple to universal kriging.

The Bayesian apparatus becomes more useful and flexible when uncertainty about the scale factor σ^2 is modelled as well. The mathematically simplest Bayesian solution is the following: Suppose the prior distribution for (σ^2, β) is such that $\sigma^2 \sim$ inverse gamma (α, γ) and $\beta | \sigma^2 \sim N_p\{\beta_0, \sigma^2 T\}$, i.e.

$$(\sigma^2, \beta) \sim \text{const.}\,(1/\sigma^2)^{\alpha+1} \exp(-\gamma/\sigma^2)\,\sigma^{-p} \exp\{-\tfrac{1}{2}(\beta - \beta_0)'T^{-1}(\beta - \beta_0)/\sigma^2\}.$$

Then calculations show that (σ^2, β) given data Z_{dat} is exactly of the same type, but with updated parameters:

$$(\sigma^2, \beta)|\text{data} \sim \text{inverse gamma}(\widetilde{\alpha}, \widetilde{\gamma}) \times N_p\{\widetilde{\beta}, \sigma^2 G_T\}.$$

Here $\widetilde{\alpha} = \alpha + \frac{1}{2}n$ and $\widetilde{\gamma} = \gamma + \frac{1}{2}n\widehat{\sigma}^2 + \frac{1}{2}(\widehat{\beta} - \beta_0)'L_T(\widehat{\beta} - \beta_0)$, writing $\widehat{\sigma}^2 = (Z_{\text{dat}} - F\widehat{\beta})'K^{-1}(Z_{\text{dat}} - F\widehat{\beta})/n$ for the non-Bayesian estimator and $L_T = T^{-1}G_T H^{-1}$. In particular the Bayesian predictor is as in (3.7) above, and the Bayes estimate of σ^2 is

$$\widetilde{\sigma}^2 = E\{\sigma^2|\text{data}\} = \frac{\alpha - 1}{\alpha - 1 + n/2}\sigma_0^2 + \frac{n/2}{\alpha - 1 + n/2}\{\widehat{\sigma}^2 + (\widehat{\beta} - \beta_0)'L_T(\widehat{\beta} - \beta_0)/n\},$$

where $\sigma_0^2 = E\sigma^2 = \gamma/(\alpha - 1)$ is the prior guess value. The Bayesian prediction error is as in (3.8) but with $\widetilde{\sigma}^2$ replacing σ^2.

Once more the traditional methods emerge in the limiting case of vague Bayesian ignorance, which here corresponds to $\alpha \to 1$, $\gamma \to 0$, and $T \to \infty$.

3.1.D. Simulation. Suppose a simulated realisation $Z_s(.)$ of a fully specified Gaußian random function is needed, perhaps conditioned on some observed values. First of all this means in practice that $Z_s(x)$ is to be simulated on some dense finite lattice of points only. Hence the problem seems simple, since textbooks on multivariate statistics give answers to such questions in terms of simple linear algebra. Such direct methods must involve matrix inversion, perhaps via Cholesky decomposition, and work well on good computers if the dimension of the problem is less than 3000. But in many spatial problems the grid net contains more than 10^6 points, and in such cases smarter simulation algorithms are called for.

One general approach to conditional simulation of the residual process $Z_r(x) = Z(x) - m(x, \beta)$, with associated residual observations $Z_r(x_i) = Z(x_i) - m(x_i, \beta)$ for $i = 1, \ldots, n$, is by decomposition. Let $Z_r(x) = \widehat{Z}_r(x) + \{Z_0(x) - \widehat{Z}_0(x)\}$, with $\widehat{Z}_r(.)$ the simple Kriging predictor based on the observations, $Z_0(.)$ an arbitrary random function with characteristics identical to $Z_r(x)$, and $\widehat{Z}_0(x)$ the simple Kriging predictor based on $Z_0(x_i)$-data. From the orthogonality of $Z_r(.)$ and $\widehat{Z}_r(.)$ it is easy to see that the decomposition is correct. Using this trick it suffices to simulate a random function with zero mean and covariance function $K(x,y)$ unconditionally.

The 'turning band' procedure of Matheron (1973) provides a general tool for simulating random functions with a specified covariance structure. Several procedures working in the spectral domain are also available, see Ripley (1986, Ch. 4).

Spatial and spatial-temporal problems often require simulation on extremely large grid nets, for which the procedures mentioned above will be too slow, even on very fast machines. In Omre, Sølna, and Tjelmeland (1992) some very fast procedures for simulating random functions are presented and evaluated. The procedures use Markov characteristics valid in one dimension and generalise the idea to higher dimensions. The traditional procedures for simulation of fractal processes, see Feder (1988), are in the same spirit. The screening sequential procedure defined in Omre, Sølna, and Tjelmeland (1992) is considerably more reliable than the traditional fractal procedures, however, albeit somewhat slower.

3.1.E. Estimating the covariance function. A point of some importance which has attracted renewed interest recently is that of the specification and estimation of the covariance function K. In the geostatistics tradition the K function has typically been regarded as 'given and fixed' once 'guessed at', which results in underestimation of interpolation variance, and, sometimes, suboptimal interpolation. Observe that the definition of and the interpretation of K and σ^2 in (3.2) are dependent upon the chosen regression surface model. If one adds a term to a previous regression trend, then K and σ^2 have changed meanings, and σ^2 will in fact tend to be smaller.

Consequences of using incorrect covariance functions have recently been studied by Watkins and Al-Bouitiahi (1990) and Stein (1990a, b). Various methods for estimating parameters in such functions have been proposed, and a couple of these and a new one will be mentioned here.

Let us structure the problem somewhat and assume stationarity and isotropy, say $\sigma^2 K(x,y) = \sigma^2 R(\|x-y\|)$, identified by putting $R(0)=1$, so that σ^2 is the variance of $Z(x)$ and $R(r)$ is the correlation between $Z(x)$ and $Z(y)$ whenever the locations are distance r apart. A nonparametric procedure which can be used with sufficient data is to group together all pairs of points with inter-distance in $(r-\delta, r+\delta)$, say, and estimate the covariance $R(r)$ based on these. This suggestion amounts to

$$\widehat{\sigma}^2\widehat{R}(r) = \sum_{i,j} w(d_{ij})\{z(x_i)-m(x_i,\widehat{\beta})\}\{z(x_j)-m(x_j,\widehat{\beta})\}/\sum_{i,j} w(d_{ij}), \tag{3.9}$$

where the sums are over all $n(n-1)/2$ pairs, and $d_{ij} = \|x_i - x_j\|$ is the inter-distance between locations, but where $w(d)$ is 1 only for $d \in (r-\delta, r+\delta)$ and 0 outside. Somewhat more ambitiously a kernel type weighting of all pairs of data can be proposed. There are some difficulties with the direct use of estimators like (3.9), since one wants to ensure positive definitess of the covariance function to be used in Kriging. Therefore (3.9) type estimators are more often used as a means of deciding on some particular parametrised covariance function. Robustness issues are discussed in Omre (1984).

For parametric models $R(r) = R_\theta(r)$ there is an ongoing dispute over the merits of the maximum likelihood estimator. Maximimising the likelihood over β gives $\widehat{\beta}_\theta =$

$(F'K_\theta^{-1}F)^{-1}F'K_\theta^{-1}Z_{\rm dat}$, and then over σ gives $\widehat\sigma_\theta^2 = Q_\theta/n$, where $Q_\theta = Q_\theta(\widehat\beta_\theta) = (Z_{\rm dat} - F\widehat\beta_\theta)'K_\theta^{-1}(Z_{\rm dat} - F\widehat\beta_\theta)$. Here K_θ is the matrix of $R_\theta(d_{ij})$. The resulting profile likelihood must finally be maximised over θ. This amounts to minimising the rather intricate function

$$-\log L(\widehat\beta_\theta, \widehat\sigma_\theta, \theta) = \tfrac12 n\log(Q_\theta/n) + \tfrac12\log\{\det(K_\theta)\} + \tfrac12 n. \tag{3.10}$$

There are first of all numerical problems associated with minimising this difficult and possibly multimodal function, and secondly it is not clear that using the maximum likelihood estimator should be a good choice per se. See the dispute of Mardia and Marshall (1984), Warnes and Ripley (1987), Ripley (1988, Chapter 2), and Mardia and Watkins (1989). Other estimation methods have also been proposed, see Switzer (1984), Stein (1987), and Vecchia (1989). Pseudo-likelihood methods in the manner of Besag (1974) and Jensen and Møller (1991) can also be used.

Let us briefly describe yet another method, the maximum quasi-likelihood procedure of Hjort (1992). This is really a class of methods, and the simplest among them is the following: Consider

$$\mathrm{ql}(\beta,\sigma,\theta) = \prod_{i<j} g(z_i, z_j | d_{ij}, \beta, \sigma, \theta), \tag{3.11}$$

where the product is over all $N = n(n-1)/2$ pairs of distinct observations, and the g-term is the model-given probability density of $(Z(x_i), Z(x_j))$ for points lying distance d_{ij} apart. Maximising this is easily carried out, as indicated below, without numerical problems. Why is maximising ql a sensible procedure? Suppose $g(z, z'|r)$ is the *true* probability density for a pair $(Z(x), Z(x'))$ with inter-distance r. Divide the distance range $[0,\infty)$ into small intervals, and sort for each interval together those pairs in log ql that have inter-distance d_{ij} close to the corresponding distance, say r. An ergodic argument shows that

$$N^{-1}\log\mathrm{ql}(\beta,\sigma,\theta) \doteq \int_0^\infty \Big[\int\!\!\int g(z,z'|r)\log g(z,z'|r,\beta,\sigma,\theta)\,dz dz'\Big]\,H(dr),$$

in which $H(dr)$ is the distribution of the distance $\|x - x'\|$ between a randomly drawn pair of points. Hence maximising ql aims at finding the parameter values that minimise the particular distance function

$$\Delta\big[g(.,.|.), g(.,.|.,\beta,\sigma,\theta)\big] = \int_0^\infty \Delta_r\big[g(.,.|r), g(.,.|r,\beta,\sigma,\theta)\big]\,dH(r),$$

in which the 'inner distance function' between the true density g_r and the modelled density g_r^* for $(Z(x), Z(x'))$ is the Kullback–Leibler one, $\int\int g_r\log\{g_r/g_r^*\}\,dzdz'$. In particular the proposed maximum ql method leads to consistent parameter estimates under suitable mild regularity conditions, but we avoid here the precise definition of the asymptotic framework.

Let us see how this works out in the three-parameter model in which $Z(x) \sim N\{\beta,\sigma^2\}$ and the covariance is $\sigma^2 R_\theta(r)$ for points lying distance r apart. As with the ordinary likelihood method the program is to maximise w.r.t. β, then over σ, and finally over θ. This leads to the following, where we take the liberty of using the same notation as for the ml case above: Let first $\widehat\beta_\theta$ minimise

$$Q_\theta(\beta) = \sum_{i<j}\frac12\frac{(z_i-\beta)^2 + (z_j-\beta)^2 - 2R_\theta(d_{ij})(z_i-\beta)(z_j-\beta)}{1 - R_\theta(d_{ij})^2},$$

indeed

$$\widehat{\beta}_\theta = \sum_{i<j} \frac{(z_i + z_j)/2}{1 + R_\theta(d_{ij})} \Big/ \sum_{i<j} \frac{1}{1 + R_\theta(d_{ij})}.$$

Then let $\widehat{\sigma}_\theta^2 = Q_\theta(\widehat{\beta}_\theta)/N = Q_\theta/N$. The remaining task is to minimise

$$-\log \mathrm{ql}(\widehat{\beta}_\theta, \widehat{\sigma}_\theta, \theta) = N \log(Q_\theta/N) + \sum_{i<j} \tfrac{1}{2} \log\{1 - R_\theta(d_{ij})^2\} + N \tag{3.12}$$

w.r.t. θ, compare (3.10).

There is a connection to the simple nonparametric correlation function estimator (3.9), in that if the particular model which postulates piece-wise constant $R(.)$ is used, then the ql-solution can be shown to be close to (3.9), and the related quasi likelihood which only uses data pairs with approximate distance r comes even closer.

The virtues of the ql method are that the numerical maximisation problem is much simpler than for the ordinary likelihood method, its relatively wide applicability, that its behaviour is better understood, and that it in fact behaves well. It does not claim to be optimal, and in the asymptotic framework where the region expands to produce nearly independent copies the ml is better. This framework is somewhat inappropriate, however.

Instead of using all pairs one could take the product over all $g(z_i, z_{n(i)}|d_i, \beta, \sigma, \theta)$ terms, where $z_{n(i)}$ is nearest neighbour to z_i, with interdistance d_i. Reasoning similar to above shows that this estimation procedure aims at minimising a different distance criterion from true model to parametric approximand, using the $H_0(dr)$ distribution for nearest neighbour distances instead of $H(dr)$ for an arbitrary distance. And there are several related alternative methods. The two procedures above care only about data-pairwise aspects of the model, and would not necessarily be good enough for prediction purposes, for example. One could with some additional efforts use three data points at a time, to fit the empirical three-point-sets distribution to the model. A fuller account is given in Hjort (1992).

3.2. Mosaic processes. Here we describe processes that divide the reference space into a set of disjoint segments and assign a label to each segment. The Markov Random Fields (mrf's), defined on regular lattices, are enjoying increased popularity, though mixed with a widened understanding of the inherent limits and difficulties of the approach. The fundamental simulation scheme called the Metropolis algorithm is explained. Some recently developed amendments and alternative models, including constrained mrf's and semi-mrf's, are then discussed. Finally a couple of non-lattice situations are considered.

3.2.A. Markov Random Fields. We are concerned with stochastic models for the distribution of classes on lattices. One class of such models is the class of mrf's. The following is a brief description of mrf's and some of the statistical properties of such models. We discuss how to estimate parameters of such models, based on an observed 'true scene', and describe methods to simulate realisations of mrf's. One needs to be able to simulate both unconditionally and data-conditionally from a specified mrf. Global constraints that one sometimes needs to be able to impose on simulated scenes include preservation of information in some locations and the desire to keep frequencies of some or all classes near specified levels.

For a given lattice system of sites we first need to introduce the notion of a clique. Because of the strong association to image analysis we shall mainly think of the sites as picture elements, or pixels. Assume a system of neighbourhoods has been defined. Then define a clique Q as a set of pixels all of which are neighbours of each other. Note the sociological appropriateness of the term. If 'neighbours' means nearest neighbours, not including the diagonal ones, then all cliques are of the type

$$\{(i,j),(i+1,j)\} = \begin{matrix} & \\ * & * \end{matrix} \quad \text{or} \quad \{(i,j),(i,j+1)\} = \begin{matrix} * \\ * \end{matrix}.$$

If also diagonal neighbours are included, so that each site has eight neighbours, then there are nine types of cliques:

$$\begin{matrix} & \\ * & * \end{matrix} \qquad \begin{matrix} * \\ * \end{matrix} \qquad \begin{matrix} & * \\ * & \end{matrix} \qquad \begin{matrix} * & \\ & * \end{matrix} \qquad \begin{matrix} * & * \\ & * \end{matrix} \qquad \begin{matrix} * & \\ * & * \end{matrix} \qquad \begin{matrix} * & * \\ * & \end{matrix} \qquad \begin{matrix} & * \\ * & * \end{matrix} \qquad \begin{matrix} * & * \\ * & * \end{matrix} \tag{3.13}$$

The mrf class of probability distributions, or Gibbs processes, are those that satisfy

$$p(\mathbf{x}) = p(x_1,\ldots,x_N) = \text{const.}\exp\Big[\sum_{i=1}^{N}\alpha_i(x_i) + \sum_{Q} V_Q(x_Q)\Big], \tag{3.14}$$

where $\mathbf{x} = (x_1,\ldots,x_N)$ is a long vector of class labels, say among $\{1,\ldots,K\}$, in N sites or pixel locations; $V_Q(x_Q) = V_Q(x_{Q,1},\ldots,x_{Q,m(Q)})$ is the 'potential' associated with clique Q; $\alpha_i(1),\ldots,\alpha_i(K)$ are class and position dependent parameters that can be tied to the prior probabilities for the various classes; and the sum is over all cliques. One important consequence is that

$$p_i(k|\text{rest}) = \Pr\{\text{class} = k \text{ in pixel } i|\text{rest}\} = \frac{\exp\{\alpha_i(k) + A_i(k,x_{\partial i})\}}{\sum_{l=1}^{K}\exp\{\alpha_i(l) + A_i(l,x_{\partial i})\}}, \tag{3.15}$$

in which $x_{\partial i}$ is the collection of classes in the neighbouring pixels lying around pixel i. In fact $A_i(k,x_{\partial i}) = \sum_{Q:i\in Q} V_Q(x_Q;\, x_i = k)$. This means in particular that $p_i(k|\text{rest})$ depends upon only ∂i, i.e.

$$p_i(k|\text{rest}) = p_i(k|x_{\partial i}). \tag{3.16}$$

This is the Markov property. The probabilities (3.16) are called the local characteristics of the mrf. One could call $A_i(k,\partial x_i)$ the award function for window $\{i\} \cup \partial i$ around pixel i. The model encourages realisations with high awards.

The remarkable Hammersley–Clifford–Besag theorem identifies processes having the Markov property (3.16) with those having the Gibbs property (3.14), under a positivity condition, see Besag (1974). When faced with the task of constructing a suitable mrf to describe a certain phenomenon it is usually simpler to think 'local Markov' in terms of award functions and local characteristics than thinking 'global Gibbs' in terms of the potentials.

The following mrf is among the structurally simplest, but has proved useful in image restoration (see 3.4.C below) and in other areas: Use 3×3 neighbourhoods, and cliques of size two only in (3.13), use class-dependent but position-independent $\alpha_i(x_i) = \alpha(x_i)$, and encourage spatial continuity by putting $V_{(i,j)}(x_i, x_j) = \beta I\{x_i = x_j\}$ in (3.14). This spatial mosaic model has $K + 1$ parameters and local characteristics

$$p_i(k|\text{rest}) = \frac{\exp\{\alpha(k) + \beta H_i(k, x_{\partial i})\}}{\sum_{l=1}^K \exp\{\alpha(l) + \beta H_i(l, x_{\partial i})\}}, \tag{3.17}$$

in which $H_i(x_i, x_{\partial i})$ is the number of x_i's neighbours that agree with it. The award is a value in $0, \beta, 2\beta, \ldots, 8\beta$.

The mrf's obviously form a very wide class. Including other cliques carefully chosen from larger neighbourhoods and perhaps finer parameterisation than a crude β for each gives one the possibility of including various types of prior knowledge about local structure into the model. In Application 2.3.B described in Section 2 we fitted mrf's with $K = 12$ classes that came in four subgroups and 5×5-windows with up to 16 different cliques and up to 6 different β-parameters, see Hjort, Holden, and Omre (1989). In Application 2.5.B similarly complex mrf's have been used to model handwritten numbers, see Pripp (1990).

REMARK. It is instructive to compare the 2-D Markov property to the corresponding 1-D one, i.e. for Markov chains $\{x_n\}$. The classical definition of Markov-ness in the chain case is that the distribution of some x_n given the complete past depends on x_{n-1} only. The alternative characterisation that the distribution of x_n given both past and future depends on the nearest neighbours only lends itself much more naturally to higher dimensions. □

3.2.B. Parameter estimation from a single scene. Consider for concreteness a mrf with local characteristics of the form (3.17), but with a more general award function structure

$$A_i(x_i, x_{\partial i}) = \beta_1 H_i^{(1)}(x_i, x_{\partial i}) + \cdots + \beta_p H_i^{(p)}(x_i, x_{\partial i}) = \beta' H_i(x_i, x_{\partial i}),$$

for certain parameters $\beta_1, \ldots, \beta_p$ and certain simple functions $H_i^{(j)}(x_i, x_{\partial i})$. The task is to obtain estimates for $\alpha(k)$'s and β's (and perhaps further parameters, see 3.4 below), from a single realisation $\mathbf{x}$ of the assumed mrf process. The $\alpha(k)$'s are tied to the prior probabilities in pixel i, but in a rather involved way, because of interaction with the β's.

This is in one way a simply structured exponential model of classical form, say $p(\mathbf{x}) = c(\beta)\exp(\beta' V(\mathbf{x}))$ (having subsumed $\alpha(k)$'s in new β's). The maximum likelihood method is seen to be equivalent to solving $V^{(j)}(\mathbf{x}) = \mu^{(j)}(\beta_1, \ldots, \beta_p)$ for $j = 1, \ldots, p$, where $\mu^{(j)}(\beta) = -\partial \log c(\beta)/\partial\beta$ is the expected value of $V^{(j)}(\mathbf{x})$ under the model. These equations cannot be solved directly, due to the formidable normalisation constant $c(\beta)$, defined as a sum of K^N terms. This is the 'partition function' of statistical mechanics, and to give an idea of its complexity it suffices to mention that a Nobel Prize was awarded Nils Onsager for just providing an approximation. But ml estimates can be computed after all, through the use of extensive simulations, see the idea sketched in Künsch (1986). Pickard (1987) managed the simplest case of two equally likely classes and a single β parameter.

The alternative maximum pseudo-likelihood method is much simpler to implement, and has become the method of popular choice. It consists of maximising $\text{pl} = \prod_{i=1}^N p_i(x_i | x_{\partial i})$ w.r.t. the parameters of the model. In the case considered

$$\log \text{pl} = \sum_{i=1}^N \Big[\alpha(x_i) + \beta' H_i(x_i, x_{\partial i}) - \log\Big(\sum_{l=1}^K \exp\{\alpha(l) + \beta' H_i(l, x_{\partial i})\}\Big)\Big], \tag{3.18}$$

and this function can be maximised numerically w.r.t. the parameters $\beta_1, \ldots, \beta_p$ and the parameters of $\alpha(k)$. To give expressions for partial derivatives, let $E_i V_i(\cdot, x_{\partial i})$ denote the mean of $V_i(X_i, x_{\partial i})$ conditional on $x_{\partial i}$, so that $X_i = k$ with probability $p_i(k|x_{\partial i})$, and let $\mathrm{VAR}_i V_i(\cdot, x_{\partial i})$ be the accompanying variance matrix. Then

$$\frac{\partial \log \mathrm{pl}}{\partial \beta_j} = \sum_{i=1}^{N} \{V_i^{(j)}(x_i, x_{\partial i}) - E_i V_i^{(j)}(\cdot, x_{\partial i})\},$$

$$\frac{\partial^2 \log \mathrm{pl}}{\partial \beta_j \partial \beta_m} = -\sum_{i=1}^{N} \{\mathrm{VAR}_i V_i(\cdot, x_{\partial i})\}_{j,m},$$

which shows that $\log \mathrm{pl}$ is concave and well-behaved as a function of β.

A natural first step is to employ parameter-free prior probabilities $\exp\{\alpha(k)\} = \pi(k)$, for example position-independent ones and taken from some 'prior scene', so that $\log \mathrm{pl}$ needs to be maximised only w.r.t. $\beta_1, \ldots, \beta_p$. The maximisation could if necessary go on in an iterational manner. If $\alpha(k)$ is treated as an unknown parameter then $\partial \log \mathrm{pl}/\partial \alpha(k) = 0$ leads to the natural equation $\pi_k(\mathrm{x}) = (1/N)\sum_{i=1}^{N} I\{x_i = k\} = (1/N)\sum_{i=1}^{N} p_i(k|x_{\partial i})$. In Application 2.3.B we have also had occasion to use and fit mrf's with non-linear exponents. All in all parameter estimation using maximum pseudo-likelihood requires some reliable maximisation algorithms, along with a flexibly structured environment to handle such data structures, but is not a major obstacle.

REMARK. Why does pseudo-likelihood work? And is it clear that ordinary maximum likelihood works, if arduously carried through? Again it is instructive to consider the one-dimensional case of Markov chains. Suppose data $\{x_a : a = 0, \ldots, n\}$ are observed from some stationary process and are to be fitted to some parametric first-order Markov chain model $\Pr\{X_{a+1} = j | X_a = i\} = p_\beta(j|i)$. Let $p_\beta(i) = \Pr\{X_a = i\}$ be the accompanying marginal distribution, which is the equilibrium distribution. The ml procedure and the pl procedure maximise respectively

$$L(\beta) = \prod_{a=1}^{n} p_\beta(x_a | x_{a-1}) = \prod_{i,j} p_\beta(j|i)^{N(i,j)}$$

and

$$\mathrm{pl}(\beta) = \prod_{a=1}^{n-1} p_\beta(x_a | x_{a-1}, x_{a+1}) = \prod_{i,j,k} p_\beta(j|i,k)^{N(i,j,k)}$$

in self-explanatory notation.

To examine the aims of ml and pl let us merely postulate that the true underlying model for the chain is some stationary distribution with $\Pr\{X_a = i, X_{a+1} = j\} = p(i,j) = p(i)p(j|i)$ and $\Pr\{X_a = i, X_{a+1} = j, X_{a+2} = k\} = p(i,j,k)$. By ergodic arguments $N(i,j)/n$ and $N(i,j,k)/n$ tend to $p(i,j)$ and $p(i,j,k)$ in probability. Hence

$$\frac{1}{n} \log L(\beta) \to_p \lambda_1(\beta) = \sum_{i,j} p(i,j) \log p_\beta(j|i) = \sum_i p(i) \sum_j p(j|i) \log p_\beta(j|i)$$

and

$$\frac{1}{n}\log \mathrm{pl}(\beta) \to_p \lambda_{\mathrm{pl}}(\beta) = \sum_{i,j,k} p(i,j,k)\log p_\beta(j\,|\,i,k)$$
$$= \sum_{i,k} p(i,.,k)\sum_j p(j\,|\,i,k)\log p_\beta(j\,|\,i,k),$$

in which $p(i,.,k)$ is the sum of $p(i,j,k)$ over all j. It follows that ml and pl in general aim at different 'least false' or 'most appropriate' parameter values. The ml procedure aims at and will be consistent for the parameter value β_0 which is least false according to the distance measure

$$\mathrm{dist}_{\mathrm{l}}\{\mathrm{truth},\mathrm{model}\} = \sum_i p(i)\sum_j p(j\,|\,i)\log\frac{p(j\,|\,i)}{p_\beta(j\,|\,i)},$$

a weighted sum of Kullback–Leibler distances between true and modelled transition probabilities. The pl procedure, on the other hand, aims at and is consistent for the second parameter value β_1 that minimises the different distance measure

$$\mathrm{dist}_{\mathrm{pl}}\{\mathrm{truth},\mathrm{model}\} = \sum_{i,k} p(i,.,k)\sum_j p(j\,|\,i,k)\log\frac{p(j\,|\,i,k)}{p_\beta(j\,|\,i,k)},$$

another weighted sum of Kullback–Leibler distances, this time between true and modelled local characteristics $\Pr\{X_a = j|X_{a-1} = i, X_{a+1} = k\}$. One may also study limit distributions in this framework. The ml is somewhat better on the model's home turf.

This discussion is pertinent considering our proclaimed view that models should be fitted and 'adapted' but not necessarily trusted.

3.2.C. Unconditional simulation. The task considered is that of simulating realisations of a specified mrf. This amounts to simulating from a discrete probability distribution $p(\mathbf{x})$, see (3.14), on an enormous but finite space, the set S of all K^N possible combinations of classes on the given lattice. In application example 2.3.B mentioned in Section 2 we worked with $K = 12$ classes and for example $N = 200 \times 100$ sites or pixels in the scene, which leads to enormous numbers of size $10^{20,000}$ and the like for the number of different scenes. Numbers become mind-boggling in 3-D! Ordinary methods can of course not cope with this kind of magnitude of the problem.

The simulation tricks to be used employ Markov chain Monte Carlo methods. Assume that a huge transition matrix for a Markov chain with state space S has elements $m(\mathbf{x},\mathbf{x}')$ that satisfy the reversibility criterion

$$p(\mathbf{x})m(\mathbf{x},\mathbf{x}') = p(\mathbf{x}')m(\mathbf{x}',\mathbf{x}) \qquad (3.19)$$

for all possible scenes, in which $p(\mathbf{x})$ is the mrf distribution given in (3.14). Then one can show that $p(.)$ is the equilibrium distribution for the Markov chain. To sample from $p(.)$, therefore, one might choose a convenient transition matrix with elements $m(.,.)$ obeying (3.19), and then run it until equilibrium seems to have settled in.

There are several possibilities for choice of $m(.,.)$. A convenient class of such can be described as follows. Choose first a symmetric transition matrix with elements $q(\mathbf{x},\mathbf{x}')$ that are mostly equal to zero. Assume the simulation chain has come to scene $\mathbf{x} = (x_1, \ldots, x_N)$. Select a potential new scene $\mathbf{x}' = (x'_1, \ldots, x'_N)$ from $q(\mathbf{x}, .)$, and move from $\mathbf{x}$ to $\mathbf{x}'$ with probability $\min\{1, p(\mathbf{x}')/p(\mathbf{x})\}$, otherwise remain at $\mathbf{x}$. This is the Metropolis algorithm, or perhaps 'the class of Metropolis algorithms'. One can check that (3.19) holds. The basic idea behind this simulation trick seems to be due to Metropolis, see Metropolis, Rosenbluth, Rosenbluth, Teller, and Teller (1953), and Hastings (1970) and Ripley (1987, Ch. 4) for more statistical accounts.

It remains to specify $q(.,.)$, and again several options are available. One possibility is to have $q(\mathbf{x}, \mathbf{x}')$ positive only if $\mathbf{x}$ and $\mathbf{x}'$ differ at a single site. If this site is i, and $\mathbf{x} = (x_1, \ldots, k, \ldots, x_N)$ and $\mathbf{x}' = (x_1, \ldots, l, \ldots, x_N)$, then

$$\frac{p(\mathbf{x}')}{p(\mathbf{x})} = \frac{p_i(l|\text{rest})}{p_i(k|\text{rest})} = \frac{\exp\{\alpha_i(l) + A_i(l, x_{\partial i})\}}{\exp\{\alpha_i(k) + A_i(k, x_{\partial i})\}},$$

see (3.15). One feasible simulation method, for generating a single realisation $\mathbf{x}$, is therefore as follows: Start out with some initial scene, for example with class labels simulated independently in different pixels, from the prior probabilities $\pi_i(k)$. Carry out complete iteration cycles until apparent equilibrium, where one iteration cycle means a full scan over the scene. And when such a scan visits site i, choose class label l randomly, and let x_i change from its current label k to l with probability $\min\{1, p_i(l|\text{rest})/p_i(k|\text{rest})\}$.

Among several other convenient methods the so-called Gibbs sampler is perhaps the most popular. It consists of running complete iteration cycles until convergence, as above, with the following schedule for changing class labels during a full scan. If the current t'th generation scene is $\mathbf{x}_t = (x_{1,t}, \ldots, x_{N,t})$, choose a random class lable $x_{i,t+1} = k$ for site i according to the local probabilities $p_i(k|\mathbf{x}_t - \{i\}) = p_i(k|\text{rest}_t)$. Only empirical evidence can be given for preferring one simulation scheme to another. The 'current folklore', in this hectic but still young field of stochastic simulation, seems to favour the Gibbs sampler. Some references are Geman and Geman (1984), Gidas (1985), Ripley (1987), and Tjelmeland and Holden (1992).

3.2.D. Constrained simulation. A pleasing facet of the mrf simulation scheme is that one can condition on known class values in some locations. Just go on running the Markov simulation chain as in the previous subsection, for example the Gibbs sampler, but with the class labels fixed at their known values, at all sites where such labels are known.

In some situations realisations of the mrf are only close to reality if the areas covered by each class are somewhat close to prior conceptions. It is therefore important to be able to constrain simulated realisations of an mrf to have class proportions equal to or close to specified values. This is not an easy problem, and some confusion surrounds the few methods that have been proposed in the literature. One possibility is a spin exchange method due to Flinn, see Hjort, Holden, and Omre (1989) for a brief review. Another and in many ways more promising avenue is to consider a new stochastic model with probability distribution

$$p_\sigma(\mathbf{x}) = p_\sigma(x_1, \ldots, x_N) = \text{const.}\, p(x_1, \ldots, x_N)\, \exp\{-\sigma\Delta(x_1, \ldots, x_N)\}, \tag{3.20}$$

in which $\Delta(x_1, \ldots, x_N) = \sum_{k=1}^{K}(N_k/N - \pi_k^0)^2$ is a measure of discrepancy between the class frequencies of the scene $\mathbf{x}$ and the specified class frequencies. It is for each given σ

possible to simulate from $p_\sigma(.)$, by methods similar to those outlined above, even though this random field is not any longer a mrf w.r.t. the neighbourhood system. The idea is then to let σ slowly increase as the Markov simulation chain moves on. The result is that the observed class proportions are forced towards the prescribed π_k^0's.

Let us elaborate this point. The local characteristics of the new model are of the form

$$\begin{aligned} p_\sigma(x_i = k|\text{rest}) &= \frac{p_\sigma(x_1,\ldots,k,\ldots,c_N)}{\sum_{l=1}^K p_\sigma(x_1,\ldots,l,\ldots,x_N)} \\ &= \frac{\exp\left[\alpha_i(k) + A_i(k,x_{\partial i}) - \sigma\Delta(x_1,\ldots,k,\ldots,x_N)\right]}{\sum_{l=1}^K \exp\left[\alpha_i(l) + A_i(l,x_{\partial i}) - \sigma\Delta(x_1,\ldots,l,\ldots,x_N)\right]}. \end{aligned}$$

This expression is generally valid for any given Δ-function of discrepancy between observed and ideal characteristics of the scene $\mathbf{x} = (x_1,\ldots,x_N)$. With the present Δ-function further simplification is possible, see Hjort, Holden, and Omre (1989), and it is not difficult to use the Gibbs sampler, as follows. Complete iteration cycles of simulated scenes are run until apparent equilibrium, where one cycle is a full scan over the scene. During one such scan, suppose the current scene is $\mathbf{x} = (x_1,\ldots,k_0,\ldots,x_N)$. Then move from k_0 to k with probability $p_\sigma(x_i = k|\text{rest})$.

REMARK. This approach is useful also for other $\Delta(\mathbf{x})$-measures of discrepancy between observed and specified characteristics of the scene. It has been used in various forms in projects we have worked on, also for marked point processes (see Sections 3.3 and 4.3). It was also proposed in a remark by Green (1986) in the context of mrf's for image restoration. □

3.2.E. Semi-mrf and other mosaic processes. Yes, there are others, and the mrf's have perhaps had too much attention during the last few years. Let us here briefly mention some other approaches for modelling mosaic type phenomena.

In some applications the boundaries between class patches are approximately linear, and the resulting mosaic image is polygonal. A natural approach is therefore to model the boundaries themselves, and perhaps model class labels separately afterwards. Switzer (1965) gives a class of Poisson line models, which has been used by Owen (1984) and Hjort (1985a) in image reconstruction problems, cf. 3.4.B below. The Switzer process has a Markov property along line transects, but is not spatially Markovian; the distribution of lines and class labels in the interior of a convex bounded region given what is outside the region is not determined by knowledge of lines and class labels on the boundary. A more complex process which has this spatial Markov property has been introduced by Arak and Surgailis (1989). Clifford and Middleton (1989) outline its use in image reconstruction. There is also a differently motivated approach based on coverage processes, covered by Hall (1988). Yet another method involves tesellations, Voronoi cells, etcetera, see Ripley (1981, Ch. 4).

Let us finally describe a semi-mrf approach that aims at combining some of the convenient features of the mrf methods with some larger-scale modifications. A realisation $\mathbf{x}$ on a lattice defines 'bodies', maximal connected sets of sites that belong to the same class. There are several possibilities for making this intuitive notion mathematically precise; see Holden and Tjelmeland (1990) for one definition that is even valid in 3-D. The idea is that users often know something about the typical sizes and forms and directions of bodies, at least for some of the classes. If bodies of sites from class 2 tend to be elliptical, for example, one can try to specify distributions of the angle and the axis lengths, and then build a model that is locally a mrf but encourages such bodies to take place, using a more complicated version of (3.20). One would also want to be able to gear such a model towards respecting certain borders on the scene, or towards respecting prior information of the type 'bodies from class 3 very rarely touch bodies from class 4'. The challenge is to build a sufficiently general and flexible model that can do this and which makes it possible to simulate realisations. This rather ambitious scheme is carried out in Holden and Tjelmeland (1990) and in Tjelmeland and Holden (1992), using models of the form

$$p(\mathbf{x}) = \text{const.}\, p_0(\mathbf{x}) \exp\Big\{\sum_{b=1}^{B} \gamma_b W_{\text{class}(B_b)}(B_b, f(B_b)) - \sum_{d=1}^{D} \sigma_d \Delta_d(\mathbf{x})\Big\},$$

where $p_0(\mathbf{x})$ is some ordinary mrf, perhaps with 5×5 windows, the B_b's are bodies with features $f(B_b)$ like size and form, the W's are award functions that encourage bodies to meet certaiun specifications, and the Δ_d's are certain discrepancy functions. This model has been used to build a program system that produces simulations of reservoir architecture and reservoir properties for oil companies; see the references mentioned.

3.3. Event processes. Here we briefly review some theory for spatial point processes. To solve problems associated with applications described in 2.3.C, 2.3.D, and 2.4.B, for example, one typically needs to model both location of points and associated 'marks'. This is one of the combinations of processes we treat in 3.4. It will be seen that natural and simple models sometimes are easy to construct, but that parameter estimation and model verification typically become difficult tasks. Simulation based inference and use becomes important.

3.3.A. Spatial point processes. How can we model the geographical positions of a collection of points, or small objects, in a given region? The simplest possibility is a Poisson process with constant intensity λ, say, which postulates that the number of points falling in disjoint regions are independent and Poisson distributed with parameters equal to λ times the areas of the regions. A wider class of models emerges by allowing the intensity to vary, perhaps even stochastically. Many important phenomena are not well modelled by even such varying-intensity or doubly stochastic Poisson processes, however. A typical feature is that the smallest inter-point distances are not as small as they would be under Poisson-ness.

A rich class of models for point patterns is the pairwise interaction processes, with density (Radon–Nikodym derivative) $f(\{x_1, \ldots, x_n\}) = \text{const.} \prod_{i=1}^{n} g(x_i) \prod_{i<j} h(\|x_i - x_j\|)$ w.r.t. the Poisson point process (with unit intensity, say). Here $g(x)$ is some nonnegative function of geographical position, often taken to be constant; $h(r)$ is some nonnegative function of the distance r between points, usually bounded by 1; and the integration constant is unwieldy. One is usually content to study models for fixed number of points n, where the pairwise interaction model says

$$f_n(x_1, \ldots, x_n) = \text{const.} \prod_{i=1}^{n} g(x_i) \prod_{i<j} h(\|x_i - x_j\|).$$

There are some measure-theoretic details to work through here; see Lotwick and Silverman (1981) and Baddeley and Møller (1989) for good accounts. Typical examples include

$$h(r) = \begin{cases} \gamma & \text{if } r < \rho, \\ 1 & \text{if } r \geq \rho, \end{cases}$$

which gives the so-called Strauss model, and other simple functions that in some way climb from 0 (or from some extra parameter ε) to 1 when r runs from 0 to ρ. The special case $\gamma = 0$ is possible in the Strauss model, and corresponds to a Poisson process which is never allowed to have points closer to each other than ρ; this is also called a hard core process with hard core distance ρ.

With these choices for $h(.)$ there is an upper limit after which no interaction occurs, and the product above is only over all neighbour pairs, where being neighbours means $\|x_i - x_j\| < \rho$. This invites Markov connections. Indeed the random collection $X = \{x_1, \ldots, x_n\}$ has a spatial Markov property, see Baddeley and Møller (1989). General references for modelling spatial point patterns include Ripley (1977, 1981, 1988, 1989a, b) and Stoyan, Kendall, and Mecke (1987). Some geological applications are described in Omre (1992).

3.3.B. How to simulate. An operational definition of 'understanding a model' is that one should be able to simulate realisations from it. For the Strauss model with $\gamma = 0$, for example, one could conceivably generate points from the Poisson model (which for fixed n means simulating from the uniform distribution in the region considered) and only keep those realisations that have smallest distance at least ρ. This can be seriously inefficient, and better methods are called for.

What seems now to be the best way is that of the spatial birth-and-death processes introduced for this task by Ripley (1977) and Ripley and Kelly (1977). The scheme is (usually) to delete one of the n points at random and then add back another one, with probability

$$\Pr\{\text{add } x_n | x_1, \ldots, x_{n-1}\} = \frac{f_n(x_1, \ldots, x_n)}{f_{n-1}(x_1, \ldots, x_{n-1})} = g(x_n) \prod_{i=1}^{n-1} h(\|x_i - x_n\|)$$

assigned to position x_n. The point is that this birth-and-death process has a unique equlibrium distribution which is exactly the point process with density f. Note that the probability above only depends on the new point and its neighbours, in case of a h-function with finite range. The simulation is usually carried out using some appropriate rejection sampling scheme. Cleverness in doing this is often essential for the algorithm to work fast enough.

3.3.C. How to read a point pattern. There is a need to summarise the main features of a given picture of point locations. One can think of a 'first order' summary picture, where the intensity of points per unit area is estimated in some smoothing fashion. This part is related to the $g(x)$-function of 3.3.A. When the intensity can reasonably be assumed to be homogeneous over a region one needs a suitable 'second order' summary. The method of choice here has become Ripley's K or L functions. The $K(t)$ function is a measure related to the covariance between the number of points falling in two areas, and under ideal Poisson conditions $K(t) = \pi t^2$. This is the motivation for studying $L(t) = \sqrt{K(t)/\pi}$ instead. We refer to Ripley (1981, 1988) and to Stoyan, Kendall, and Mecke (1987) for proper definitions and constructions of estimators that in various ways take edge effects into account. These summary curves can be used to detect non-Poisson behaviour, to suggest other models, and to estimate parameters in such.

If the 'points' have associated areas, for example, then other summary characteristics are needed as well. Ripley (1988, Ch. 6) surveys several such based on morhology and Serra calculus. See also 3.4.H below for more general processes that combine point locations with 'marks'.

3.3.D. Estimating parameters. Even a simple-looking model like the Strauss model with $g = 1$ is notoriously difficult to estimate from data. Maximum likelihood estimation is difficult because of the intractable integration constant, but can be carried out through simulation procedures. One Monte Carlo method is described in in Ripley (1988, Ch. 4), and the rudiments of a general stochastic approximation method are presented in Moyeed and Baddeley (1990), following an idea of Künsch. Versions of pseudo-likelihood methods are studied in Särkkä (1989) and in Jensen and Møller (1991). Another method via conditioning of Palm probabilites has been developed by Takacs and Fiksel; see Fiksel (1988) and Särkkä (1989), who points out connections to pseudo-likelihood again. Nonparametric estimation of the $h(r)$ function is very difficult to do with reasonable precision, and is perhaps only feasible with very large sample sizes. It can nevertheless be carried out, see Diggle, Gates, and Stallard (1987), and be used as a data analytic summary.

3.4. Combinations. In this final subsection a couple of naturally occurring cross-situations are discussed, in which Gaußian random functions, mosaic processes, and event processes appear in combination.

3.4.A. Hidden Markov fields and image restoration. The following situation occurs naturally in image analysis applications. There is an underlying true image $\mathbf{x}$ with value x_i in pixel i, but corrupting noise is present and $y_i = x_i + \varepsilon_i$ is observed instead. More generally there could be a vector y_i carrying information about the true x_i, for example in the form of $y_i|x_i \sim N_d\{\mu(x_i), \Sigma(x_i)\}$.

In some situations there is a low number of possible values for x_i, say $1, \ldots, K$, which suggests using mosaic models of the type discussed in 3.2 for this 'hidden truth'. Thus the land cover classes in a remote sensing application could be modelled as a mrf with an appropriate neighbourhood structure. In other situations there is a larger number of possible x_i-values, and the $\mathbf{x}$ process could be viewed as a discretisation of a continuous random function. The noise is typically assumed to be Gaußian and independent from pixel to pixel given the $\mathbf{x}$ labels. In applications we have worked with involving fine-resolution multi-channel satellite data the measurements from the same underlying class have indeed been quite Gaußian, but have exhibited strong autocorrelation. In other situations the independent white noise assumption seems to be quite realistic.

Let us consider the case of a hidden mosaic process $\mathbf{x}$ with independent Gaußian observations $\mathbf{y}$ on top of it, say $y_i|\{x_i = k\} \sim f(y_i|x_i) = N_d\{\mu(k), \Sigma\}$ for definiteness. The restoration problem is to estimate the full image $\mathbf{x}$ from the observed $\mathbf{y}$. This can be viewed as a spatial classification task. The simplest solution is to carry out ordinary discriminant analysis for each pixel, that is, use as $\widehat{x}_i$ the class label k that maximises $\pi(k)f(y_i|k)$, where $\pi(1),\ldots,\pi(K)$ are the prior probabilities for the K classes. Of course the parameters $\mu(1),\ldots,\mu(K),\Sigma$ must have been estimated from some initial training stage. In some applications the class densities have large pairwise interdistances and this simple non-contextual method is sufficient. In other applications it is not, and contextual methods can offer significant improvements. We discuss two major approaches below, the 'local modelling' developed by Hjort and Mohn (1984, 1987) and others and the mrf based one developed by Geman and Geman (1984), Besag (1986) and others. Other approaches are mentioned in 3.4.D.

3.4.B. An approach based on neighbourhood models. Let us see where basic statistical decision theory leads us in the present spatial context. Assume that the loss incurred when we assign label $\widehat{x}_i$ to pixel i, whose true label is x_i, is of the type

$$L(x_i,\widehat{x}_i)=\begin{cases}0 & \text{if } \widehat{x}_i=x_i \text{ (correct decision)},\\ 1 & \text{if } \widehat{x}_i\neq x_i \text{ and } \widehat{x}_i\in\{1,\ldots,K\} \text{ (wrong decision)},\\ t & \text{if } \widehat{x}_i=D \text{ (being in doubt)},\end{cases}\tag{3.21}$$

in which t is a threshold between 0 and 1. Thus the possibility of being in doubt and state nothing about x_i is reserved, having in mind, for example, mixed pixels in some remote sensing application. Now, if the total measure of consequence is the average of the individual loss-contributions, i.e. the misclassification rate plus t times the doubt rate, then the optimal rule becomes

$$\widehat{x}_i=\begin{cases}k & \text{if } k \text{ maximises } P_i\{k|\mathrm{y}\},\\ & \text{and this maximum exceeds } 1-t;\\ D & \text{if } P_i\{k|\mathrm{y}\}\ \leq 1-t \text{ for each } k.\end{cases}\tag{3.22}$$

Two points to note here are that all the data in principle are conditioned on in the posterior probabilities $P_i\{k|\mathrm{y}\}$, and that the rule classifies one pixel at a time.

In practice one has to limit oneself to a small subset $y_{N(i)}$, containing at least y_i, of all the data. If $y_{N(i)}$ is chosen to consist of y_i and its four immediate neighbours, for example, then the natural approximation to (3.22) is the rule that maximises

$$\begin{aligned}P_i\{k|y_{N(i)}\}&=\text{const. }\pi(k)\ f(y_{N(i)}|c_i=k)\\ &=\text{const. }\pi(k)\sum_{a,b,c,d} g(a,b,c,d|k)\ h(y_{N(i)}|k,a,b,c,d).\end{aligned}\tag{3.23}$$

Here the two basic stochastic elements of the problem enter in a natural and illuminating way: $g(a,b,c,d|k)$ is the conditional probability of getting class configurations a,b,c,d given class k in the centre pixel, and is tied to the $\mathbf{x}$ process. And $h(y_{N(i)}|k,a,b,c,d)$ is the density, in dimension $5d$, for the five vectors in question, given that the underlying classes are k,a,b,c,d. The summation in (3.23) is, in general, over all K^4 configurations. The rule based on (3.23) is an approximation to (3.22), but we emphasise that it also enjoys a natural optimality property by itself, namely that of achieving lowest expected average loss among all rules using the neighbour information $y_{N(i)}$ for the i-th decision.

For each specification of global, simultaneous models for the processes **x** and for **y** given **x** formulae for g and h above can in principle be derived, after which we have a contextual classification algorithm. It is not really necessary for us to derive g and h from fully given, simultaneous probability distributions, however; we may if we wish forget the full scene and come up with realistic local models for the pixel neighbourhood alone, i.e. model g and h above directly. Even if some proposed local g-model should turn out to be inconsistent with a full model for **x**, say, we are allowed to view it merely as a convenient approximation to the complex schemes Nature employs when she distributes class labels over the scene.

Another typical feature in these problems is also illustrated in formula (3.23): the models we use must not only be realistic and fittable, but also feasible in the sense of not needing to much computing time. A satellite scene can contain about a million pixels, and a rule that needs to sum K^4 terms for each class before it can decide on a class label for a pixel will be useless in most cases. Accordingly we should look for clever approximations and/or for convenient model choices that lead to reduced and simplified expressions. One such clever version of the general (3.23) is the following: suppose that y_i-vectors given the underlying classes are independent, and let $g(a,b,c,d|k) = p(a|k)p(b|k)p(c|k)p(d|k)$, where the $p(a|k)$'s are neighbour transition probabilities (which must be estimated). (The Markov mesh model for classes on a lattice studied by Pickard (1977) has in fact this multiplicative property.) Then (3.23) simplifies to

$$P_i\{k|y_{N(i)}\} = \text{const. } \pi(k)f(y_i|k)\, T_k(y_{i1}) \cdot \cdot\, T_k(y_{i4}), \quad T_k(y) = \sum_{m=1}^{K} p(m|k)f(y|m), \quad (3.24)$$

where the y_{ij}'s stem from the four neighbour pixels. This produces the classification rule reached by Hjort and Mohn (1984), Haslett (1985), and others, from somewhat different perspectives.

Hjort and Mohn (1985) obtained a natural generalisation of this rule to the case where spatial autocorrelation between y_i's is allowed for. Specifically,

$$P_i\{k|y_{N(i)}\} = \text{const. } \pi(k)f(y_i|k)\, U_k(y_i, y_{i1}) \cdot \cdot\, U_k(y_i, y_{i4}), \quad (3.25)$$

where the U-functions are appropriate generalisations of the T-functions appearing in (3.24). They also provide evidence that such autocorrelation is prominently present with high resolution satellite data and ought to be taken into account. Hjort and Mohn (1984) and Sæbø et al. (1985) consider other variations on theme (3.23) as well.

The reasoning above applies equally well to larger neighbourhoods than the cross, but exact expressions based on the appropriate generalisation of (3.23) quickly become long and untractable. Again we feel that the statistician should not be afraid of constructing pragmatic approximations, even if they should lead him outside the safe ground of exact expressions under exact models. For the 3×3 pixel box with eight neighbours, for example, we may use a formula similar to (3.24), with four more terms entering the product, involving transition probabilities for diagonal neighbours, say $q(\cdot|k)$, which can be expressed in terms of the $p(\cdot|\cdot)$'s. This produces a valid classification algorithm with good error rate properties, although it, in fact, cannot be deduced from a bona fide global model for the classes.

A natural question is how much gain there is in being (more) sophisticated and cpu-consuming, by including neighbours at all, and by including say eight neighbours instead of only four. Hjort (1985a) studies one particular eight-neighbour method of the type (3.23), by an appropriate generalisation of a four-neighbour method due to Owen (1984). Exact formulae for error rates cannot be obtained, but they can be expressed via probabilities for events involving nine or fewer (univariate, even if the y_i's are multivariate) independent normal variates, and can as such be evaluated by computer simulation. (In this way we do not have to simulate the scenes or portions of the scene itself.) Some numerical information is presented in Hjort and Mohn (1987), and indicates first of all that using context can lead to appreciably increased accuracy, and secondly that using larger neighbourhoods usually will be worth the extra trouble and cpu-time. This is also supported by experience from simulation studies, see for example Hjort, Mohn and Storvik (1987).

3.4.C. Markov random field approaches. The loss function (3.21) is 'local' in nature, and corresponds essentially to viewing pixel-wise error rate as the basic quality measure. A radically different suggestion is the 'global' loss measure

$$L(\mathbf{x},\widehat{\mathbf{x}}) = \begin{cases} 0 & \text{if } \textit{every} \text{ pixel is correctly classified;} \\ 1 & \text{if one or more pixels are misclassified.} \end{cases} \tag{3.26}$$

The optimal rule in this case becomes: find $\widehat{\mathbf{x}} = (\widehat{x}_1, \ldots, \widehat{x}_N)$ to maximise the posterior probability

$$p(\mathbf{x}|\mathbf{y}) = \text{const.}\, p(\mathbf{x})\, f(\mathbf{y}|\mathbf{x}).$$

This requires first of all full model specifications for $\mathbf{x}$ and $\mathbf{y}$ (as opposed to only 'local models'). Secondly, it may appear practically impossible to find this maximum a posteriori scene, because of the enormous number K^N of different possibilities to search through. But modern ideas from numerical-probabilistical optimisation made it possible for both Geman and Geman (1984) and Besag (1986), in two important papers, to give satisfactory solutions, for the broad family of mrf prior distributions studied in 3.2.

Consider for illustration the simplest type of mrf (3.17), with a single β parameter in addition to class-parameters $\alpha(k)$. Assume also that the y_i's are conditionally independent. Then

$$\begin{aligned} p(\mathbf{x}|\mathbf{y}) &= \text{const.}\, p(\mathbf{x})\, f(\mathbf{y}|\mathbf{x}) \\ &= \text{const. } \exp\Big[\sum_{i=1}^{N}\{\alpha(x_i) + \log f(y_i|x_i)\} + \beta \sum_{i<j} I\{x_i = x_j\}\Big]. \end{aligned}$$

Accordingly $\mathbf{x}$ given data is again a mrf, only with updated $\alpha(x_i)$'s. Geman and Geman (1984) discuss a 'statistical cooling' technique from combinatorial optimisation for coming at least close to the maximum a posteriori picture, which is the optimal solution w.r.t. loss function (3.26). It is computationally demanding and requires several hundred iterative scans over the full scene. See Marroquin, Mitter, and Poggio (1987) for considerations about massive parallel processors and speed, and for applications of mrf's to computer vision. Besag (1986), on the other hand, has proposed a much simpler computational scheme that in effect, in a coordinate-ascent way, goes for a *local* maximum of the posterior distribution. The intuitively plausible idea is to start with an initial estimate $\bar{\mathbf{x}}$ for the scene, and then update $\bar{\mathbf{x}}$ to a perhaps better $\widehat{\mathbf{x}}$ by finding $\widehat{x}_i = k$ to maximise

$$p_i(x_i = k|\mathbf{y}, \bar{\mathbf{x}}_{S-i}) = \text{const.} \exp\bigl[\alpha(k) + \beta H_i(k, \bar{x}_{\partial i})\bigr]\, f(y_i|k), \tag{3.27}$$

with notation as in (3.17). Note that this is like ordinary discriminant analysis but with neighbour-influenced 'prior' probabilities $\pi(k) = \text{const.} \exp[\alpha(k) + \beta H_i(k, \bar{x}_{\partial i})]$. In this way the full scene is swept over, in some order, and we have a new, updated estimate $\widehat{\mathbf{x}}$. The process is iterated until convergence; usually 6–10 times suffice. The starting point is ordinarily that corresponding to $\beta = 0$, i.e. the noncontextual, but the 'iterated conditional modes' method could equally well use a contextual classification as its starting point. It has been argued that smaller values of β should be used for the first couple of iterations.

It is our experience from high resolution satellite data that realistic models must allow positive spatial correlation for y_i-vectors given the scene. A simple model that serves to illustrate the general principle and the wider potential of the mrf approach is the following:

$$f(\mathbf{y}|\mathbf{x}) = \text{const.} \exp\Bigl\{-\tfrac{1}{2}\Bigl[\sum_i (y_i - \mu(x_i))'\Sigma^{-1}(y_i - \mu(x_i)) \\ - \sum_{i<j} \gamma_{ij}(y_i - \mu(x_i))'\Sigma^{-1}(y_j - \mu(x_j))\Bigr]\Bigr\},$$

in which $\gamma_{ij} = \frac{1}{2}\gamma$ when i and j are immediate (first order) neighbours and zero otherwise. This is a Gaußian mrf, or conditional autoregressive scheme, with corresponding local characteristics

$$y_i|\mathbf{x}, \mathbf{y}_{S-i} \sim N\{\mu(x_i) + \gamma(\bar{y}_{\partial i} - \bar{\mu}_{\partial i}), \Sigma\}, \tag{3.28}$$

writing $\bar{y}_{\partial i}$ for the average of the four immediate y_j neighbours to y_i and similarly $\bar{\mu}_{\partial i}$ for the average of the four accompanying $\mu(x_j)$'s. It is easily seen that $\mathbf{x}$ given $\mathbf{y}$ again is a mrf. An appropriately modified version of the Geman and Geman method is capable of coming close to the simultaneous optimisation of $p(\mathbf{x}|\mathbf{y})$, which is seen to mean maximising

$$\sum_i \bigl[\alpha(x_i) - \tfrac{1}{2}(y_i - \mu(x_i))'\Sigma^{-1}(y_i - \mu(x_i))\bigr] \\ + \sum_{i<j} \bigl[\beta I\{x_i = x_j\} + \tfrac{1}{2}\gamma(y_i - \mu(x_i))'\Sigma^{-1}(y_j - \mu(x_j))\bigr],$$

where the second sum is over all pairs of neighbours. The natural generalisation of Besag's method to the present spatial correlation model is simpler, and amounts to maximising for each i, and for the current estimate $\bar{\mathbf{x}}$ of the rest of the scene,

$$p_i(x_i = k|\mathbf{y}, \bar{\mathbf{x}}_{S-i}) = \text{const.} \exp\bigl[\alpha(k) + \beta H_i(k, \bar{x}_{\partial i})\bigr]\, f(y_i|k, \bar{\mathbf{x}}_{S-i}, \mathbf{y}_{S-i}). \tag{3.29}$$

Thus the conditional mode step again acts like discriminant analysis, but this time with both neighbour-corrected prior probability and neighbour-corrected class density.

3.4.D. Other approaches to classification. Let us briefly touch upon some other spatial classification techniques. Underlying the previous methods are the loss functions (3.21) and

(3.26). A simple intermediate loss function that is less crude than (3.21) but nevertheless has a 'contextual element' is $L =$ number of misclassified 2×2 blocks of pixels. The optimal rule becomes one of simultaneously classifying four pixels, by maximising the posterior probability given data over the K^4 possible outcomes. Hjort (1987) has worked out simple rules of this type based on a geometric probability model for classes, under which only $6K^2 - 5K$ of the possible configurations have positive probability. This geometrical model used the Switzer process for Poisson lines mentioned in 3.2.F.

Relaxation procedures is a term used for algorithms that iteratively adjust posterior probabilities based on estimated or known spatial relationships among the class labels. Some of these use wider and wider neighbourhoods as the iterations go on. They are perhaps best understood in terms of connections to mrf models, and to analysis of incomplete data, see Kay and Titterington (1986) and Fiskum (1986), and Section 4.2 below.

Other references of interest include Switzer and Green (1984) and Switzer and Ingebritsen (1987) on min/max autocorrelation factors that aim to separate noise from signal; Conradsen and Nielsen (1987), studying the benefits of using texture-type features derived from neighbourhoods; Green and Titterington (1987) who study recursive procedures under an interesting time-sequence of image models; Esbensen and Geladi (1989) where soft bi-linear modelling is used, Greig, Porteus, and Seheult (1989) who demonstrate the maximum a posteriori image algorithm exactly for the two class case; Owen (1989), where the smoothing parameters of Besag type methods are studied; and Taxt and Bølviken (1991), where new restoration algorithms are motivated through an analogy with quantum physics.

3.4.E. Predicting a continuous variable. In several remote sensing applications one is as interested in estimating a 'ground parameter' as in classifying pixels into ground classes. Imagine that z_i is such a variable of interest, associated with ground surface element no. i. In a water quality application of MSS- and LANDSAT-satellite data we have worked on there are in fact several z_i's of interest: the amount of plankton in sea element no. i, along with turbidity, water transparency, and other measures of water quality. In an application to forestry surveillance the total 'tree mass volume' for each 20m×20m element on the ground was of interest. With luck these z_i's are correlated with the remotely sensed y_i-vectors, and predictions based on these can be made. Examples of this sort abound in the remote sensing literature, and make it clear that many important surveillance tasks now can be carried out with the help of remote sensing, ideally combined with ground truth masurements from land stations.

Let us for convenience still use y_i to denote the vector of pertinent observations at pixel no. i, for example spectral data, possibly transformed, and possibly supplemented with other available covariates thought to be useful for the prediction of z_i. (In the water quality application, the components of y_i are two chromaticity indices supplemented with topographic information.) Let us also keep z_i one-dimensional (extensions are straightforward). A useful mathematical assumption, used as a vehicle for producing good prediction procedures, is

$$\begin{pmatrix} z_i \\ y_i \end{pmatrix} | (x_i = k) \sim N\{\begin{pmatrix} \nu_k \\ \mu_k \end{pmatrix}, \begin{pmatrix} {\tau_k}^2 & {\omega_k}' \\ \omega_k & \Sigma \end{pmatrix}\}.$$

Thus z_i in pixel i is viewed as a realisation of a random variable. The natural predictor, if we know that the pixel in question is of ground type k, is

$$\widehat{z}_i(k) = E\{z_i|y_i, x_i = k\} = \nu_k + \omega_k'\Sigma^{-1}(y_i - \mu_k), \tag{3.30}$$

and the conditional variance $\sigma(k)^2 = \tau_k^2 - \omega_k'\Sigma^{-1}\omega_k$ can be used to construct prediction intervals for z_i. Without knowledge of the pixel's class one might weight these with the posterior probabilities $P_i\{k|y_i\}$ to form a (non-contextual) predictor.

There are several ways to incorporate spatial context in the method. One strategy that uses a spatial model for a continuous residual function is explained and illustrated in Høst, Omre, and Sæbø (1989). Let us now examine some other contextual alternatives that use spatial models for the underlying classes.

3.4.F. Predictors constructed from neighbourhood models. Hjort and Mohn (1987) derived prediction rules with variance measures for this framework. Assume that z_i's given y and x are independent, with $z_i|(y_i, x_i) \sim f(z_i|y_i, x_i)$, a normal with mean $\widehat{z}_i(x_i)$ and variance $\widehat{\sigma}(x_i)^2$. The predictors take the form

$$\widehat{z}_i = E\{z_i|y_{N(i)}\} = \sum_{k=1}^{K} P_i\{k|y_{N(i)}\}\,\widehat{z}_i(k).$$

One readily shows that z_i given data $y_{N(i)}$, i.e. the information from pixel i and its neighbours, is distributed as a mixture of the densities $f(z_i|y_i, x_i)$ with $P_i\{k|y_{N(i)}\}$ as weights. Accordingly

$$\mathrm{Var}\{z_i|y_{N(i)}\} = \sum_{k=1}^{K} P_i\{k|y_{N(i)}\}\,\{\sigma(k)^2 + (\widehat{z}_i(k) - \widehat{z}_i)^2\},$$

which is of use when confidence intervals are called for. Observe that if a contextual classification is carried out using the 'local modelling' method then the extra computational burden needed to compute predictors and standard deviations is mild.

3.4.G. Markov random field methods. Assume that $\mathbf{x}$ is a mrf with distribution (3.14), that $\mathbf{y}$ given $\mathbf{x}$ is a Gaußian mrf with local characteristics (3.28), and that z_i's are conditionally independent as above. Then one can show that $(\mathbf{y}, \mathbf{z})$ has a simultaneous mrf distribution given $\mathbf{x}$, and that $(\mathbf{x}, \mathbf{y}, \mathbf{z})$ is a simultaneous mrf. The most important fact is that the unobserved processes $(\mathbf{x}, \mathbf{z})$ given the data $\mathbf{y}$, the Bayesian posterior distribution, is yet another mrf, with local characteristics

$$(x_i, z_i)|(\mathbf{y}, \mathbf{x}_{S-i}, \mathbf{z}_{S-i}) \sim \text{const.}\ \exp\bigl[\alpha(x_i) + \beta H_i(x_i, x_{\partial i})\bigr]\ f(y_i|\mathbf{x}, \mathbf{y}_{S-i})\, f(z_i|y_i, x_i), \tag{3.31}$$

cf. (3.17) and (3.28). This generalises the result (3.29).

Besag's method of taking iterative conditional modes can be generalised to the present state of affairs, with both $\mathbf{x}$ and $\mathbf{z}$ to be estimated from the image data $\mathbf{y}$. This is done in Hjort and Mohn (1987, Section 4). The best method depends on the specific loss function used. When the loss function is $I\{\widehat{\mathbf{x}} \neq \mathbf{x}\}$ plus average squared prediction error then the

Bayes solution is as follows: First use the usual Besag method (in this case, as explained around (3.29)) to arrive at the scene estimate $\widehat{\mathbf{x}}$. Then compute

$$\begin{aligned}\widehat{z}_i &= E\{z_i|\mathbf{y},\widehat{\mathbf{x}}_{S-i},\mathbf{z}_{S-i}\}\\ &= \frac{\sum_{k=1}^{K}\exp\left[\alpha(k)+\beta H_i(k,\widehat{x}_{\partial i})\right] f(y_i|k,\widehat{\mathbf{x}}_{S-i},\mathbf{y}_{S-i})\,\widehat{z}_i(k)}{\sum_{k=1}^{K}\exp\left[\alpha(k)+\beta H_i(k,\widehat{x}_{\partial i})\right] f(y_i|k,\widehat{\mathbf{x}}_{S-i},\mathbf{y}_{S-i})}.\end{aligned}$$

Note that the autocorrelation parameter γ enters via $f(y_i|\mathbf{x},\mathbf{y}_{S-i})$.

In this case $\widehat{z}_i$ emerged as an explicit function of the finally classified scene $\widehat{\mathbf{x}}$. This is because we assumed (3.33) to hold. In models where z_i's must be taken interdependent, given scene and $\mathbf{y}$-data, a simultaneous, iterational updating of $\mathbf{x}$ and $\mathbf{z}$ may be called for. An example is given in Hjort and Mohn (1987, Section 4).

3.4.H. Marked point processes. Suppose there is a mark or set of attributes z_i associated with each point x_i of a spatial point process. An example with a 4-dimensional mark for each point is described in 4.3 below. If the marks live in a mark space $\mathcal{Z}$ then the process with outcomes (x_i, z_i) is just a spatial point process in some appropriate $\mathcal{X} \times \mathcal{Z}$, so the most important parts of the theory presented in 3.3 carry over to marked point processes. In particular, simulation of realisations can be carried out using a spatial birth and death process. The hardest and most vital task is often simply that of building a good model, with distance functions and pairwise interaction functions, that produces realistic outcomes. A general reference with theory and examples is Stoyan, Kendall, and Mecke (1987).

3.4.I. Estimation problems. There are challenging estimation problems associated with several of the models described. Hjort (1985b) and Hjort and Mohn (1987) develop estimation methods for many of the image models mentioned in 3.4.B. In particular they describe methods that utilise unclassified vectors via estimation of mixture distributions. Besag (1986) proposes an iteration scheme to simultaneously restore an image and estimate the parameters of the mrf model used for $\mathbf{x}$, used in 3.4.C, assuming the y_i's to be conditionally independent. This scheme is somewhat biased and inconsistent, as pointed out along with a remedy in Hjort and Mohn (1987). Lakshmanan and Derin (1989) describe a simulated annealing method that stops at regular intervals to estimate the mrf parameters. Veijanen (1990) gives another method for imperfectly observed mrf's and proves consistency. Georgsen and Omre (1992) considers estimation in a model that combines fibre processes with a Gaußian random function.

4. Some worked-through examples of applications

4.1. Depth conversion of seismic data [Omre and Halvorsen (1989)]. The petroleum reservoirs in the North Sea are located at a depth of approximately 3000 m and have an areal extent of typically $3.0 \times 5.0\,\mathrm{km}^2$. In the reservoir the hydrocarbons tend to migrate upwards in the structures until they are trapped under a syncline of non-permeable geologic layers, usually shale rich horizons. The mapping of these horizons is important both for exploration purposes and for prediction of hydrocarbon volume in situ.

Fortunately these non-permeable horizons tend to have properties very different from the porous reservoir, and can be identified from seismic data. Seismic data can be collected in an unexpensive way from ships, and vast amounts with good areal coverage is usually available. The seismic reflection signal has geographical reference horizontally and reflection time reference vertically. After seismic cleaning, which is a discipline in itself, a relatively reliable seismic reflection time surface $\{t(x): x \in D\}$ is obtained, see Figure 4.1. The challenge is to convert this into a map of depths to the horizon $\{z(x): x \in D\}$. This could of course be done by simply multiplying reflection time and signal velocity. The fact that the signal velocity varies considerably, both vertically and laterally, complicates this.

Two other sources of information are available for the depth conversion. The first is the knowledge of the geophysicists. The areal extent of some of these horizons is often huge and it also covers other reservoirs. Hence experience from other areas of the North Sea is relevant. In addition the physical understanding of packing of reservoir rock provides some constraints on the vertical velocity profile. Secondly, exact depth observations $z(x_1), \dots, z(x_n)$ are available in certain well positions, see Figure 4.1. The fact that the four first wells are the most shallow ones indicates preferential drilling and non-representative positioning of the observations in the design space. Note, however, that the seismic reflections have a support of $100 \times 100\,\mathrm{m}^2$ of the horizon while the support of well observations is $0.2 \times 0.2\,\mathrm{m}^2$. Hence the former must be considered as weakly smoothed.

The stochastic model used for merging the various pieces of information in this study is of the form

$$\begin{aligned} Z(x) &= V(x)t(x) + \varepsilon(x) \\ &= \left\{B_1 + B_2 t(x) + B_3 \frac{x_1 - x_{1,\mathrm{min}}}{x_{1,\mathrm{max}} - x_{1,\mathrm{min}}}\right\} t(x) + \varepsilon(x), \end{aligned} \tag{4.1}$$

where $\varepsilon(x)$ is a continuous residual surface, compensating for the smoothing in the seismic signal, with correlation structure $\sigma^2 K(x-y)$. In other words, the signal velocity increases with depth according to the increase in reflection time and there exists a lateral trend in the East-West or x_1-direction. Geophysical knowledge is included through carefully assessed prior distributions on B_1, B_2, B_3. The model is accordingly within the Bayesian Kriging framework as discussed in Section 3.1.D.

The example is from a study of a huge offshore gas field in the North Sea. A set of parameters, intended to be as realistic as possible, were defined in cooperation with geophysicists in a Norwegian oil company. The sensitivity to the influence of the prior knowledge was evaluated. The changes in the predictions over time, i.e. as a function of the available wells, was also studied. The study is based on

$$\begin{aligned} \sigma &= 200.0\,\mathrm{m}; \\ K(\Delta x) &= \begin{cases} 1 - \frac{3}{2}\frac{\Delta x}{2800} + \frac{1}{2}\left(\frac{\Delta x}{2800}\right)^3 & \text{if } 0 \le \Delta x \le 2800, \\ 0 & \text{if } \Delta x \ge 2800; \end{cases} \\ B = \begin{pmatrix} B_1 \\ B_2 \\ B_3 \end{pmatrix} &\sim N_3\left\{ \begin{pmatrix} 6.0 \cdot 10^{-1} \\ 2.0 \cdot 10^{-4} \\ 7.0 \cdot 10^{-2} \end{pmatrix}, \tau^2 \begin{pmatrix} 3.0 \cdot 10^{-3} & 0 & 0 \\ 0 & 1.0 \cdot 10^{-8} & 0 \\ 0 & 0 & 5.0 \cdot 10^{-4} \end{pmatrix} \right\}. \end{aligned} \tag{4.2}$$

The scale parameter τ was varied in order to evaluate the sensitivity to the choice of prior distribution. In Table 4.1 and Figure 4.2 the results from the sensitivity of choice of τ are summarised. The evaluation is based on the three first wells only.

For τ equal to zero the coefficients B are fully specified and the underlying trend surface can be subtracted. This corresponds to what is termed simple Kriging in geostatistical terminology. The observations $z(x_1), \ldots, z(x_n)$ will in this case have influence on the residuals $\{\varepsilon(x): x \in D\}$ only. This makes the observations create cone-like surfaces in their immediate neighbourhood. The case of τ going to infinity corresponds to there being no available prior knowledge about the coefficients, and the resulting method coincides with what is called universal Kriging. In this case the observations $z(x_1), \ldots, z(x_n)$ will be the only source of information for both B_1, B_2, B_3 and the residuals. This may give unreliable results based on the first few wells since they a priori are known to be preferentially located in shallow areas. The intermediate cases with finite τ constitute trade-off cases between user experience and the available observations, as discussed in Section 3.1. Note that in the posterior distribution the off-diagonal terms in the covariance matrix for B are non-zero, since all the parameters draw on the information in the three wells.

The development of the predictions over time can be evaluated by adding one well at a time. In Table 4.2 and Figure 4.3 results from this study are summarised. The prior distribution is based on $\tau = 1$. Note that the model in this application is used for interpolation. When assessing the hydrocarbon volume in situ with associated uncertainty measures one would use the model as basis for stochastic simulation.

The regression surface contains three unknown parameters, so a solution in the traditional setting requires at least three wells. In the Bayesian setting a solution exists regardless of the number of observations. The Bayesian model provides a prior guess on the surface, along with uncertainty measures, and the initial estimate is updated when new observations are made available. From an operational point of view in petroleum exploration this is meaningful, and it provides the opportunity to evaluate the information content in each datum. Note also that the posterior variances of the parameters decline monotonically with increasing number of wells, as they should.

We view the use of the Bayesian machine here as appropriate and non-controversial, in spite of the somewhat subjective and surely non-perfect determination of the prior distribution. The geophysical knowledge is substantial and is of a form which naturally can be quantified through the parameters of the model as defined above. A lot of expert effort and experience has gone into the determination of the prior parameters. The setting of these was not an entirely Bayesian affair but had more of the empirical Bayes flavour, in that also other available indirect data sources were used, partly in informal ways via plots etc.

Reliable estimators for the spatial correlation function $K(.)$ and the standard deviation parameter σ are not simple to obtain with so few data points available. Often experience from evaluation of other reservoirs with many more wells must be exploited. This suggests using the extended Bayesian apparatus of the type described in 3.1.C, with an inverse gamma prior distribution for σ^2 and a 'hyper prior' distribution for τ^2, and perhaps with a prior for the covariance matrix of B. In Abrahamsen, Omre, and Lia (1991) and Abrahamsen (1992) the model is extended to solve a multi-layer seismic depth inversion problem, providing solutions for observations from non-vertical wells.

4.2. Identification of heart dysfunction [Taxt, Lundervold, and Angelsen (1990)]. The objective of the study is to evaluate the left ventricular volume of the heart and the cardiac output fraction based on data from time-repeated two-dimensional echocardiography, so-called ultrasound techniques. This will allow significant improvements of present diagnostic capabilities for heart dysfunction. The methodological challenge is to combine prior knowledge with pattern recognition techniques to identify moving boundaries of specific structures in time-varying images with low local contrast and a large noise component.

Time-varying ultrasound images are extensively used as a routine diagnostic tool in the examination of the cardiac function. The images are collected at 25–35 Hz which is appropriate for evaluating the heart activity with contraction cycles down to 0.3 seconds. Each image is collected in polar coordinates (r, θ), with the origin at the probe of the ultrasound equipment. The reflections u are assigned integer-values in the range from 0 to 255. In the study 20 consecutive images were available, covering more than two complete cardiac cycles. The data are accordingly of the form $u_t(r_i, \theta_j) \in \{0, \ldots, 255\}$ for $i = 1, \ldots, 512$, $j = 1, \ldots, 128$, $t = 1, \ldots, 20$. Since the reference system is not orthogonal an inverse polar transformation was used to get $u_t(x_i, y_j)$ instead. The time reference was treated as a third dimension in the problem, hence defining a 3-D image. To reduce the computational load the grey level resolution was reduced to 32. Thus data are of the form

$$v_{ijk} = u_k(x_i, y_j) \in \{0, \ldots, 31\} \quad \text{for } i = 1, \ldots, N_i,\ j = 1, \ldots, N_j,\ k = 1, \ldots, 20. \qquad (4.3)$$

In Figure 4.4 a cross section of the 3-D image at constant k is displayed.

Two noise reduction algorithms have been used in this study. A relaxation procedure of the type mentioned in Section 3.4 is the basis for the first one. The relaxation procedure is adapted to the noise reduction problem as follows: use as (one-dimensional) feature vector the grey level itself; use as the set of possible classification classes simply the possible grey levels $c \in \{0, \ldots, 31\}$; and use class-conditional feature vector density $f_c \sim N\{c, \sigma^2\}$ combined with transition probabilities $p(d|c) = \frac{1}{31}\{1 - p(c|c)\}$ for $d \neq c$.

To describe how the relaxation simulation scheme works, let C^l_{ijk} denote temporary classification for pixel (i, j, k) at iteration no. l, let V_{ijk} be a neighbourhood of (i, j, k), and let V^2_{ijk} be the neighbours plus all their neighbours again. Then

$$\begin{aligned} \Pr\{C^{l+1}_{ijk} &= c | C^l_{mno} \text{ for } (m,n,o) \in V^2_{ijk}\} \\ &= \text{const.} \exp\{-(c - C^l_{ijk})^2/2\sigma^2\} \\ &\times \sum_{(m,n,o) \in V_{ijk}} \Big[p(c|c)\Pr\{C^l_{mno} = c|\cdot\} + \frac{1}{31}\{1 - p(c|c)\}[1 - \Pr\{C^l_{mno} = c|\cdot\}]\Big]. \end{aligned} \qquad (4.4)$$

The initiation of the procedure is done by determining $\Pr\{C^0_{ijk} = c|\cdot\}$ from a non-contextual Gaußian model assuming $\pi_c = 1/32$, and using of course $c^0_{ijk} = v_{ijk}$ in all positions as the initial image. The parameter values used in the actual study were $p(c|c) = 0.90$ and $\sigma = 7.41$. The former was subjectively assigned while the latter was estimated from a training set of data. The neighbourhood V_{ijk} used is of size 3 × 3 × 3.

The relaxation was carried out in five iterations, after which each pixel was assigned the most probable grey level according to the estimated posterior probabilities. The resulting noise reduced image for a particular time-index is displayed in Figure 4.5. This image is much smoother than the original one in the sense that noise seems to be removed. Note that the edges seem to be partially smoothed away as well, however.

Besag's method of iterated conditional modes, as presented in Section 3.4, provides the basis for the other noise reduction algorithm. Corresponding adaptations as for the relaxation procedure were made. The archetypical Besag model contains class-parameters $\alpha_1, \ldots, \alpha_{32}$ and a single β for neighbourhood interaction. The α_c's were taken class independent in the study reported on here. The resulting Besag iteration equation becomes

$$\Pr\{C_{ijk}^{l+1} = c | C_{mno}^{l} \text{ for } (m,n,o) \in V_{ijk}\} = \text{const.} \exp\{-(c - C_{ijk})^2/2\sigma^2 + \beta H^l(c, V_{ijk})\}, \tag{4.5}$$

where $H^l(c, V_{ijk})$ is the number of pixels in the three-dimensional neighbourhood whose class labels agree with c at iteration l. The initiation was done as for the relaxation procedure, and the value $\beta = 0.5$ was found to be satisfactory. Iterated conditional modes were found with ten iterations. The resulting noise reduced image for one index in time is displayed in Figure 4.5. It can be seen that some of the noise has been smoothed and that the edges are resonably well reproduced.

The binarisation was performed by a locally adaptive thresholding algorithm. The results from applying this to the original and the noise reduced images in Figures 4.5 are reported in Figure 4.6. Taxt, Lundervall, and Angelsen (1990) judge the relaxation approach to be superior with respect to quality in the binary image. Based on these binary images additional cleaning by removing binary objects with small temporal extent is performed. The boundary can be determined from this cleaned image, see Storvik (1992).

This multi-stage 'one task at a time' approach to problem solving seems to be representative for many current applications in applied image analysis. It is not necessarily the best approach, however. An alternative approach to the problem would be to address the volume estimation directly from the initial images. Robust estimators may be able to reduce the influence of the noise. In a stepwise procedure the danger of filtering out important information concerning the main objective of the study is severe, hence bias can be introduced and efficiency reduced. The 'directly to the heart' approach looks attractive in that respect. The fact that it is the dynamic characteristics of the heart which are of interest calls for models for which smoothing along the time dimension is not too severe. A separate treatment of the time dimension seems necessary. See Storvik (1992).

4.3. Simulation of fault zones [Omre and Sølna (1990)]. Petroleum reservoirs in the North Sea are characterised by numerous fractures and faults. This is expected to have considerable impact on the production potential. Not merely the presence of faults but also the characteristics of the fault zone will have influence. The fault could slip along one continuous plane, or it may consist of a swarm of minor fractures. The exact flow mechanism across faults is not well understood at present. In this application a stochastic model for the break pattern is established. One fault zone will be considered and several realisations are generated. Each realisation is later taken as input to a fluid flow simulator in order to evaluate the impact of the break pattern on production.

The large faults, i.e. with offset above 20 m, can be observed on the seismic maps. They are characterised by centre line, vertical offset and lateral extension, see Figure 4.7. The smaller fractures constituting the break pattern in the fault zone are below seismic resolution, however. It is these smaller fractures which will be modelled in this study. The stochastic model is based on general structural geological knowledge. The realisations generated from the model have to be constrained by the centre line, vertical offset and lateral extension actually observed.

The stochastic model is based on the theory of marked point processes as outlined in Sections 3.3 and 3.4.H. Each fracture is defined as a marked point $m = (x, \phi, \omega, \rho, \theta)$, see Figure 4.8, in which x is the two-dimensional geographical reference point, a stochastic variable defined in the fault zone; ϕ is the orientation of fracture, constrained to be parallel to the centre line of the fault zone, ω is the stochastic width of fracture, ρ is the stochastic offset of fracture, and θ is the constant dip angle, as specified by user. The models applied in the present study specify that the joint probability for n fractures $m_1, \ldots, m_n$ is of the general form

$$f_n(m_1, \ldots, m_n) = \text{const. } \exp\Big\{-\sum_{i=1}^{n} b(m_i) - \sum_{i<j} c(m_i, m_j)\Big\} \exp\{-\sigma\Delta(m_1, \ldots, m_n)\}. \tag{4.6}$$

Here $b(m)$ takes care of the dependence structure for attributes in each marked point, $c(m_i, m_j)$ models the pairwise interaction between marked points, and $\Delta(m_1, \ldots, m_n)$ is finally a measure of deviation between the realisation $(m_1, \ldots, m_n)$ and some desired property, with accompanying strength parameter σ. Note the similarity to a technique mentioned in 3.2.D. If exact or approximate constraints of the simulated marked points are needed then such are built into the deviance measure.

The model actually employed in our study used

$$b(m_i) = b_1(x_i) + b_2(\omega_i|x_i) + b_3(\rho_i|\omega_i), \tag{4.7}$$

in which $b_1(x)$ is a function defining the fracture frequency in the fault zone dependent upon the distance from x to the centre line of the fault; $b_2(\omega|x)$ is another function defined in the fault zone where the width can be a function of the distance from x to the centre line of the fault; and $b_3(\rho|\omega)$ is a function relating the width of the fracture to the offset, taken as $(\rho - \mu\omega^2)^2/2(\omega^2\eta)^2$ for certain parameters μ and η. Note that steeper slopes in some areas of the fault zone can be realised by either higher frequencies of fractures or larger expected width of each fracture which in turn is correlated with offset. The trade-off between these two effects is governed by a parameter α. Furthermore $c(x_i, x_j)$ was taken as $c_0(x_i - x_j)$ where

$$c_0(\Delta x) = \begin{cases} k(\phi)/|\Delta x|^2 & \text{for } 0 \leq |\Delta x| \leq x_0 k(\phi)^{1/2}, \\ 1/x_0^2 & \text{for } |\Delta x| \geq x_0 k(\phi)^{1/2}, \end{cases}$$

with $(|\Delta x|, k(\phi))$ being the polar coordinates for Δx, and $k(\phi)$ representing the anisotropy factor being elliptical with major axis horizontally. Finally the $\Delta(m_1, \ldots, m_n)$ measure of deviance used, to be scaled with σ afterwards, is

$$\Delta(m_1, \ldots, m_n) = \frac{1}{|L|} \int_L \big|(\text{total offset at } u) - (\text{realised offset at } u \text{ by } \{m_1, \ldots, m_n\})\big|\, du,$$

with L being the centre line of fault and $|L|$ its length.

In the study the actual model was explored by simulation in order to see if it was suited for generating realistic realisations of break patterns in faults. In this summary the sensitivity to $b_1(x)$ and $b_2(\omega|x)$ as well as to $c_0(x_i - x_j)$ will be reported. In Figure 4.9 the fracture locations and widths are generated from a Poisson process, with strength parameter $\sigma = 0$, and only (ω, ρ)-interaction is present. In the figure the upper display is a bird's view and the locations of the fractures are exposed. Note their 'random' appearance. The middle display corresponds to facing the fault and the respective offsets can be observed. Note that the total offset in the fault is not reproduced since no global constraints are imposed. The lower display shows the average slope profile for the fault in solid line and three profiles at arbitrary locations in dotted lines. Note that the slope is linear over the fault as specified by the Poisson process. In Figures 4.10 and 4.11 the interaction function $c_0(.)$ is used, the strength parameter σ is assigned a relatively large value, and the effect of having steeper slope in the middle of the fault area is added. Note that in both figures the fractures tend to repulse each other and that the total offset is almost reproduced. In Figure 4.10 the steepness is realised by having larger width and offset in the centre, while in Figure 4.11 it is realised by having higher frequency of fractures in the centre. It is also possible to use a trade-off between the two.

The geologists have approved the results, and the study has since proceeded towards evaluation of fluid flow across the fault zone. Futher methodologial work will aim at understanding the interaction between the parameters when enforcing global constraints. Parameter estimation from observations of fractures in wells and from comparable outcrop data will also be studied.

4.4. Spatial prediction of air pollution from space-time observations [Høst, Omre, and Switzer (1991)]. The awareness of the possible consequences of changes in the environment has contributed to increasing interest in pollution monitoring. Control of international agreements on reduction of emissions to air will require careful air pollution monitoring, supplemented with a thorough statistical evaluation. Air pollution will normally be modelled as a spatial-temporal phenomenon, and the available data take the form of time series in a number of fixed locations. Challenging problems like spatial interpolation and evaluation of temporal trends in arbitrary locations remain mostly unstudied.

In the study reported on here the problem of spatial interpolation at a given time point is addressed. The air pollution data used are collected by the European Monitoring Evaluation Program (EMEP). The variable considered is sulphur concentration in units of micrograms per cubic meter, $\mu g/m^3$. The data are presently collected in more than one hundred locations all over Europe, but in this study data from the six years 1980–1985 are used, in the form of monthly averages of sulphur concentrations in 42 fixed locations. The locations provide a good areal coverage over Central Europe, see Figure 4.12. The time series are log-transformed and are denoted $\{y(x_i, t_j): i \leq 42, j \leq 72\}$, with x and t denoting geographical position and time respectively. The time series for two particular locations are presented in Figure 4.13, exposing sizeable spatial differences as well as seasonal variations.

The statistical objective we focus on is to estimate the surface $y(x, t)$, for x in the domain $\mathcal{D}$, for a given t among $\mathcal{T}$, the 72 time points used. A natural model for this purpose is

$$Y(x,t) = m(t) + M(x) + V(x,t), \quad x \in \mathcal{D},\, t \in \mathcal{T}, \tag{4.8}$$

where $m(t)$ is centred temporal drift, containing seasonal variations but independent of location, $M(x)$ is the spatial drift independent of time, and $V(x,t)$ is the centred space-time residual. We choose to represent the latter as $V(x,t) = S(x,t)U(x,t)$, where $S(x,t)$ is residual standard deviation and $U(x,t)$ is the normalised residual. The temporal drift is represented deterministically since its variation is considered to contribute only marginally to the uncertainty of the final interpolator. If the aim of the study had been temporal forecasting it would have been necessary to model the $m(t)$ function stochastically as well.

The model is defined up to second order and employs the following parameters: Spatial drift is based on an ordinary Kriging model, with

$$EM(x) = \mu_M, \quad \mathrm{Var}\{M(x) - M(x')\} = 2\gamma_M(x - x').$$

The residual standard deviation is similarly based on an ordinary Kriging model, with

$$ES(x,t) = \mu_S, \quad \mathrm{Var}\{S(x,t) - S(x',t)\} = 2\sigma_S^2\{1 - \rho_S(x - x')\}.$$

Finally the normalised residual is modelled with a location dependent correlation function, discussed in Switzer (1989), having

$$EU(x,t) = 0, \quad \mathrm{Var}\{U(x,t) - U(x',t)\} = 2\{1 - \rho_U(x, x')\}.$$

The model differs from what is traditionally being used in that the standard deviation is spatially varying and that the spatial correlation function in the residuals is location dependent. The variables and parameters of the model can be estimated from the $y(x_i, t_j)$-data. See Høst, Omre, and Switzer (1991) for development of some reasonable but not necessarily optimal estimators. It is difficult to establish exact properties of these, but they are based on a fair amount of data and should be sufficiently reliable.

The spatial interpolator for an arbitrary location x_0, at the time point t under consideration, is

$$Y^*(x_0,t) = \widehat{m}(t) + M^*(x_0) + S^*(x_0,t)U^*(x_0,t). \tag{4.9}$$

Here $\widehat{m}(.)$ is the estimate of temporal drift based on a simple smoother on the available data, $M^*(.)$ and $S^*(.)$ are ordinary Kriging predictors, and $U^*(.,.)$ is determined by the procedure for spatial interpolation discussed in Switzer (1989) and Høst, Omre, and Switzer (1991). See also the independent work of Sampson and Guttorp (1992). A model with a location specific correlation function is used. The interpolator Y^* is not optimal in the mean squared error sense since the three components M, S, U are predicted independently. The exact optimal solution cannot be expressed simply since it requires solving a fourth order minimisation problem. The interpolator (4.9) happens to be optimal in the case of independence between M, S, U, and can be shown to be close to the optimal one whenever the components are not too highly correlated. Scatter plots have indeed indicated near independence for the situation at hand.

It is worth noting that the prediction variance of (4.9) can be calculated explicitly for the case of independent M, S, U, and can be expressed as

$$\begin{aligned}\operatorname{Var}\{Y(x_0,t)-Y^*(x_0,t)\} &= \operatorname{Var}\{M(x_0)-M^*(x_0)\}\\ &\quad+\operatorname{Var}\{S(x_0,t)-S^*(x_0,t)\}\operatorname{Var}U^*(x_0,t)\\ &\quad+\operatorname{Var}\{U(x_0,t)-U^*(x_0,t)\}\,(\sigma_S^2+\mu_S^2).\end{aligned}$$

The interpolator (4.9) and its prediction variance have the 'exactness property', in the sense that observations are correctly predicted with prediction variance zero at the data locations. In general, one will obtain weights associated with the observations which are location specific and not only dependent on the configuration of data locations. This makes the interpolator different from the simple and ordinary Kriging interpolator methods. In the end the predicted sulphur concentration is obtained by the inverse log-transform.

The illustration shows the interpolated sulphur concentration over Europe for January 1984. The prediction is presented on a grid of size 375 × 450 over Europe. Figure 4.14 presents a contour map of the predicted sulphur concentration along with the pointwise 0.2 and 0.8 percentiles in the predictions. Alternative maps of presentation can be imagined and should be used whenever particular effects are to be studied or exposed.

Comparison with results obtained by use of traditional Kriging techniques for interpolation, as described in 3.1.B, show deviations both in the predictions and in the prediction variances. Traditional Kriging gives predictions in the range of about ±10% of what (4.9) produces. The fact that the approach used here is more flexible and adapts better to the available data, without overfitting, seems to indicate its superiority. Further work on evaluation of temporal trends in the average of sulphur concentration and other air quality variables over given regions is being pursued.

5. Closing remarks

There is an increasing interest in spatial and spatial-temporal methodology. Inexpensive, fast-processing computers provide the technological basis for most spatial statistical analysis. Vast amounts of automatically collected data have made new applications accessible for spatial evaluation. The experiences with and expectations for spatial and spatial-temporal statistics can tentatively be summarised as follows.

There is a wide variety of challenging applications. User groups are normally positive since they are often poorly trained in handling spatial data and realise that their evaluation is insufficient. The possibility of including user experience through 'prior guesses' is highly appreciated. Numerical results can often be supplemented with graphical displays, and this simplifies verification and interaction with the users. The main experience is however that *every problem is unique.* This is true even more so than in traditional statistics because of the modelling possibilities and the large variety of sampling designs.

One of the things to note on the methodological side is that many natural models do not admit analytical 'closed form expression' solutions. The mathematical complexity increases considerably for higher dimensions in the reference space. The untractability of Markov properties of Gaußian random functions is but one example. Efforts should be made to obtain further analytical results, although a complete 'analytical understanding' seems out of reach. To compensate for this stochastic simulation has been used extensively. It has in many cases proved successful, and valuable insight into the models has been reached. For surprisingly many models, however, simulation techniques have proved to be unreliable or too time-consuming. The disappointingly slow convergence of the Metropolis algorithm and Gibbs sampler for simulation of Markov random fields are examples of this. Further research on new models formulations with associated reliable and efficient simulation algorithms are certainly needed. The availability of vector and parallel processing computers should be taken to advantage.

Criteria for selection between different models are not developed and research along such lines should be initiated. For several of the most often used models there is a lack of reliable estimators for the model parameters. Constructing such estimators is a difficult task, since the parameters are often interrelated and the sampling designs vary considerably. Model adaptation procedures should be cross-validated and bootstrapping should be further developed for spatial models. As can be seen, despite recent and healthy progress in the field, there seem to be more questions than answers concerning spatial and spatial-temporal statistics so far.

Space/time statistics will provide challenges for both theoretical and applied statisticians for the years to come.

Acknowledgements. We have been privileged to work in a stimulating environment at the Norwegian Computing Centre, with fellow statisticians of high standard as well as with demanding clients from several sectors of industry and research. Our work over the years has partly been supported by the Royal Norwegian Council for Scientific and Technological Research. Finally we are grateful to the programme committee of the Nordic Conference in Odense 1990 for inviting us to lecture, and to Editor Elja Arjas for encouragement and patience.

References

Abrahamsen, P. (1992). Bayesian Kriging for seismic depth conversion of a multi-layer reservoir. Proceedings *4th International Geostatistics Congress*, Troia, Portugal.

Abrahamsen, P., Omre, H., and Lia, O. (1991). Stochastic models for seismic depth conversion of geological horizons. *Society of Petroleum Engineers* 23138, 329–341.

Adler, R.J. (1984). *The Geometry of Random Fields.* Wiley, New York.

Arak, T. and Surgailis, D. (1989). Markov fields with polygonal realisations. *Probab. Theory Rel. Fields* **80**, 543–580.

Baddeley, A. and Møller, J. (1989). Nearest-neighbour Markov point processes and random sets. *Int. Statist. Rev.* **57**, 89–121.

Besag, J. (1974). Spatial interaction and the statistical analysis of lattice systems [with discussion] *J. Royal Statist. Soc. B* **36**, 192–236.

Besag, J. (1986). On the statistical analysis of dirty pictures [with discussion]. *J. Royal Statist. Soc. B* **48**, 259–302.

Box, G.E.F. and Jenkins, G. (1976). *Time Series Analysis: Forecasting and Control.* Holden-Day, Johannesburg.

Bølviken, E. and Helgeland, J. (1989). Some models and algorithms in segmented time series analysis. Technical report SAND/xx/89, Norwegian Computing Centre, Oslo.

Bølviken, E., Helgeland, J., and Storvik, G. (1991). Stochastic regime models and wireline log data. *Bull. Int. Statist. Inst.*, invited paper in the session on spatial statistics, Cairo.

Christensen, R. (1990). The equivalence of predictions from universal Kriging and intrinsic random-function Kiriging. *Math. Geol.* **22**, 655–664.

Clemetsen, R., Hurst, A., Omre, H., and Knarud, H. (1989). A computer program for evaluation of fluvial reservoirs. Proceedings *2nd International Conference on North Sea Oil and Gas Reservoirs*, ed. J. Kleppe, 373–385. Graham & Trotham, Norwegian Institute of Technology, Trondheim.

Clifford, P. and Middleton, R.D. (1989). Reconstruction of polygonal images. *Appl. Statist.* **16**, 409–422.

Conradsen, K. and Nielsen, B.K. (1987). Classification of digital images. *Proceedings 2nd Intern. Tampere Conf. in Statistics.*

Cressie, N. (1991). *Spatial Statistics With Applications.* Wiley, New York.

Davis, J.C. (1973). *Statistics and Data Analysis in Geology.* Wiley, New York.

Diggle, P.J. (1979). On parameter estimation and goodness-of-fit testing for spatial point patterns. *Biometrics* **35**, 87–101.

Diggle, P.J. (1983). *Statistical Analysis of Spatial Point Patterns.* Academic Press, London.

Diggle, P.J., Gates, D.J., and Stallard, A. (1987). A nonparametric estimation for pairwise interaction processes. *Biometrika* **74**, 763–770.

Esbensen, K. and Geladi, P. (1989). Strategy of Multivariate Image Analysis (MIA). *Chem. and Intelligent Lab. Syst.* **7**, 67–86.

Feder, J. (1988). *Fractals.* Plenum Press.

Fiskum, S. (1986). Relaxation methods used in supervised classification of multispectral data [in Norwegian]. Report No. 788. Norwegian Computing Centre, Oslo.

Fiksel, T. (1988). Estimation of interaction potentials of Gibbsian point processes. *Statistics* **19**, 77–80.

Geman, S. and Geman, D. (1984). Stochastic relaxation, Gibbs distributions, and the Bayesian restoration of images. *IEEE Trans. PAMI* **6**, 721–741.

Georgsen, F. and Omre, H. (1992). Combining fibre processes and Gaussian random functions for modelling fluvial reservoirs. Proceedings *4th International Geostatistics Congress*, Troia, Portugal.

Gidas, B. (1985). Nonstationary Markov chains and convergence of the annealing algorithm. *J. Statist. Phys.* **39**, 73–131.

Godtliebsen, F. (1989). *A Study of Image Improvement Techniques Applied to NMR Images.* Dr. Ing. thesis, Norwegian Institute of Technology.

Green, P.J. (1986). Discussion contribution to Besag's 'Statistical analysis of dirty pictures', *J. Royal Statist. Soc. B* **48**.

Green, P.J. and Titterington, D.M. (1987). Recursive methods in image processing. *Bull. Int. Statist. Inst.*, invited paper in the session on spatial image analysis, Tokyo, 51–67.

Greig, D.M., Porteous, B.T., and Seheult, A.H. (1989). Exact MAP estimation for binary images. *J. R. Statist. Soc.* **51**, 271–279.

Hall, P.G. (1988). *Introduction to the Theory of Coverage Processes.* Wiley, New York.

Halvorsen, K. and Strand, G.-H. (1987). Geostatistical analysis of pollution data: a study of methods. Technical report STAT/19/87, Norwegian Computing Centre, Oslo.

Haslett, J. (1985). Maximum likelihood discriminant analysis on the plane using a Markovian model of spatial context. *Pattern Recognition* **18**, 287–296.

Hastings, W.K. (1970). Monte Carlo sampling methods using Markov chains and their applications. *Biometrika* **57**, 97–109.

Helgeland, J., Hjort, N.L., and Sæbø, H.V. (1984). Spatial sampling strategies: a review and some possible applications. Technical report, Norwegian Computing Centre, Oslo.

Hjort, J. and Murray, Sir John (1912). *The Depths of the Ocean.* Cambridge University Press.

Hjort, N.L. (1985a). Neighbourhood based classification of remotely sensed data based on geometric probability models. Technical report 10/NSF, Department of Statistics, Stanford University.

Hjort, N.L. (1985b). Estimating parameters in neighbourhood based classifiers for remotely sensed data, using unclassified vectors. Technical report 12/NSF, Department of Statistics, Stanford University.

Hjort, N.L. (1986). *Statistical Symbol Recognition.* Research monograph, Norwegian Computing Centre, Oslo.

Hjort, N.L. (1987). Classification of 2 × 2 blocks of pixels in image analysis. Technical report BILD/xx/87, Norwegian Computing Centre, Oslo.

Hjort, N.L. (1992). A quasi-likelihood method for estimating parameters in spatial covariance functions. Technical report SAND/xx/92, Norwegian Computing Centre, Oslo.

Hjort, N.L. and Mohn, E. (1984). A comparison of some contextual methods in remote sensing. Proceedings *18th International Symposium on Remote Sensing of the Environment*, CNES, Paris, 1693–1072.

Hjort, N.L. and Mohn, E. (1985). On the contextual classification of data from high resolution satellites. Proceedings *4th Scandinavian Conference on Image Analysis*, 391–399. Tapir, Trondheim.

Hjort, N.L., Mohn, E., and Storvik, G. (1987). A simulation study of some contextual classification methods for remotely sensed data. *IEEE Trans. on Remote Sensing and Geosciences* **15**, 796–804.

Hjort, N.L. and Mohn, E. (1987). Topics in the statistical analysis of remotely sensed data. *Bull. Int. Statist. Inst.*, invited paper in the session on spatial image analysis, Tokyo, 23–47.

Hjort, N.L., Holden, L., and Omre, H. (1989). Modelling sedimentary facies by Markov random fields. Technical report SAND/03/89, Norwegian Computing Centre, Oslo.

Hjort, N.L. and Taxt, T. (1988). Automatic training in statistical pattern recognition. Proceedings *Int. Conference on Pattern Recognition*, Sicily 1987.

Holbæk-Hanssen, E. and Schistad, A.H. (1989). Partially unsupervised classification of SAR images of sea ice. Report No. 835, Norwegian Computing Centre, Oslo.

Holden, L. and Tjelmeland, H. (1990). A program system for simulation of reservoir architecture and reservoir properties. Technical report SAND/09/90, Norwegian Computing Centre, Oslo.

Homleid, M. (1990). TOVS data processing and the potential use of the data in numerical weather prediction models at the Norwegian Meteorological Institute. Technical report no. 83, Norwegian Meteorological Institute, Oslo.

Huijbregts, C.J. and Matheron, G. (1971). Universal Kriging. Canad. Inst. Mining Metal (special volume) **12**, 159–169.

Høiberg, J., Omre, H., and Tjelmeland, H. (1989). Large scale barriers in extensively drilled reservoirs. Proceedings *2nd European Conference on the Mathematics of Oil Recovery*, Arles, France.

Høiberg, J., Omre, H., and Tjelmeland, H. (1990). A stochastic model for shale distribution in petroleum reservoirs. Proceedings *2nd Codata Conference on Geomathematics and Geostatistics, Sciences de la Terre*, Leeds, U.K.

Høst, G., Omre, H., and Sæbø, H.V. (1989). Combining field observations and remotely sensed data in pollution monitoring: A spatial statistical approach. Technical report STAT/09/89, Norwegian Computing Centre, Oslo.

Høst, G., Omre, H., and Switzer, P. (1991). Spatial prediction of air pollution from space/time observations. Technical report STAT/xx/91, Norwegian Computing Centre, Oslo.

Jensen, J.L. and Møller, J. (1991). Pseudolikelihood for exponential family models of spatial point processes. *Ann. Appl. Probab.* **1**, 445–461.

Journel, A.G. (1983). Nonparametric estimation of spatial distributions. *Math. Geology* **15**, 445–468.

Journel, A.G. (1989). *Fundamental of Geostatistics in Five Lessons.* American Geophysical Union, Washington.

Journel, A.G. and Huijbregts, C.J. (1978). *Mining Geostatistics.* Academic Press, New York.

Kay, J.W. and Titterington, D.M. (1986). Image labelling and the statistical analysis of incomplete data. Proceedings *2nd International Conference on Image Processing and its Applications*, IEEE, Imperial College of Science and Technology, London.

Künsch, H.R. (1986). Discussion contribution to Besag's 'Statistical analysis of dirty pictures', *J. Royal Statist. Soc. B* **48**.

Künsch, H.R. (1987). Intrinsic autoregressions and related models on the lattice $\mathcal{Z}^2$. *Biometrika* **74**, 517–524.

Lakshmanan, S. and Derin, H. (1989). Simultaneous parameter estimation and segmentation of Gibbs random fields using simulated annealing. *IEEE Trans. on Pattern Analysis and Machine Intelligence* **11**, 799–813.

Le, N.D. and Zidek, J.V. (1991). Interpolation with uncertain spatial covariances: A Bayesian alternative to Kriging. Technical report, Department of Statistics, University of British Columbia, Vancouver, Canada.

Lotwick, H.W. and Silverman, B.W. (1981). Convergence of spatial birth-and-death processes. *Math. Proc. Camb. Phil. Soc.* **90**, 155–165.

Lundervold, A., Moen, K., and Taxt, T. (1988). Automatic recognition of normal and pathological tissue types in MNR-images: A feasibility study using contextual classifiation methods. Proceedings *NOBIM conference*, Oslo. Report No. 818, Norwegian Computing Centre, Oslo, 189–192.

Mardia, K.V. and Marshall, R.J. (1984). Maximum likelihood estimation of models for residual covariance in spatial regression. *Biometrika* **71**, 135–146.

Mardia, K.V. and Watkins, A.J. (1989). On multimodality of the likelihood in the spatial linear model. *Biometrika* **76**, 289–295.

Marroquin, J., Mitter, S., and Poggio, T. (1987). Probabilistic solution of ill-posed problems in computational vision. *J. Amer. Statsti. Assoc.* **82**, 76–89.

Matérn, B. (1960). *Spatial Variation.* Meddelanden från Statens Skogforskningsinstitut **49**, 1–144.

Matheron, G. (1973). The intrinsic random functions and their applications. *Adv. Appl. Probab.* **5**, 439–468.

Matheron, G. (1976). A simple substitute for conditional expectation: dijunctive Kriging. Proceedings *1st NATO Geostatistical Conference*, eds. Fabbri et al, 221–236. D. Reidel Publishing Company.

Moyeed, R.A. and Baddeley, A.J. (1989). Stochastic approximation of the MLE for a spatial point pattern. CWI technical report, Amsterdam.

Metropolis, N., Rosenbluth, A.W., Rosenbluth, M.N., Teller, A.H., and Teller, E. (1953). Equations of state calculations by fast computing machines. *J. Chem. Phys.* **21**, 1087–1092.

Omre, H. (1984). *Alternative Variogram Estimators in Geostatistics.* Ph.D. thesis, Earth Sciences Department, Stanford University.

Omre, H. (1987). Bayesian Kriging – merging observations and qualified guesses in Kriging. *Math. Geol.* **19**, 25–39.

Omre, H., Halvorsen, K., and Berteig, V. (1989). A Bayesian approach to Kriging. *Geostatistics* **I**, ed. M. Armstrong, Kluwer Academic Publishers, 109–126.

Omre, H. and Halvorsen, K. (1989). The Bayesian bridge between simple and universal Kriging. *Math. Geol.* **21**. 767–786.

Omre, H., Sølna, K., and Tjelmeland, H. (1990). Algorithms for simulating random functions. Technical report SAND/xx/90, Norwegian Computing Centre, Oslo.

Omre, H. and Sølna, K. (1990). Stochastic modelling and simulation of fault zones. Proceedings *2nd Codata Conference on Geomathematics and Geostatistics, Sciences de la Terre.*

Omre, H. (1992). Stochastic models for reservoir characterisation. In *Recent Advances in Imprved Oil Recovery Methods for North Sea Sandstone Reservoirs*, eds. S.M. Skjæveland and J. Kleppe, 141–149. Norwegian Petroleum Directorate, Stavanger.

Omre, H., Sølna, K., Dahl, N., and Tørudbakken, B. (1992). Impact of fault heterogeneity in fault zones on fluid flow. Proceedings *3rd International Conference on North Sea Oil and Gas Reservoirs.*

Omre, H., Sølna, K., and Tjelmeland, H. (1992). Simulation of random functions on large lattices. Proceedings *4th International Geostatistics Congress*, Troia, Portugal.

Owen, A. (1984). A neighbourhood-based classifier for LANDSAT data. *Ca. J. Statist.* **12**, 191–200.

Owen, A. (1989). Image segmentation via iterated conditional expectations. Technical report no. 254, Department of Statistics, Univeristy of Chicago.

Pickard, D.K. (1977). A curious binary lattice process. *J. Appl. Probab.* **14**, 717–731.

Pickard, D.K. (1987). Inference for discrete Markov random fields: the simplest nontrivial case. *J. Amer. Statist. Assoc.* **82**, 90–96.

Pilz, J. (1990). Robust Bayes linear prediction of regionalised variables. Techical report, Freiburg Universität.

Pripp, P.O. (1990). Binary Markov random fields applied to automatic recognition of hand-written symbols [in Norwegian]. Graduate thesis, Dept. of Math., University of Oslo.

Ripley, B.D. (1977). Modelling spatial patterns (with discussion). *J. R. Statist. Assoc. B* **39**, 172–212.

Ripley, B.D. (1981). *Spatial Statistics.* Wiley, New York.

Ripley, B.D. (1986). Statistics, images and pattern recognition (with discussion). *Can. J. Statist.* **14**, 83–111.

Ripley, B.D. (1987). *Stochastic Simulation.* Wiley, New York.

Ripley, B.D. (1988). *Stastical Inference for Spatial Processes.* Cambridge University Press.

Ripley, B.D. (1989a). Gibbsian interaction models. In *Spatial Statistics: Past, Present and Future,* ed. D.A. Griffiths, Image, New York.

Ripley, B.D. (1989b). The uses of spatial models as image priors. In *Spatial Statistics & Imaging*, ed. A. Possolo, *IMS Lecture Notes*, 29 pp.

Ripley, B.D. and Kelly, F.P. (1977). Markov point processes. *J. London Math. Soc.* **15**, 188–192.

Sampson, P.D. and Guttorp, P. (1992). Nonparametric estimation of nonstationary spatial covariance structure. *J. Amer. Statist. Assoc.* **87**, 108–119.

Sandjivy, L. (1984). The factorial Kriging analysis of regionalised data. Its application to geochemical prospecting. *Geostatistics for Natural Resources Characterisation* **I**, eds. G. Verly et al, 559–571. D. Reidel Publishing Company.

Särkkä, A. (1991). On parameter estimation of Gibbs point processes through the pseuso-likelihood method. Technical Report, Dept. of Statistics, University of Jyväskylä.

Schweder, T., Øien, N., and Høst, G. (1990). Estimates of the detection probability for shipboard surveys of Northeastern Atlantic minke whales, based on a parallel ship experiment. Technical report STAT/xx/90, Norwegian Computing Centre, Oslo.

Schweder, T. and Høst, G. (1991). Integrating experimental data and survey data through a simulation model to obtain estimates of $g(0)$. Proceedings *International Whaling Committee*, Cambridge.

Solow, A.R. (1990). Geostatistical cross-validation: a cautionary note. *Math. Geology* **22**, 637–639.

Stein, M. (1987). Minimum norm quadratic estimation of spatial variograms. *J. Amer. Statist. Assoc.* **82**, 765–772.

Stein, M. (1990a). Bounds on the efficiency of linear predictions using an incorrect covariance function. *Ann. Statist.* **18**, 1116–1138.

Stein, M. (1990b). A comparison of generalised cross validation and modified maximum likelihood for estimating the parameters of a stochastic process. *Ann. Statist.* **18**, 1139–1157.

Storvik, G. (1992). Time-dynamic modelling of closed curves. Technical Report, Norwegian Computing Centre, Oslo.

Storvik, G. and Switzer, P. (1992). Space-time modelling of simply connected objects: An application to detection of left ventricular cardiac boundaries from ultrasound images. Technical Report, Norwegian Computing Centre, Oslo.

Stoyan, D., Kendall, W.S., and Mecke, J. (1987). *Stochastic Geometry and Its Applications.* Akademie-Verlag, Berlin DDR.

Strand, G-H. (1989). Remote sensing of forest: An inductive approach. Report No. 824, Norwegian Computing Centre, Oslo.

Switzer, P. (1965). A random set process in the plane with a Markov property. *Ann. Math. Statist.* **36**, 1859–1863.

Switzer, P. (1984). Inference for spatial autocorrelation functions. *Geostatistics for Natural Resources Characterization*, I, 127–140. Ed. G. Verly et al. D. Reidel Publ. Comp.

Switzer, P. (1989). Non-stationary spatial covariances estimated from monitoring data. In *Geostatistics* **I**, ed. M. Armstrong, 127–138. Kluwer Academic Publishers, Amsterdam.

Switzer, P. and Green, A.A. (1984). Min/max autocorrelation factors for multivariate spatial imagery. Technical Report, Dept. of Statistics, Stanford University.

Switzer, P. and Ingebritsen, S.E. (1986). Ordering of time-difference data from multispectral imagery. *Remote Sensing of Environment* **20**, 85–94.

Sæbø, H.V., Bråten, K.B., Hjort, N.L., Llewellyn, B., and Mohn, E. (1985). *Contextual Classification of Remotely Sensed Data: Statistical Methods and Development of a System.* Report No. 768, Norwegian Coputing Centre, Oslo.

Taxt, T., Lundervold, A., and Angelsen, B. (1990). Noise reduction and segmentation in time-varying ultrasound images. Proceedings *10th International Conference on Pattern Recognition:*

Systems and Applications, Atlantic City.

Taxt, T. and Bølviken, E. (1991). Relaxation using models from quantum mechanics. *Pattern Recognition* **24**, 695–709.

Tjelmeland, H. and Holden, L. (1992). Semi-Markov random fields. Proceedings *4th International Geostatistics Congress*, Troia, Portugal.

Vecchia, A.V. (1989). Estimation and model identification for continuous spatial processes. *J. Royal Statist. Soc. B* **50**, 297–312.

Veijanen, A. (1990). An estimator for imperfectly observed Markov random fields. Research report, Department of Statistics, Helsinki.

Warnes, J.J. and Ripley, B.D. (1987). Problems with likelihood estimation of covariance functions of spatial processes. *Biometrika* **74**, 640–642.

Watkins, A.J. and Al-Boutiahi, F.H.M. (1990). On maximum likelihood estimation of parameters in incorrectly specified models for covariance for spatial data. *Math. Geol.* **22**, 151–173.

Yaglom, A.M. (1962). Some classes of random fields in n-dimensional space, related to stationary random processes. *Theory of Prob. Appl.*, 273–320.

τ	B_1	B_2	B_3	$V(x_0)$
0.0	0.6000	0.0002	0.0700	1.015
	0	0	0	
	0	0	0	
	0	0	0	
0.01	0.5991	0.00019	0.0699	1.003
	$0.296 \cdot 10^{-6}$	$-0.236 \cdot 10^{-10}$	$-0.217 \cdot 10^{-9}$	
	$-0.236 \cdot 10^{-10}$	$0.855 \cdot 10^{-12}$	$-0.133 \cdot 10^{-11}$	
	$-0.217 \cdot 10^{-9}$	$-0.133 \cdot 10^{-11}$	$0.500 \cdot 10^{-7}$	
0.1	0.5943	0.00017	0.0691	0.944
	$0.277 \cdot 10^{-4}$	$-0.141 \cdot 10^{-7}$	$-0.137 \cdot 10^{-6}$	
	$-0.141 \cdot 10^{-7}$	$0.129 \cdot 10^{-10}$	$-0.773 \cdot 10^{-9}$	
	$-0.137 \cdot 10^{-6}$	$-0.773 \cdot 10^{-9}$	$0.488 \cdot 10^{-5}$	
1.0	0.5865	0.00017	0.0501	0.938
	$0.241 \cdot 10^{-2}$	$-0.130 \cdot 10^{-5}$	$-0.309 \cdot 10^{-4}$	
	$-0.130 \cdot 10^{-5}$	$0.711 \cdot 10^{-9}$	$-0.111 \cdot 10^{-7}$	
	$-0.309 \cdot 10^{-4}$	$-0.111 \cdot 10^{-7}$	$0.152 \cdot 10^{-3}$	
10.0	0.5460	0.0002	0.0423	0.938
	$0.178 \cdot 10^{-1}$	$-0.958 \cdot 10^{-5}$	$-0.285 \cdot 10^{-3}$	
	$-0.958 \cdot 10^{-5}$	$0.518 \cdot 10^{-8}$	$0.113 \cdot 10^{-6}$	
	$-0.285 \cdot 10^{-3}$	$0.113 \cdot 10^{-6}$	$0.223 \cdot 10^{-3}$	
∞	0.5428	0.0002	0.0422	0.938
	$0.190 \cdot 10^{-1}$	$-0.102 \cdot 10^{-4}$	$-0.309 \cdot 10^{-3}$	
	$-0.102 \cdot 10^{-4}$	$0.553 \cdot 10^{-8}$	$0.127 \cdot 10^{-6}$	
	$-0.309 \cdot 10^{-3}$	$0.127 \cdot 10^{-6}$	$0.223 \cdot 10^{-3}$	

TABLE 4.1. *Posterior distribution of parameters, and the velocity at a location on the centre of the map, with $t(x) = 1900$, using specification (4.2). The table gives the posterior means and the posterior covariance matrix.*

Number of wells	B_1	B_2	B_3	$V(x_0)$
1	0.5942	0.00017	0.0699	0.944
	$0.274 \cdot 10^{-2}$	$-0.155 \cdot 10^{-5}$	$-0.572 \cdot 10^{-5}$	
	$-0.155 \cdot 10^{-5}$	$0.895 \cdot 10^{-9}$	$-0.337 \cdot 10^{-7}$	
	$-0.572 \cdot 10^{-5}$	$-0.337 \cdot 10^{-7}$	$0.500 \cdot 10^{-3}$	
3	0.5865	0.00017	0.0501	0.938
	$0.241 \cdot 10^{-2}$	$-0.130 \cdot 10^{-5}$	$-0.309 \cdot 10^{-4}$	
	$-0.130 \cdot 10^{-5}$	$0.711 \cdot 10^{-9}$	$-0.111 \cdot 10^{-7}$	
	$-0.309 \cdot 10^{-4}$	$-0.111 \cdot 10^{-7}$	$0.152 \cdot 10^{-3}$	
5	0.5581	0.00018	0.0532	0.936
	$0.131 \cdot 10^{-2}$	$-0.701 \cdot 10^{-6}$	$0.679 \cdot 10^{-4}$	
	$-0.701 \cdot 10^{-6}$	$0.385 \cdot 10^{-9}$	$0.679 \cdot 10^{-7}$	
	$0.679 \cdot 10^{-4}$	$-0.645 \cdot 10^{-7}$	$0.143 \cdot 10^{-3}$	
8	0.5654	0.00018	0.0663	0.940
	$0.127 \cdot 10^{-2}$	$-0.674 \cdot 10^{-6}$	$0.362 \cdot 10^{-4}$	
	$-0.674 \cdot 10^{-6}$	$0.364 \cdot 10^{-9}$	$-0.427 \cdot 10^{-7}$	
	$0.362 \cdot 10^{-4}$	$-0.427 \cdot 10^{-7}$	$0.102 \cdot 10^{-3}$	

TABLE 4.2. *Posterior distribution of parameters, and the velocity at a location on the centre of the map, with $t(x) = 1900$, when varying the number of wells used in the conditioning. The table gives the posterior means and the posterior covariance matrix.*

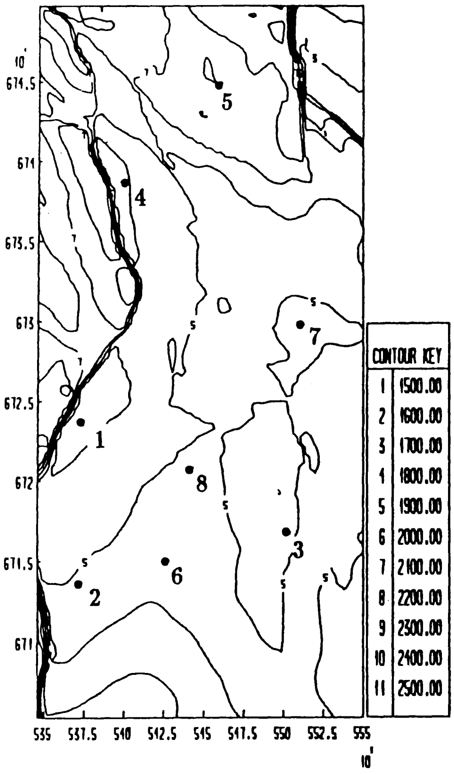

well id.	depth
1	1584.1
2	1770.3
3	1715.4
4	1586.5
5	2062.8
6	1846.7
7	1836.0
8	1784.6

FIGURE 4.1. *Map of seismic reflection times and list of depths observed in the wells.*

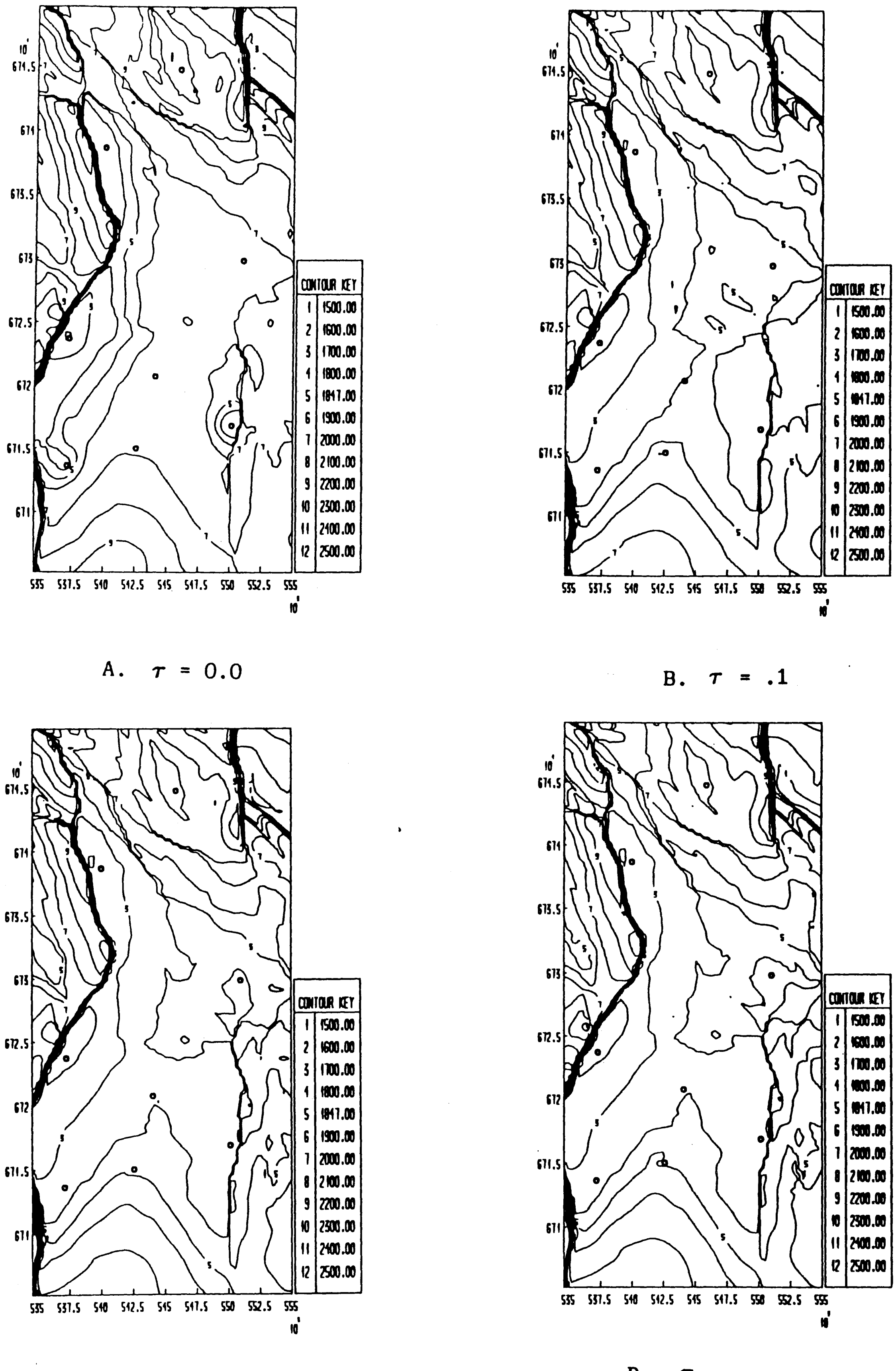

A. $\tau = 0.0$

B. $\tau = .1$

C. $\tau = 1.0$

D. $\tau = \infty$

FIGURE 4.2. *Kriging maps, using specification (4.2), for some values of the prior uncertainty parameter* τ.

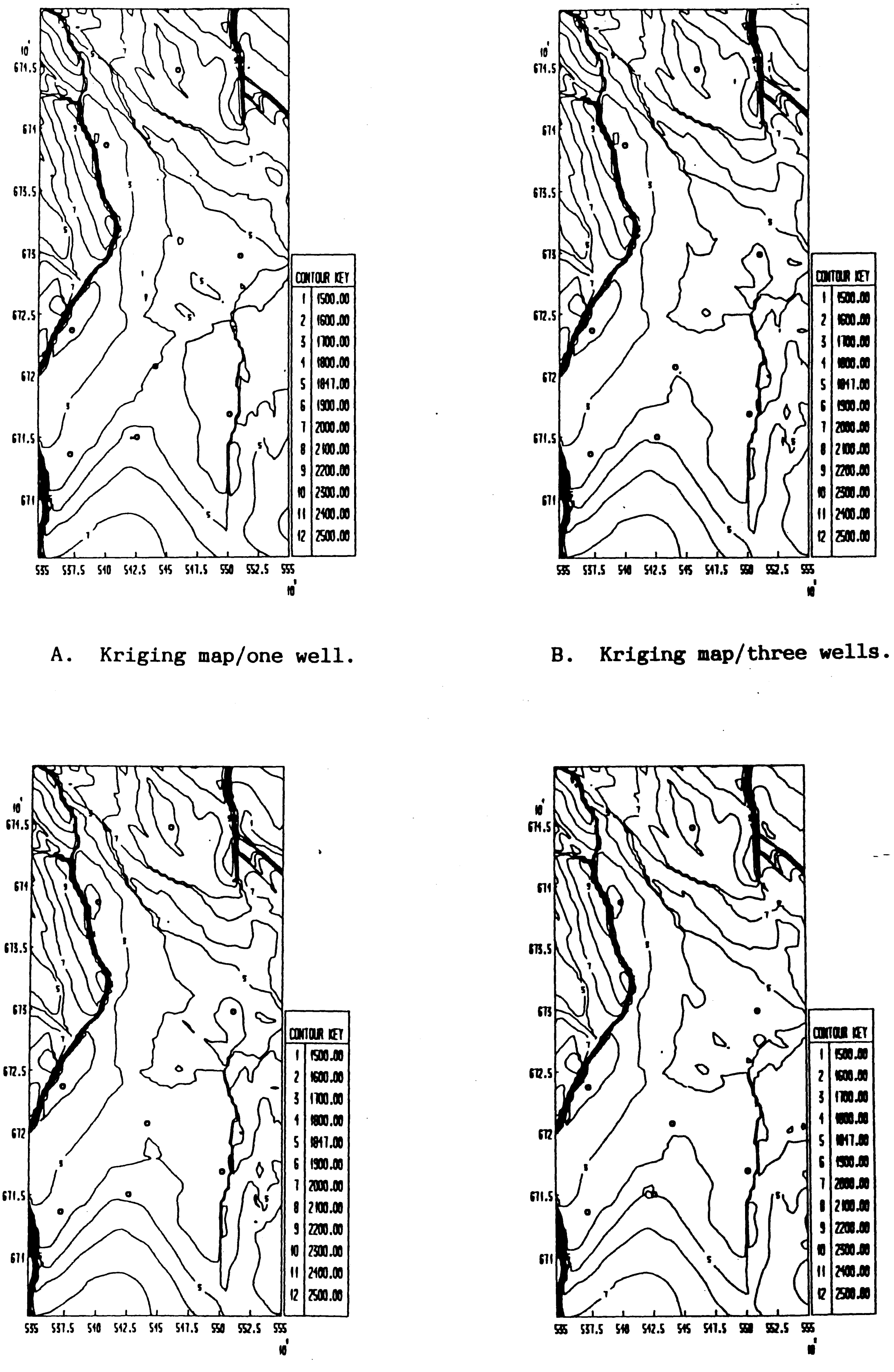

A. Kriging map/one well.

B. Kriging map/three wells.

C. Kriging map/five wells.

D. Kriging map/eight wells.

FIGURE 4.3. *Kriging maps, conditioning on respectively one, three, five, and eight wells.*

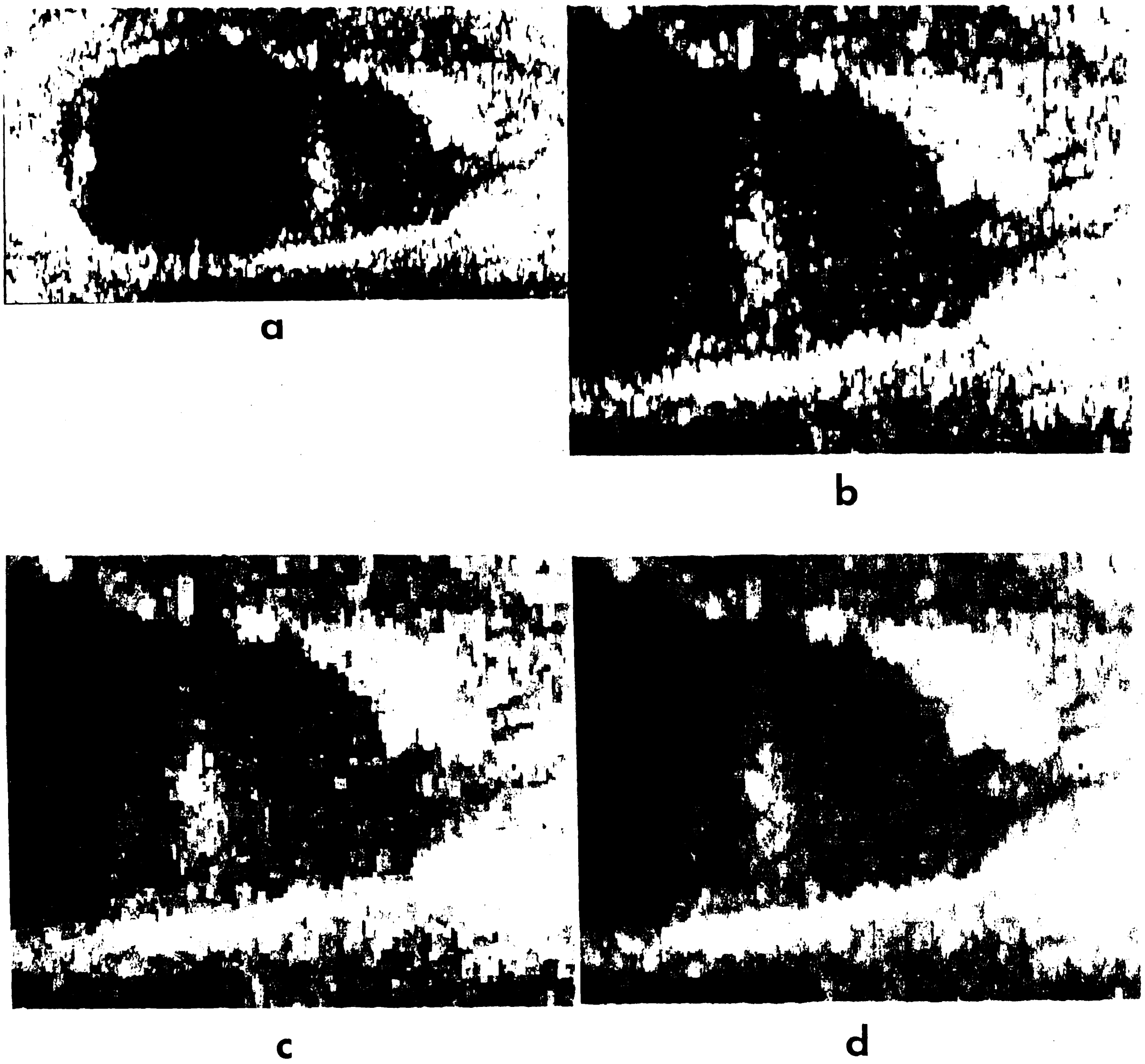

FIGURES 4.4–4.5. *(a) Typical cross section* (128 × 432) *of the 3D-image at constant k, represented as an image in polar coordinates (abscissa is length, ordinate is angle). The broad band in the left ventricular lumen is noise. (b) is a magnified part of (a). (c) is the same detail as in (b), but after application of the Besag noise reduction method. (d) is again the same detail as in (b), but after application of the relaxation noise reduction method.*

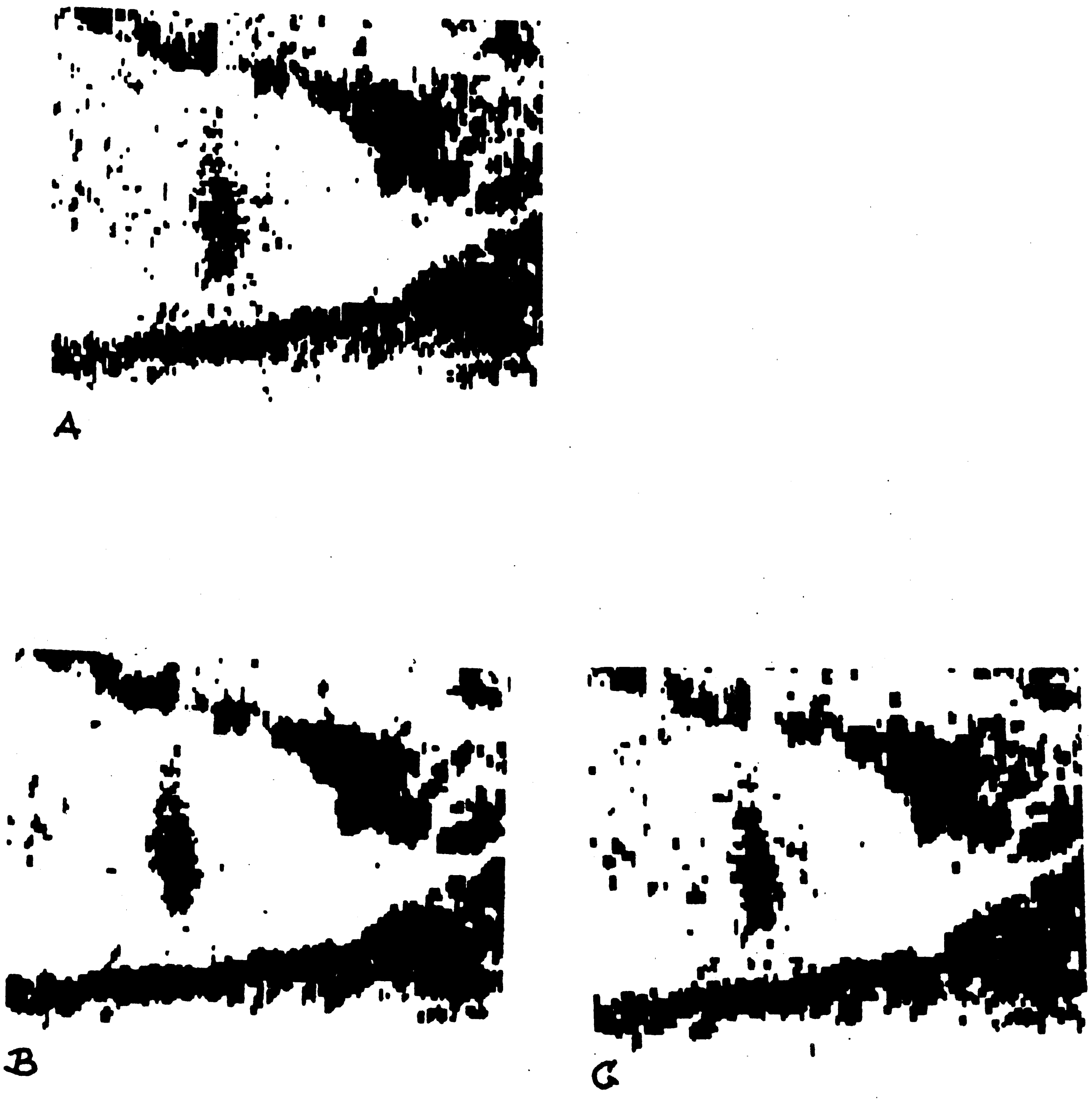

FIGURE 4.6. *Three images of a given section of the heart. (a): binarisation of original image; (b): binarisation of image after relaxation noise reduction method; (c): binarisation of image after Besag noise reduction method.*

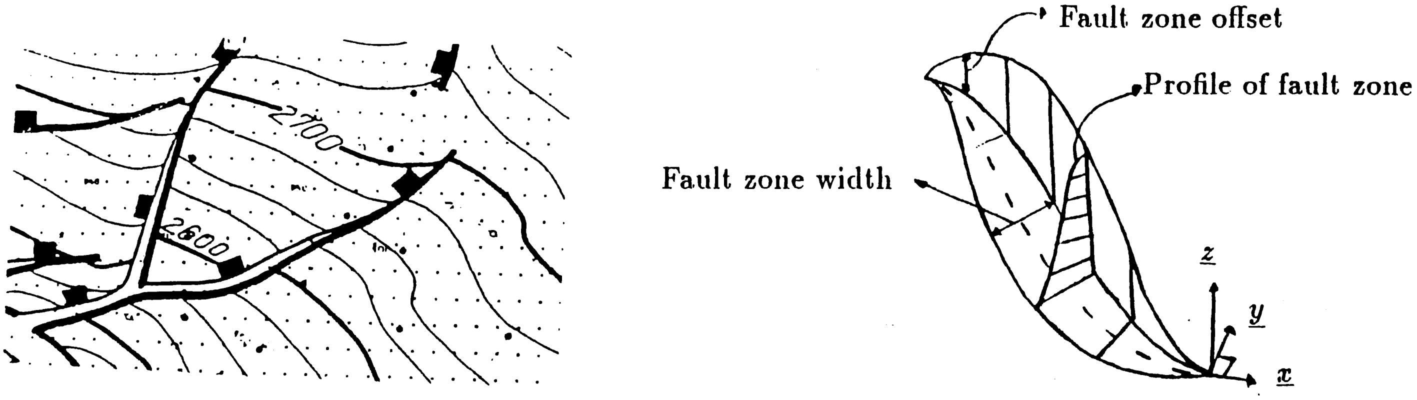

a. Seismic map.

b. Parameterization of fault zone.

FIGURE 4.7. *The large fault zones. Left, seismic map; right, parametrisation of fault zone.*

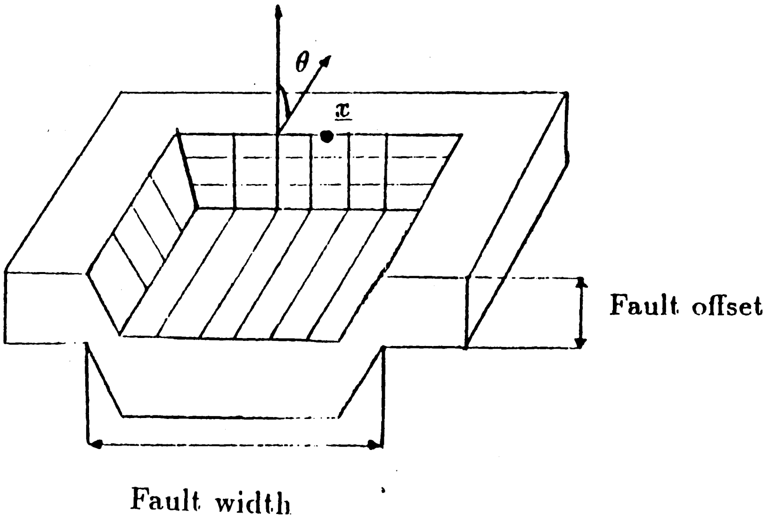

FIGURE 4.8. *Parameterisation of a fracture.*

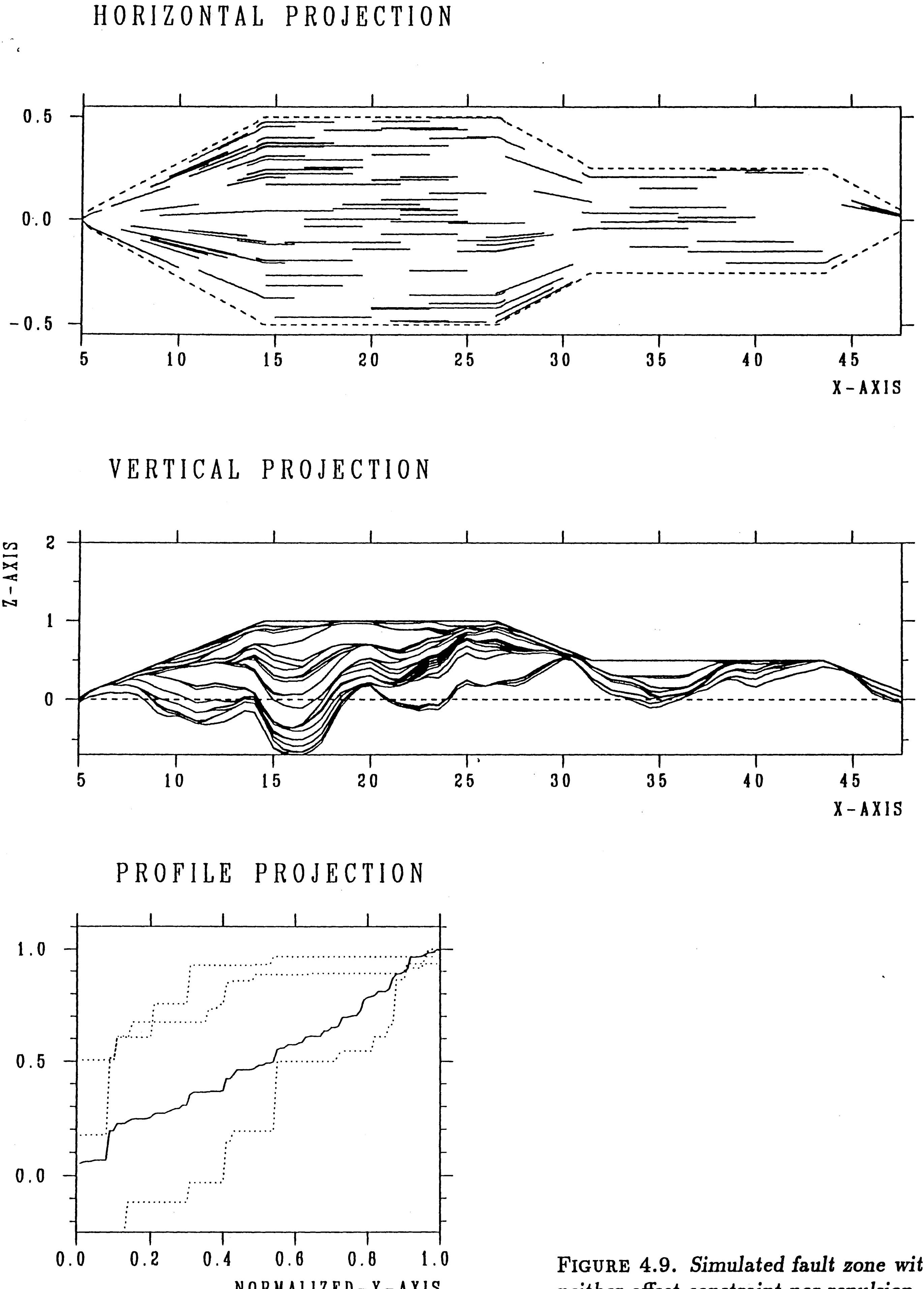

HORIZONTAL PROJECTION

VERTICAL PROJECTION

PROFILE PROJECTION

FIGURE 4.9. *Simulated fault zone with neither offset constraint nor repulsion.*

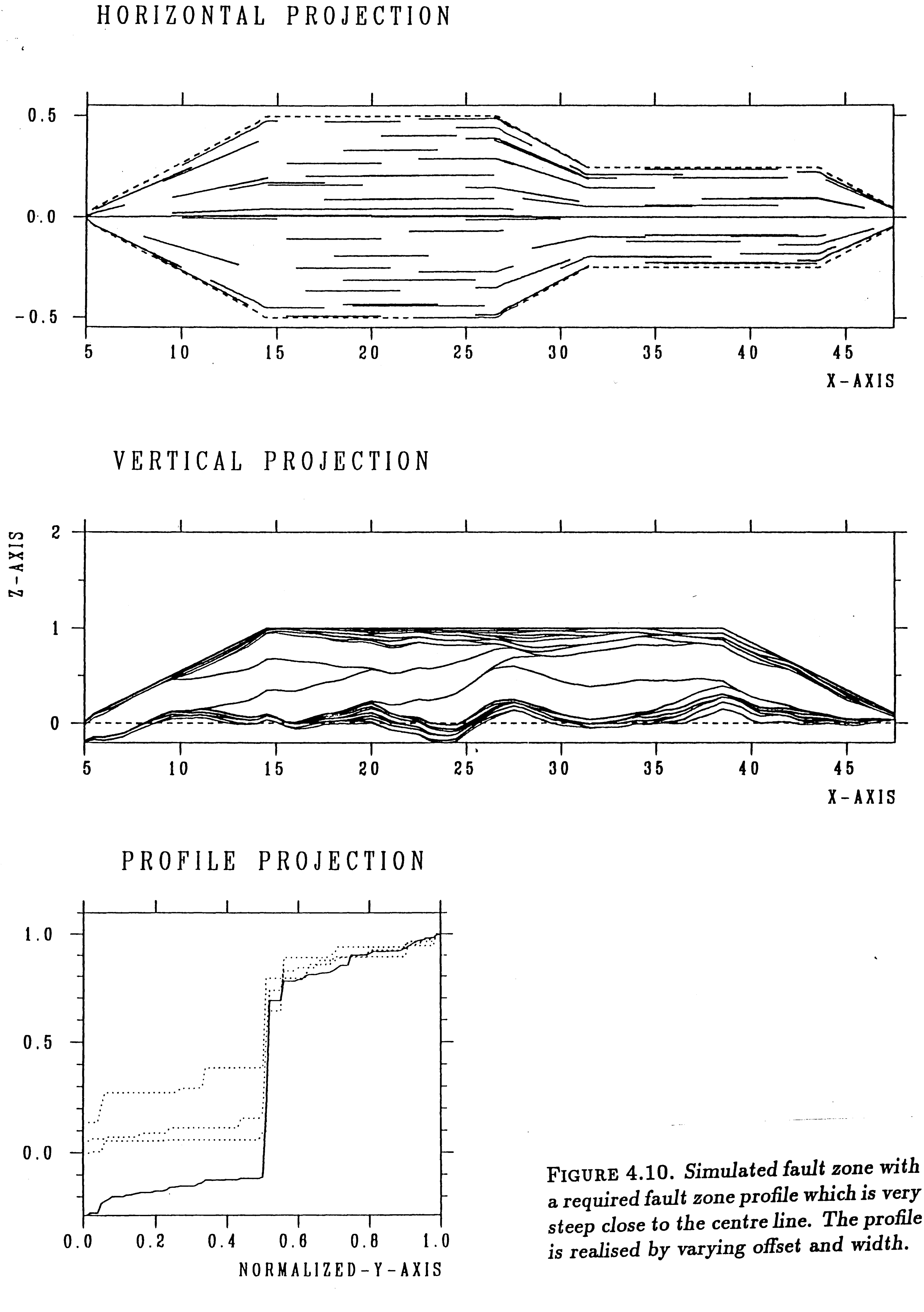
HORIZONTAL PROJECTION

VERTICAL PROJECTION

PROFILE PROJECTION

FIGURE 4.10. *Simulated fault zone with a required fault zone profile which is very steep close to the centre line. The profile is realised by varying offset and width.*

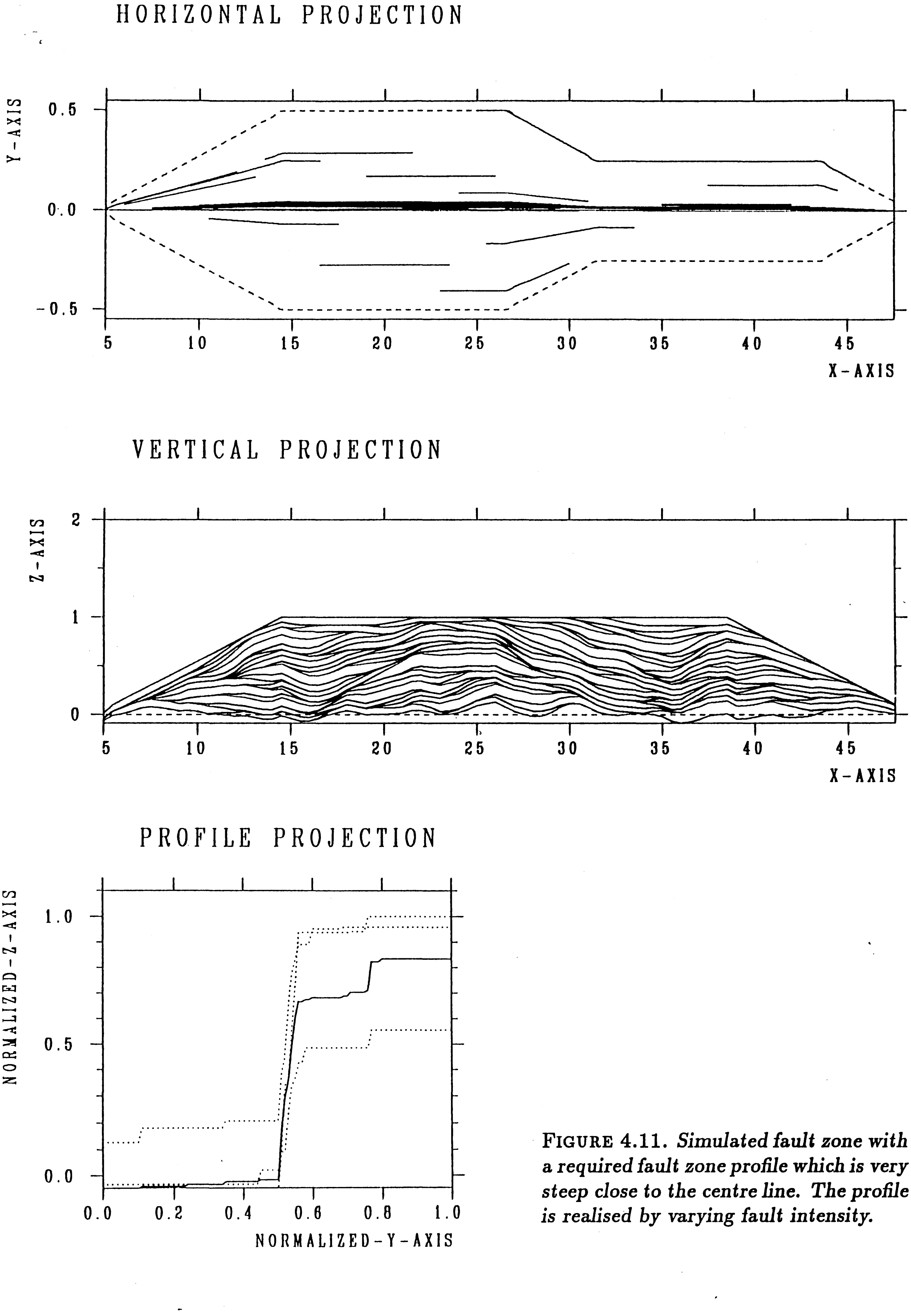

FIGURE 4.11. *Simulated fault zone with a required fault zone profile which is very steep close to the centre line. The profile is realised by varying fault intensity.*

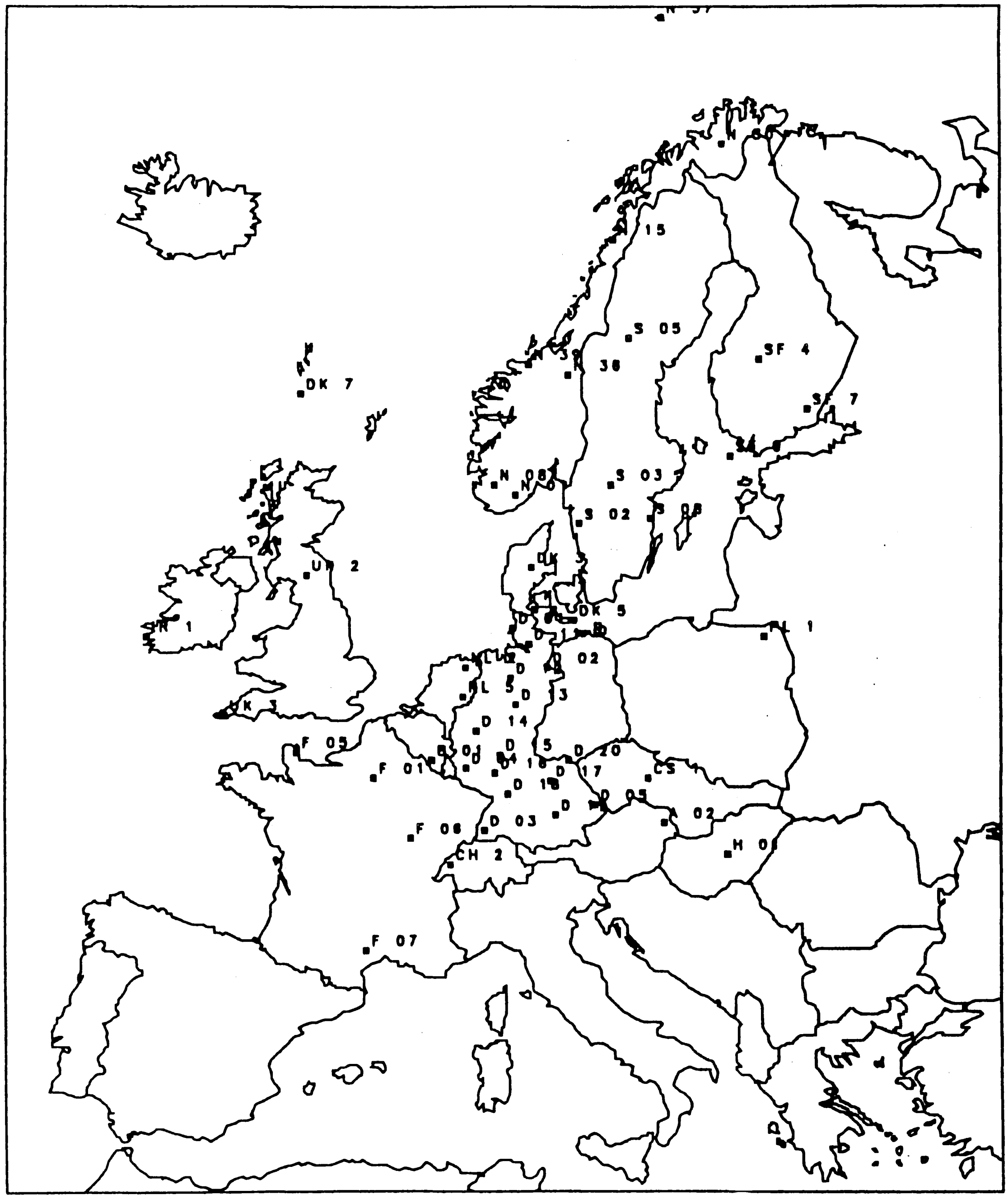

FIGURE 4.12. *Locations where sulphur coincentration is measured by the European Monitoring Evaluation Programme.*

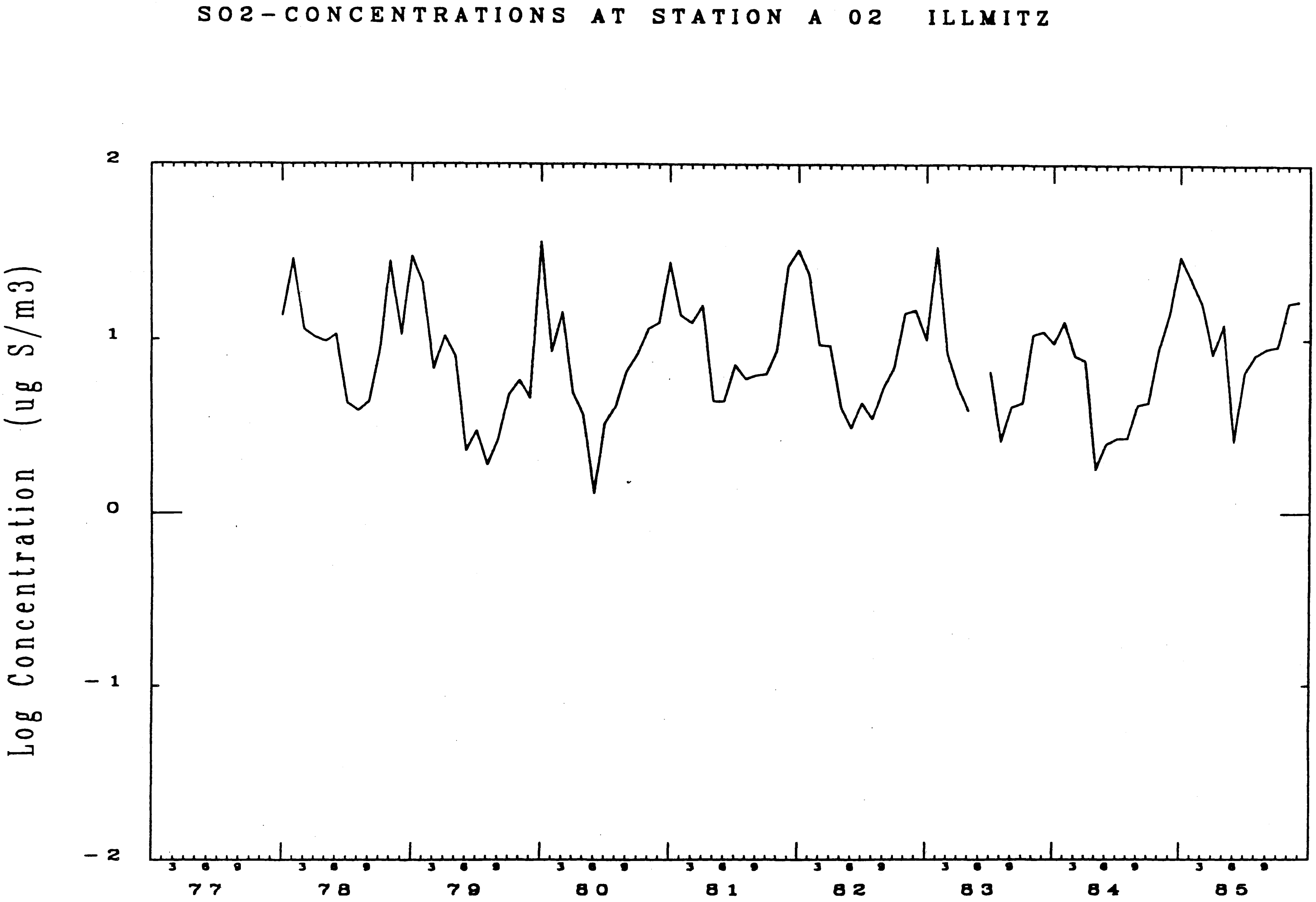

FIGURE 4.13. *Sulphur concentration time series for two particular locations.*

SO2-CONCENTRATIONS AT STATION N 01 BIRKENES

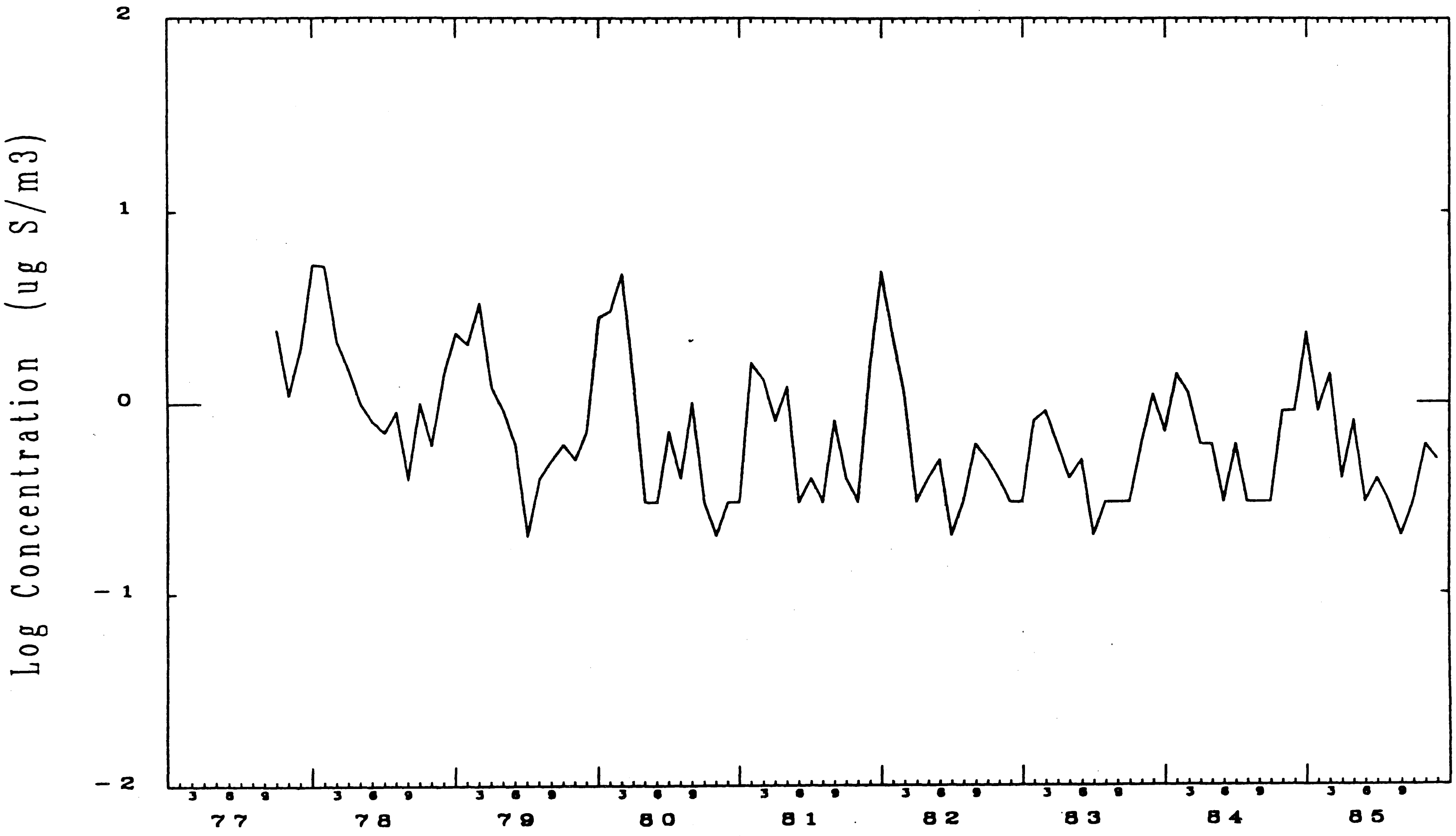

Figure 4.13B

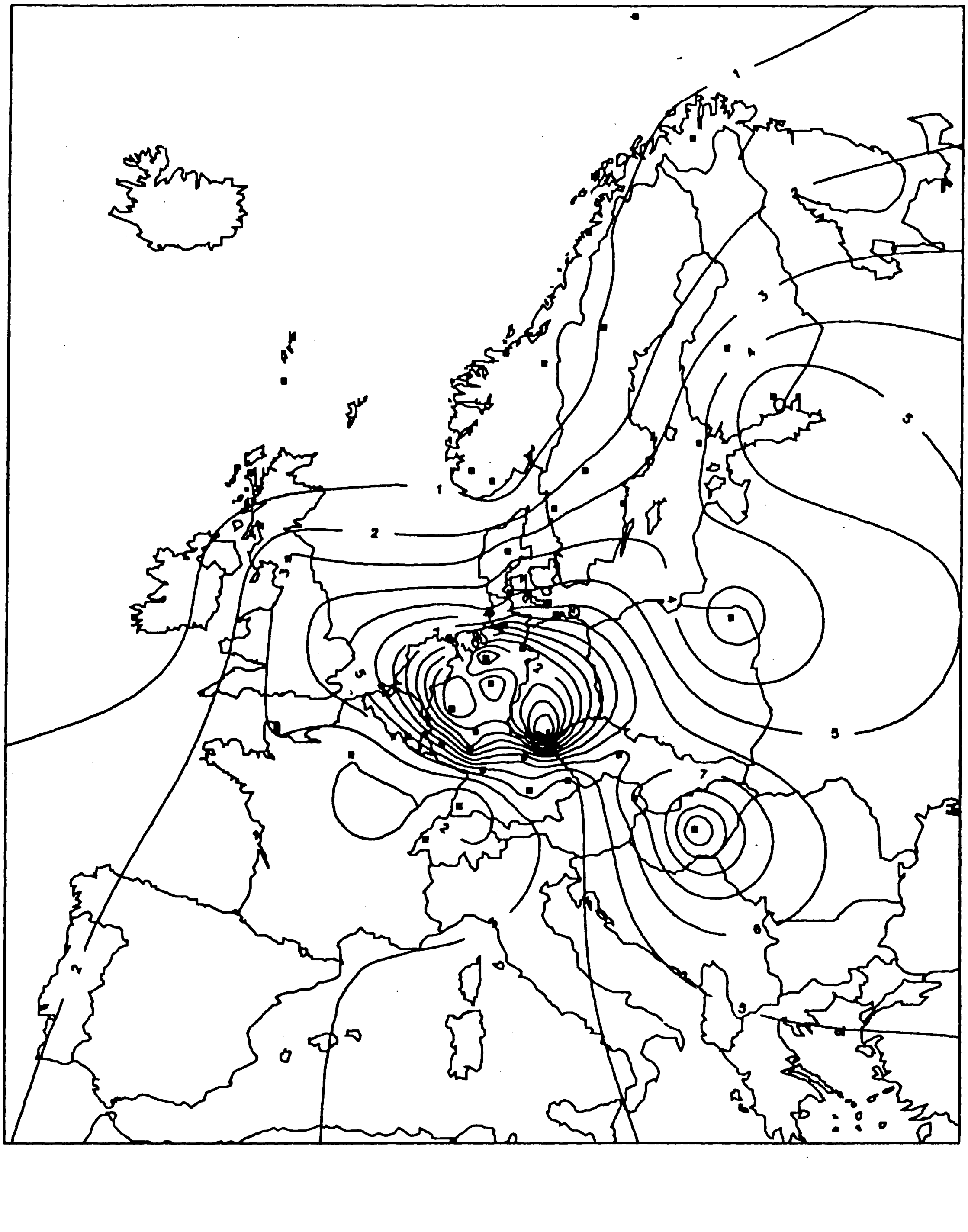

FIGURE 4.14. *Contour map of the predicted sulphur concentration, along with the pointwise 0.2 and 0.8 percentiles in the predictions.*

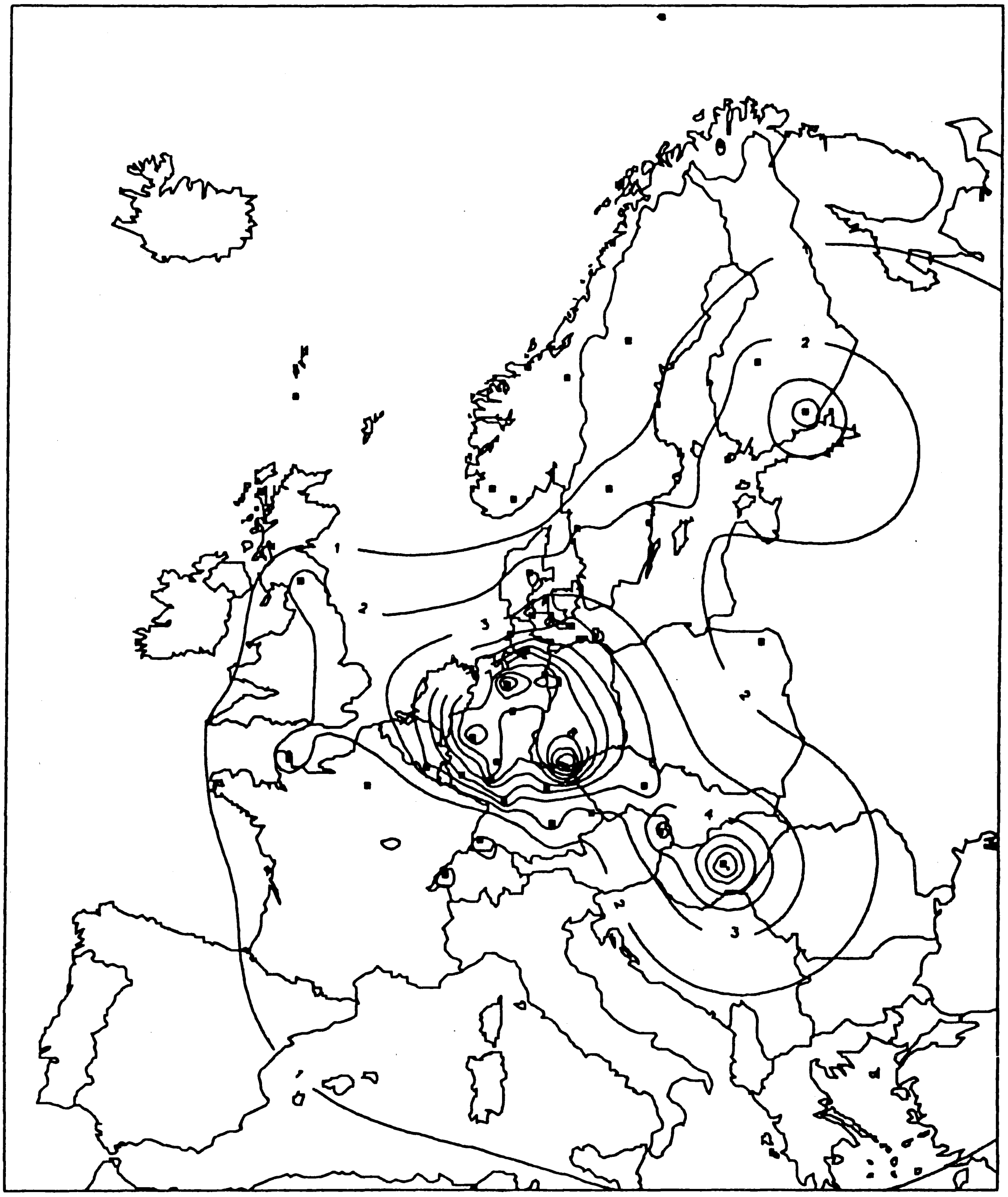

Uncertainty in Z(x,t)

Time: 12:48:34 Date: 14-DEC-90

0.20 - [illegible]!

Figure 4.14 . B

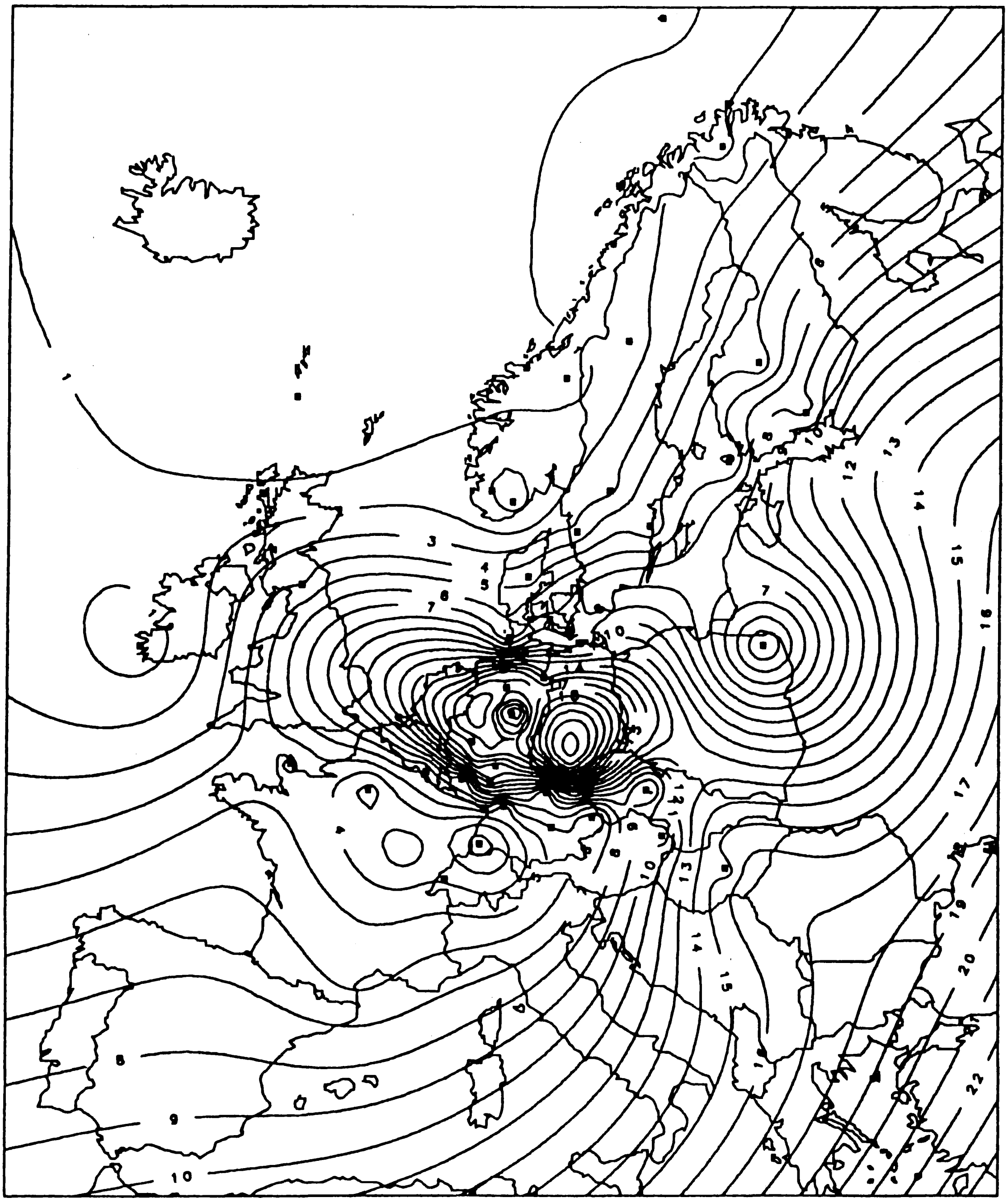

Uncertainty in Z(x,t)

Time: 12:25:15 Date: 14-DEC-90

Figure 4.14.c